The Response of Transformers to Geomagnetically Induced-like Currents

Prepared by: **Hilary K Chisepo**

Supervisor: **Professor CT Gaunt**

May 2014

Dissertation presented for the degree of ***Master of Science in Engineering***

Department of Electrical Engineering

University of Cape Town

The copyright of this thesis vests in the author. No quotation from it or information derived from it is to be published without full acknowledgement of the source. The thesis is to be used for private study or non-commercial research purposes only.

Published by the University of Cape Town (UCT) in terms of the non-exclusive license granted to UCT by the author.

University of Cape Town

DECLARATION

I know the meaning of plagiarism and declare that all the work in the document, save for that which is properly acknowledged and the normal guidance of my supervisor, is my own.

Signature of author:

HILARY KUDZAI CHISEPO

Department of Electrical Engineering,

University of Cape Town,

South Africa

April 2014

ABSTRACT

Geomagnetically induced currents (GICs) occur as a direct consequence of abnormal space weather and have been known to have adverse effects on power systems. GICs enter the networks through the neutrals of grounded power transformers and they bring about a myriad of problems ranging from incipient transformer damage to the complete black-out of power systems. The problems that come with GICs have been in the limelight of power systems research for over two decades now. The main and most strategic component at risk is the power transformer. The effects of severe geomagnetic disturbances have not only caused overwhelming damage in classic auroral regions, but have also been observed in regions incorrectly considered to be low GIC-risk, such as Southern Africa. Laboratory testing of different core types of transformers to GIC-like currents is of considerable value in order to adequately characterize transformer response. This dissertation discusses the development and implementation of a rigorously developed protocol for characterizing and testing transformers with GIC-like currents based on their magnetization curve characteristics. The differences between reactive and non-active power in the context of transformers and GICs are investigated thoroughly and their impact on power networks are analysed. The implementation of this protocol in the laboratory and simulation environments has therefore led to a sound characterization of the transformers' electrical and magnetic response. This developed protocol can also be useful when extended to investigate the response of large power transformers, particularly for the generation of mitigation parameters that are valuable to power utilities.

ACKNOWLEDGEMENTS

I would like to take this opportunity to thank my supervisor Professor Gaunt for not only your guidance and assistance but also for your passion and drive for excellence, which is contagious. Professor Gaunt, I am indebted to you for the support you have given me as your student, for the confidence you showed in my abilities and for the numerous opportunities that you opened for me during my Masters degree.

A big thank you to Dr. Ron Herman and Mrs Kehinde Awodele for all your invaluable insights and experience you gladly offered at our weekly seminars.

David Oyedokun, my mentor and my friend, for such a high achiever thank you for cutting me some slack and making me realize that I can be 'more powerful'.

Special thanks is owed to Dr. Pierre Cilliers and his team from the South African National Space Agency (SANSA) for your collaboration with us which afforded us access to your invaluable knowledge of the problem, coming from your elevated space science background.

I would also like to thank Chris Wozniak and his team for assisting with setting up and commissioning the isolated power supply which was a very important aspect in the experimental procedure.

Thanks to all my fellow studends for making this experience very fruitful.

Tine-tariro Matambo, my friend thank you for proofreading this dissertation and for giving all your much needed 'genius comments'.

Finally, to my parents I am very grateful for your unequivocal faith in me, your guidance and support, which have made it possible for me to achieve this.

…Hilary

TABLE OF CONTENTS

LIST OF TABLES

LIST OF FIGURES

NOMENCLATURE

HV	High Voltage
LV	Low Voltage
MV	Medium Voltage
I_{mag}	Magnetizing current
V_{knee}	Knee point voltage
Q	Reactive power or non-active power unless otherwise specified
Q_{MVar}	Reactive power
Q_{MM}	Non-active power
3p-3s	A bank of three single phase transformer units
3p-3L	A three phase three limb transformer
3p-5L	A three phase five limb transformer
GIC	Geomagnetically induced current
GMD	Geomagnetic disturbance
MTS	Main Transmission System
THD	Total Harmonic Distortion
TDD	Total Demand Distortion
NLL	No Load Losses
Req	Electrical equivalent circuit resistance element
Xeq	Electrical equivalent circuit leakage reactance element
KI	Key Indicator
QOS	Quality of supply
TuT	Transformer under test
TRFR	Transformer

Measured Results – refers to measurements taken in the laboratory

Simulated Results – refers to results modelled in the simulation software

General power theory, new method (of calculating power), general formula – the calculations developed by Malengret & Gaunt (2011, and companion papers); Gaunt & Malengret (2012).

1 INTRODUCTION

Literature has reported various conclusions concerning the susceptibility of different types of transformers to GIC damage; some of which is contradictory or solely based on research comments. This report aims to develop a protocol for rigorously testing transformers with GIC-like currents in order to characterize their electrical and magnetic response. Having developed this protocol, different types of bench-scale transformers will be tested, and measured results will be contrasted with some modelled results in an electromagnetic transients program (EMTP) environment. Additional tests on larger capacity transformers will then be performed in order to test the protocol at bigger scale. The relationship between GIC and VAR demand has been reported to be linear. While various aspects of transformer behaviour due to dc excitation will be investigated, particular attention will be given to the differences between reactive power and non-active power, and the calculation algorithms thereof. Analyses of these differences may lead to a more sound characterization of transformer response and its effect on the interpretation of energy transfer efficiency across power networks.

1.1 Background

Solar activity gives rise to abnormal space weather conditions which, through a complex interaction of events, lead to geomagnetic disturbances (GMDs). This then causes geomagnetically induced currents (GICs) to flow through the earth which may pose risk to manmade structures. Approximately every 11 years, solar disturbances occur on the surface of the sun and the most significant phenomenon that is experienced is a coronal mass ejection (CME) which has energy and moves almost at the speed of light. If the earth happens to be within the trajectory of these CMEs, it normally takes them a few days to reach it (Thomson, *et al*., 2010). These CMEs then interact with the Earth's near space environment (magnetosphere) where periodic variations of the resultant geomagnetic field and ionospheric currents lead to changes in the electric field intensity penetrating the Earth's surface. According to Faradays law of electromagnetic induction, GICs flow through the ground and enter power networks through grounded transformer neutrals; effectively forming a loop (see Figure 1). GMDs have also been known to cause problems with pipelines and communication systems.

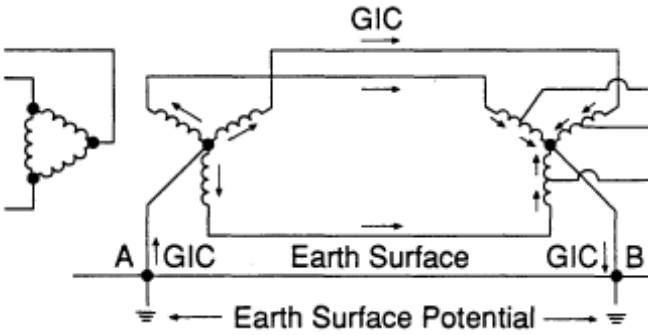

Figure 1: Induced Earth surface potential producing a GIC in a power system involving wye transformers (Albertson, *et al.*, 1993).

When two power transformers are widely separated by high voltage (HV) overhead transmission lines and a geomagnetic disturbance (GMD) occurs, a GIC is induced and seeks to move in the path of 'true earth' (Gaunt & Coetzee, 2007; Gaunt, 2014). This GIC then flows into the neutral of one transformer, and moves along the transmission line, into the second transformer and out through its neutral. The frequency of this GIC is in the order of milliHertz (mHz), typically less than 1 Hz, whereas the nominal operating frequency of power systems is 50 Hz (in South Africa. 60 Hz in the U.S.A. and Canada). Consequently, GICs are termed as *quasi-dc* currents in power engineering as they most assuredly induce the same effects as those of dc excitation in transformers. Dc excitation causes interference with the co-ordination of the transformers magnetic circuit, driving it into the half cycle saturation of its core and consequently bringing about multiple instantaneous and cumulative damaging effects (Heindl, *et al.*, 2011).

1.2 Motivation

Power networks in Southern Africa have been considered to have low GIC-risk but recent research suggests otherwise (Gaunt & Coetzee, 2007; Pinto, *et al.*, 2005). For instance Gaunt and Coetzee's study (2007) reports multiple power transformers at the Tutuka, Matimba and Lethabo power stations that may have been affected by the so-called 'Halloween Storm' in October 2003 – a severe GMD. Early on, Koen (2002) had identified that based on their locations in the Eskom main transmission system (MTS), the aforementioned power stations are among the most susceptible to GICs. This was then confirmed by the sudden onset of 'gassing' in several transformers in the network occurring simultaneously during this significant geomagnetic storm. Some of these transformers experienced cumulative damage and had to be taken out of service weeks after the geomagnetic disturbance (GMD). Transformer failures are costly, disruptive to utility

operations and may cause major power outages as in the instance of the Hydro-Quebec power station in 1989 (Kappenman & Albertson, 1990; Bolduc, 2002).

A renewed awareness of GIC-risk is therefore needed and understanding the behavioural characteristics of transformers, which are a vital component in power systems, in relation to GIC may be of considerable value for a good many reasons inter alia:

a) adequately maintaining or restoring stability in power networks,
b) damage prevention and mitigation of GIC effects on transformers,
c) aiding in network reliability and customer interruption cost (CIC) studies,
d) possibility of setting standards in large scale testing and industrial specifications.

The physics underlying the GIC effect in power systems is quite well-known i.e. the ionosphere – magnetosphere interaction leading to electromagnetic induction through the ground. However, no structured way of testing transformers has been developed or outlined. Also, the conflicting reports in literature concerning the core type of a transformer and its susceptibility to GIC damage further consolidates the need to undertake a laboratory testing protocol.

The North American Electric Reliability Corporation (NERC) is reported (U.S.A. FERC, 2013) to have set goals (May 2012) in a three year plan to:

"… (2) performing comprehensive tests of transformers to GIC…

(4) developing analytical tools for system planners and operators to reliably manage geomagnetic disturbance impacts."

The above extract consolidates the need in power utilities for more knowledge on transformer response and its impact on power system reliability.

Finally, a thorough procedure for testing transformers may be useful in identifying some key parameters that can be used by power utilities' operations and control during or before a potentially consequential GMD for mitigation.

1.3 Hypothesis

Based on the aspects outlined above, the hypothesis of this study is as follows:

"The development of a rigorous testing protocol for transformers subjected to GIC-like currents is needed for a better understanding of the response."

1.3.1 Research questions

The research questions that will enable the testing of the hypothesis are the following:

(a) What are the available methods of laboratory testing and monitoring that will facilitate measurements in compliance with the most up to date power calculation conventions?
(b) In relation to (a), what are the differences between reactive and non-active power in the context of transformers and GICs?
(c) How does the sizing of a transformer in terms of VA rating and operating voltage relate to the magnitude GICs?
(d) What is the effect of reducing the transformer voltage in the presence of GIC?
(e) Is there a standard for defining the relative size of the dc imposed on a particular transformer?
(f) For the same rated capacity (VA) and voltage, what is the differential transformer core structure's response to dc?
(g) How accurate is the carefully chosen simulation software in modelling actual transformers' responses to dc?

1.4 Scope and Limitations

The development of three phase transformer models with relation to GIC was demonstrated in earlier reports (Amuanyena & Gaunt, 2002; Dlamini, 2008) at the University of Cape Town. The main focus of this study is to develop a rigorous laboratory protocol that enables the undertaking of exhaustive transformer tests. In other words this study seeks to answer the (seemingly) simple question, "How can transformers be tested for the effects of dc excitation in a scientifically structured manner, and in a carefully controlled laboratory environment?"

The central focus will be the electrical and magnetic response based on laboratory scale transformers. The thermal and noise responses will not be investigated.

The laboratory tests are to be compared with simulations modelled in the software that is chosen after undertaking a literature survey. The software's transformer models must incorporate non-linear behaviour of a saturated transformer core.

While the bulk of experiments are limited to the low voltage, low capacity range (400V, 900VA), further tests are done with transformers of a higher capacity (48kVA) solely to demonstrate the reproducibility of the developed protocol.

1.5 Dissertation outline

Chapter 1 introduced the topic under investigation, and presented motivation for the research. The hypothesis and the research questions to test it were also outlined.

Chapter 2 will present the undertaking of a comprehensive literature survey based on the aforementioned research questions. An attempt to tackle areas where there is little insight or contradictory conclusions will be carried out in the rest of the study.

Chapter 3 introduces the some of the theories that will be used in the testing of the protocol outlines the chief objectives that will be addressed in the study. Here, the purpose of the investigation and the various domains that will be considered are expanded on. Based on the existing studies critically analysed in *Chapter 2,* the concept of the need for a rigorous "step-by-step" procedure is introduced along with its justification before ushering the reader into the Laboratory protocol.

Chapter 4 lays a solid foundation for the theories that will be used to develop the laboratory procedure. The steps leading up to the definition of the 'knee point' of the magnetization curve, and consequently the role of the corresponding magnetising current as a reference for imposed dc magnitudes is comprehensively described. Variable dependency in the presence of dc is established thus aiding in the deciding of relevant test procedures. A comparative power calculation study is undertaken which involves implications on the non-active power aspect in transformers.

Chapter 5 takes the theories from *Chapter 4* and incorporates them in a three phase bench scale experimental protocol. The experimental and simulation procedures are outlined in

detail; first for the three phase bank system which is the hub of most aspects of the investigations, and then for the multi-limb transformers.

Chapter 6 is the discussion of the results presented in *Chapters 5* and *6*.

Chapter 7 shows how the developed protocol is applied to different transformer core type systems of comparable voltage rating and capacity. Additional tests are also performed on a transformer system of a much larger capacity (48kVA, 380/415V) to demonstrate its adaptability.

Chapter 8 In addition to addressing the research questions and the industrial relevance of outcomes of this study, this chapter draws conclusions on the validity of the hypothesis.

2 LITERATURE REVIEW

2.1 Historical background to GIC studies

The history of geomagnetic disturbances has been recorded for about 160 years starting with one of the first instances between 1846 and 1847 where W.H Barlow reported "spontaneous electric currents observed in the wires on the electric telegraph" (Kappenman & Albertson, 1990). In 1859, telegraph lines in the U.S.A, the highest technology of that time, were reported to have operated for over an hour "with the aid of celestial batteries alone" in the words of G.B Prescott, an engineer with a telegraph company in the U.S.A. This GMD is commonly referred to as the 'Solar Super Storm' and it is the largest geomagnetic storm ever recorded (ibid). The effects of GIC on power systems were then noted in 1940 and research was commenced in the late 1960s.In March 1989, the Hydro-Quebec power system experienced a complete black-out of its system due to a severe geomagnetic storm. There was a power outage for several hours and overall resultant damages amounting to a total of 13.2 million dollars (Bolduc, 2002). The impact of this severe GMD alone then ignited serious research on the effects of GICs on various man made systems. Research over the past thirty years has brought great insight as far as understanding of the phenomenon and implementing mitigating measures are concerned. In their work, Thomson *et al.* (2010) summarize the present knowledge of GICs and recommend areas for future research in this interdisciplinary field of study.

2.2 Science behind the phenomenon

The GIC effect is caused by solar activity which brings rise to the interaction of the ionosphere and the magnetosphere of the earth. When these GICs flow in the earth they then cause various problems on manmade systems such as power system networks, pipelines and communication systems. This section gives a brief overview on the different parts played by each activity involved in a geomagnetic disturbance.

2.2.1 Solar cycle

Approximately every 11 years major disturbances happen on the surface of the sun due to the sun's magnetic activity cycle (See Figure 2).Large amounts of charged particles called coronal mass ejections (CMEs) are then launched into space. If the Earth happens to be within the trajectory of some of these particles, collision with its protective magnetosphere coupled with various other complex interactions cause changes in the ionospheric current systems and this happens within days (Molinski, 2002; Thomson, *et al.*, 2010). These current systems cause large magnetic variations that induce electric fields in the solid Earth.

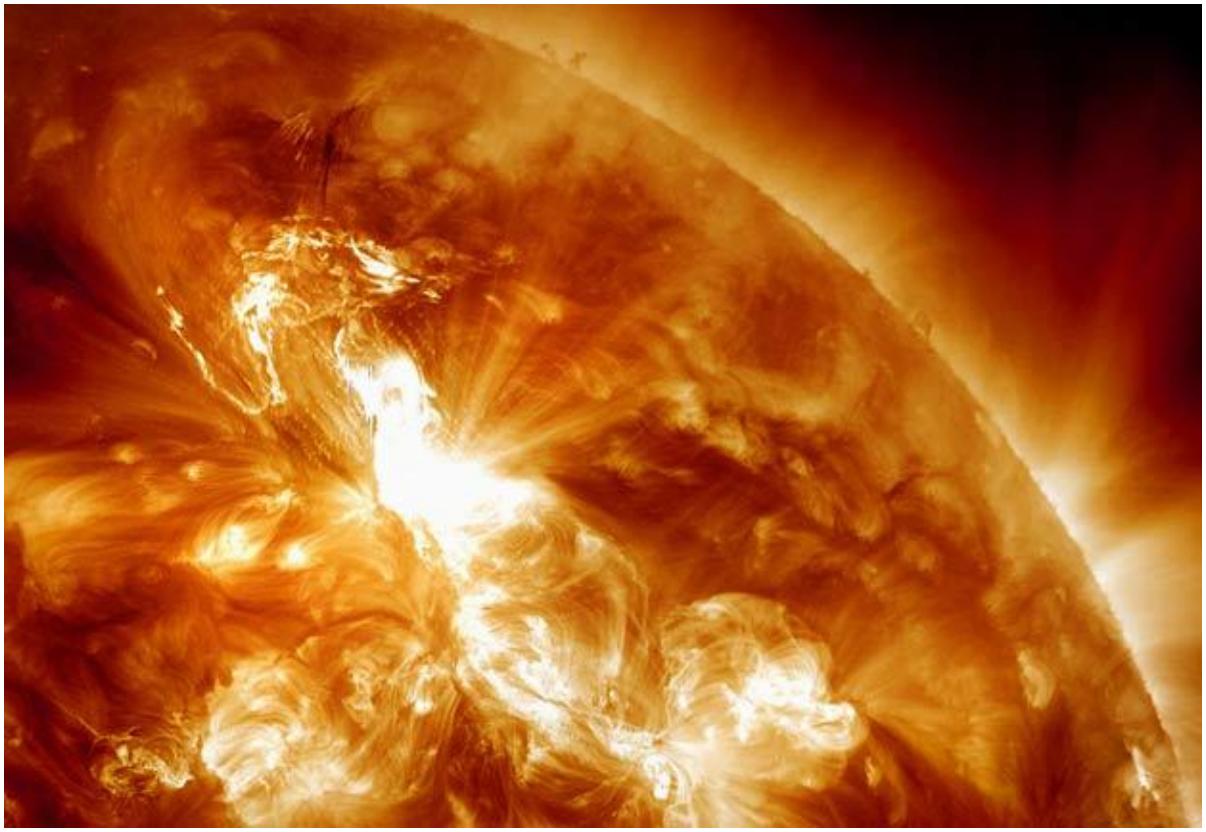

Figure 2: Image taken by NASA on the 22nd of January, 2012 showing a solar flare erupting on the Sun's surface about the north-eastern hemisphere (Public Intelligence, 2012).

The magnetosphere is the Earth's near space environment whose vector quantities are determined by the earth's intrinsic magnetic field. The time varying ionospheric currents are currents that exist in the ionosphere environment as a result of solar radiation. This ionosphere-magnetosphere interaction induces the flow of quasi dc according to Faraday's law of electromagnetic induction. Solar storms that lead to high levels of GICs are statistically more likely during periods close to the solar maximum and the descending phase of the solar cycle, but not limited to those times. In other words GIC risk is always present as stipulated by Thomson *et al.* (2010) in a comprehensive inter-disciplinary study of geomagnetic hazards.

2.2.2 Factors affecting GIC

Boteler *et al.(*1998) defined two sets of factors that determine the nature and effect of the GIC:

(a) The geophysical parameters that determine the size of the electric fields namely:

- The earth's resistivity which varies from location to location i.e. as a function of space by as much as five orders of magnitude (Molinski, 2002; Thomson *et al*., 2009). Contrasts in conductivity such as at a coastline also affect magnitude of

GIC as they can produce larger electric fields because of the charge accumulation at the coast.

- Ionospheric currents which vary as a function of time and space
- Proximity of power systems to auroral zones and the auroral electrojet currents flowing in the ionosphere there. The auroral zone may expand during a GMD.

(b) The engineering characteristics that determine the response of the system to that electric field:

- Transformer type and connection. For instance, the choice of transformers in Finland has meant that they normally operate well below their highest capacity, even though Finland experiences large GMDs no significant problems have occurred there. (This theory is only valid if it can be proved that lightness of load is a function of the severity of damage. More on this will be discussed in later in this study).
- Station grounding
- Electrical resistance
- Lengths and resistances of transmission lines
- Power system orientation.

In the past it has been incorrectly assumed that only countries at higher latitudes close to the auroral zones are susceptible to GIC. At these latitudes, the 'auroral electrojets' induce mostly east west electric fields which means that power networks in that orientation will experience the largest voltage difference across them (Thomson, *et al.,* 2010). However in some cases north-south orientation may be very important where GIC susceptibility is concerned (Ngwira, 2008). Lower and mid-latitudes may also experience high levels of GIC for a plethora of reasons. One of these reasons is that the auroral zone may expand during a severe GMD as in the case of the March 13 1989 storm, the auroral oval had expanded significantly westwards and eastwards. This was the cause of the burn out of the transformer at the Salem generating station on the US east coast (Boteler *et al.,* 1998). Another example proving that GICs have been demonstrated to affect power systems at all latitudes is the damage to a South African transformer three weeks after the Halloween storm of October 2003 (Thomson, *et al.*, 2010). See Figure 3 below.

Figure 3: Disruption of the winding and insulation after initiation of damage during Halloween storm of October 2003 (Thomson *et al*., 2010).

Thomson *et al.* (2010) identified some similar factors that pose GIC risk to power grids. One of these factors omitted from the above findings is the fact that:

- the rate of change of the Earth's magnetic field is actually the dominant cause of GIC in power grids. Accurate prediction of GIC risk is therefore contingent upon accurate prediction of variations in the magnetic field, commonly referred to as $\frac{dB}{dt}$.

2.2.3 GIC Effect on Power systems

The effect of GICs on power systems is important to this study. The main component of power systems that causes disruptions is the grounded power transformer subjected to GIC flow. Below is a brief outline of the effects of GIC.

2.2.3.1 GIC Peaks in transformer neutrals

When there is a severe GMD and GIC flows, power systems experience peaks of GIC in their various components. The typical duration of these peaks can be anywhere between 2 and 15 minutes, but not limited to that range (Pulkkinen, *et al*., 2009). Most of these GIC peaks are associated with sub-storm intensifications e.g. occurrence of localized ionospheric structures during the storm. Figure 4 shows the recorded GIC peaks in the power systems of Finland and Scotland during the April 2002 storm.

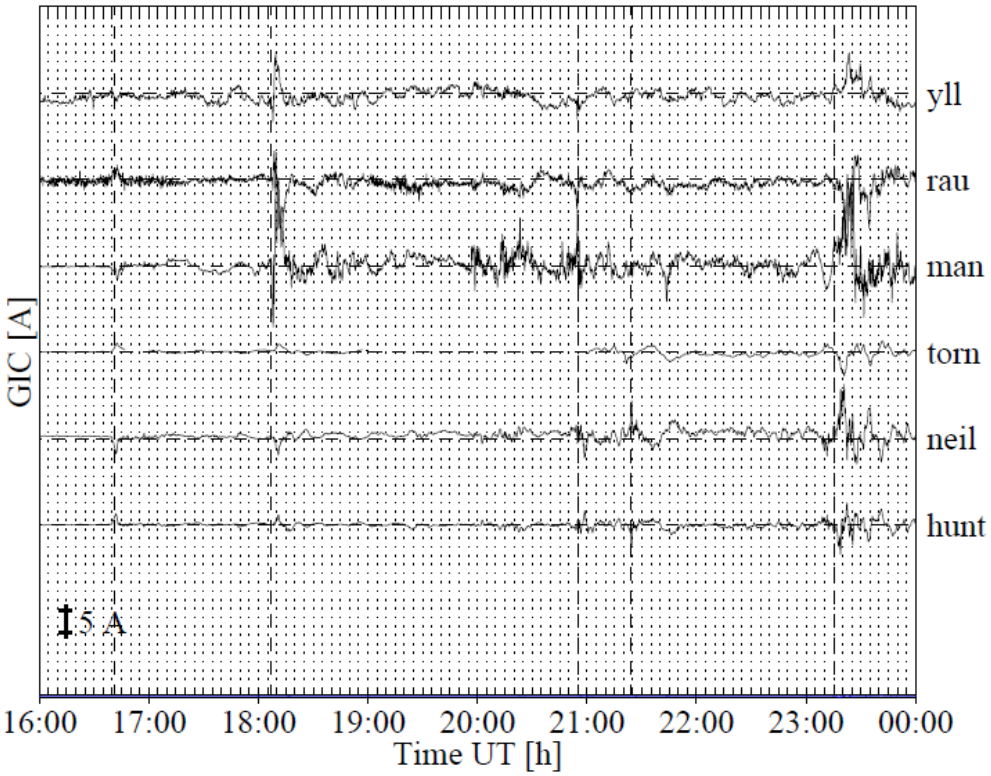

Figure 4: GIC recorded at the Scottish and Finnish power transformer neutrals and in the Finnish pipeline on 6 April 2002. Yll = Yllikkala, rau = Rauma, man = Manstala, torn = Tornes, neil = Neilston, hunt = Hunterson. The vertical lines indicate the times 16:41, 18:07, 20:55, 21:24 and 23:15 UT respectively (Pulkkinen, *et al*., 2009).

2.2.3.2 Simultaneous effect of GIC at multiple points across large scale networks

Global and continental space weather impacts are distinguished from localised terrestrial disturbances such as lightning, ice or severe hail storms here. When it comes to the analysis of power system failure, GICs require a different approach in comparison to standard approaches that normally assume independence of events of initiating system faults (Thomson, *et al.*, 2010). It would not be surprising therefore to find that various transformers at different points in a power network experienced similar problems around the same time frame during a severe storm, as reported by Gaunt and Coetzee (2007).

2.2.4 The effects of GIC in a grounded transformer

This section discusses response of a transformer during the GIC event. The areas of focus shall be split into two sections: (a) the electrical and magnetic response (b) stress experienced by the transformer.

2.2.4.1 Electrical and magnetic response

When a quasi-dc GIC is introduced into the neutrals of a transformer it causes an offset in the sinusoidal AC voltage. This then introduces disturbances in the co-ordination of the magnetic circuit of the transformer driving its core into half cycle saturation (the dc offset voltage is a derivative of the magnetic flux density). For a transformer that is operating close to its rated parameters, even a small GIC can drive its core into half cycle saturation. As the core saturates permeability tends to 1 (an ideal transformer has a permeability of ∞) causing the magnetic flux to fill the whole space of winding with a flux distribution very different from the one under normal operating conditions. The losses that then arise with the leakage flux may cause localised heating in different parts of the transformer core and steel tank. The (dc) excitation due to GIC also causes the magnetizing current of the transformer to increase significantly, lagging the system voltage by 90°, generating both even and odd harmonics and bringing about an increased demand for VARs (Kappenman & Albertson, 1990; Bolduc, *et al.*, 2000; Berge, *et al.*, 2011).

2.2.4.2 Stress experience by the transformer

The distortion for the magnetization co-ordination of the transformer brings rise to the following problems as summarized by Amuanyena (2002).

- Production of harmonics.
- Unusual swing in real and reactive (non-active) power (VAR) flow.
- Voltage collapse at the output.
- Intense stray flux.
- Temperature rise and gas formation.
- Increased audible noise (vibrations).

Of these key indicators (KIs), those that will be analysed in this study are those that are directly related to the core structure of the transformer from an electrical and magnetic perspective. Therefore KIs that will be analysed are (a) reactive and non-active power absorption, (b) voltage and current harmonics (c) magnetic saturation of the core, and (d) voltage collapse. Temperature rise and audible noise will not be focused on in this study.

2.3 Transformer theory

The conventional understanding of transformer response to GIC was briefly described in section 2.2.4. This section is aimed at introducing transformer theory and identifying the different types of transformers that are used in industry. Reports from literature are also referred to with regard to the core type of the transformer and its response to GIC.

2.3.1 The Ideal Transformer

The transformer is one of the most common and strategic nonlinear devices in power systems, whose nonlinearity is brought about by the magnetizing characteristics of its iron core (Abdulsalam, *et al.*, 1996). It is a static machine having two or more electrical circuits coupled by a common magnetic circuit, that uses the principles of electromagnetic mutual induction (Sen, 1997).This device either steps up voltage or steps it down, also altering the current but without affecting the frequency unless harmonics are introduced. A transformer consists of two or more windings that are coupled by a mutual magnetic field. A typical coupling core used in industry is the ferromagnetic core as it provides the tight coupling and high flux densities required in power engineering applications. Transformers operate on two fundamental laws comprehensively defined by Griffiths (1999):

(a) Ampere's law - This law stipulates that an electric current produces a magnetic field.

(b) Faradays law of electromagnetic conduction.

This law stipulates that a changing magnetic field within a coil of wire induces an electric field across the ends of the coil. This induced voltage is proportional to the rate of change of flux and the number of turns in the coil. As shown in equation 2.1 below:

$$v_1 = e_1 = N_1 \frac{d\varphi}{dt} \tag{2.1}$$

Where v_1 is the applied voltage, e_1 is the induced voltage in the primary coil of N_1 turns with a flux φ changing at a rate $d\varphi/dt$ webers per second. The core flux links the secondary winding and induces a voltage e_2:

$$v_2 = e_2 = N_2 \frac{d\varphi}{dt} \tag{2.2}$$

Where v_2 is the voltage at the terminal and it is the same as the induced voltage e_2,and N_2 is the number of turns in the secondary coil. In an ideal transformer, winding resistances are

negligible (thus making v_1 and $e_1$equal), zero flux leakage and therefore zero core losses are assumed and the core has permeability of infinity (Sen, 1997).

A turns ratio *a* can then be formed by combining equations 2.1 and 2.2 as shown below:

$$\frac{v_1}{v_2} = \frac{N_1}{N_2} = \frac{i_2}{i_1} = a \tag{2.3}$$

Another important relationship is introduced by equation 2.3. If a load is connected at the terminals of v_2, a current i_2 will flow in the secondary windings providing a magnetomotive force (mmf) $N_2 i_2$ for the core. Instantaneously, a current i_1 is caused to flow in the primary winding so as to create a counter mmf$N_1 i_1$ that opposes $N_2 i_2$. This is because the net mmf F_{core} required in establishing a flux in the ideal core is zero (see equation 2.4) in accordance to the theories of Ampere's law and the law of conservation of energy. This also means that ideally the instantaneous input power would be equal to the instantaneous output power.

$$N_1 i_1 - N_2 i_2 = 0 = F_{core} \tag{2.4}$$

$$N_1 i_1 = N_2 i_2 \tag{2.5}$$

2.3.2 Impedance transfer

In order to simplify the electrical circuit of the ideal transformer from a magnetically coupled circuit to a simple circuit, the impedance on the primary Z_1 may be transferred to the secondary side (with its own impedance Z_2) and vice versa yielding the following equations (Sen, 1997):

$$Z_1 = a^2 Z_2 = Z_2' \tag{2.6}$$

The equation above stipulates that an impedanceZ_2 connected across the secondary terminals will appear as an impedance Z'$_2$ looking into the primary. Z_2 here is obtained by dividing the secondary voltage V_2 by the secondary current I_2.

2.3.3 The Practical Transformer

The practical transformer exhibits imperfections that are a departure from the ideal case. This is because the windings have resistances, not all windings link the same flux, core losses occur when the core is subjected to a sinusoidal flux and the permeability of the core material is finite. As currents flow through the windings of the transformer, a resultant mutual flux φ_m is established and is theoretically confined to the magnetic core. A very small amount of the flux however links only one winding and does not link the other. This flux is known as leakage flux φ_l. The leakage path is air and the leakage flux which varies linearly with current can be accounted for by an inductance called the leakage inductance. The interested reader is referred to Sen (1997) for the equations accounting for the leakage inductance in each winding.

Abdulsalam *et al.* (2006) and Sen (1997) illustrated the transformer electrical equivalent circuit that can be used in the analysis of a practical transformer. This equivalent circuit represents effectively an ideal transformer plus external impedances that account for the imperfections of the actual transformer. A practical core having finite permeability would require a magnetizing current i_m to establish a flux in the core and this effect is represented by a magnetizing inductance L_m. The core loss is represented by a resistance *Rc* (r_{mj} in the diagram). Figure 5 below represents the electric equivalent circuit:

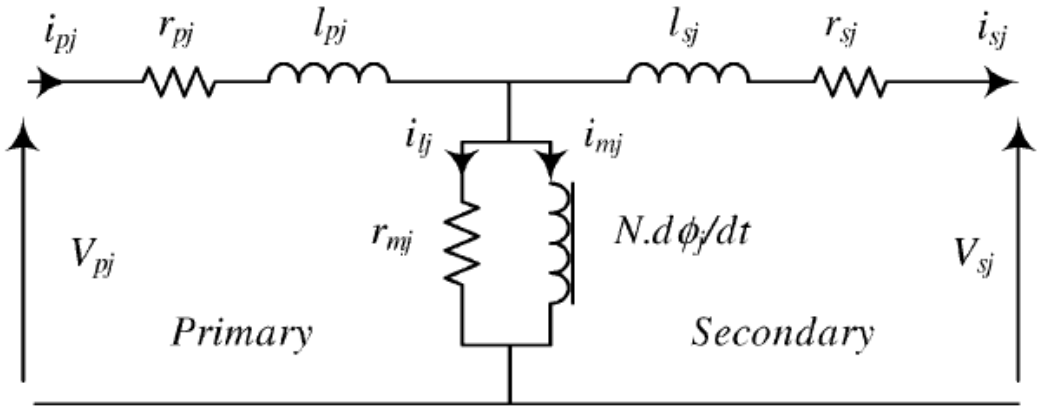

Figure 5: Transformer electrical equivalent circuit referred to from the primary side (per phase) (Abdulsalam, *et al.*, 1996).

2.3.4 No load state

In the no load condition, if a voltage is applied either to the high voltage side or the low voltage side the nature of voltagev_1 is given by equation 2.7 below:

$$v_1 = \sqrt{2} v_p \cos 2\pi f t \tag{2.7}$$

Where v_p is the peak voltage, f is the frequency in hertz and t is the period of the wave. It is important to note the there is a difference between the applied voltage v_1 and the induced voltage e_1 in the primary coil which occurs naturally because of the winding resistance and the leakage flux. Consequently an excitation current i_e flows which is made up of two components: (i) the magnetizing current i_m which lags the applied voltage by 90° and (ii) the core loss current i_c which is in phase with the voltage (Jenneson, 2002)

$$i_e = i_m + i_c \tag{2.8}$$

The excitation current has a very special property which causes it to have a significant third harmonic. This is due to the non-linear magnetic characteristic of the core described by a hysteresis loop and results in a non-sinusoidal “peaky” waveform (Massachusetts Institute of Technology, 1944; Fehr, 2004). Harmonics are one of the most relevant analytical tools in this GIC study and it is of paramount importance that they are adequately understood. The next section (2.3.5) gives a brief overview on harmonics with close attention to the excitation current and the effects of GIC generated harmonics in the transformer windings.

2.3.5 Harmonics

The waveform of the excitation current i_e consists of a dominant frequency called the fundamental frequency with a time period *T* and frequency *f.* In addition to a dominant component at the fundamental frequency, i_e also contains other waveforms that contain components at unwanted frequencies that are odd integer multiples of the fundamental frequency (odd harmonics).These harmonics can be calculated by the rigorous means of Fourier analysis or processed in real-time by electronic equipment. The most significant excitation current harmonic component is the 3rd harmonic, with a total harmonic distortion (THD) of about 41.5 % for a typical transformer core (Massachusetts Institute of Technology, 1944).

Transformers under GIC stress are known to experience problems from the arising triplen (3^{rd}, 6^{th}, 9^{th}, etc.) harmonics (Price, 2002). These harmonics are at integer multiples of the fundamental frequency e.g. for f = 50 Hz, the 6^{th} harmonic will be at 300 Hz. The problem that arises with harmonics in power systems is their adverse effects on relay switches during FACT operation. If the harmonics that are caused by GIC exceed certain limits, it leads to the mal-operation of relays which causes static VAr compensators to not supply the required non-active power to avoid voltage drops (voltage drops are caused by the change in the self-inductance of the transformer whose impedance is jωL which is a function of the frequency).

2.3.6 Core saturation and hysteresis

2.3.6.1 The *B-H* loop

Whenever there is a magnetic field intensity *H*, a magnetic flux density will be produced and this relations is denoted by the equation below:

$$B = \mu H$$

Weber/m^2 (2.9)

Where μ is the permeability of the iron core which is a product of the permeability of free space μ_0 ($4\pi 10^{-7}$ Henry/meter) and the relative permeability of core μ_r. This relationship is illustrated in Figure 6. As the magnetic intensity is *H* increased, by increasing the current *i*(Ampere's law) the magnetization of the core also increase:

$$\oint H \cdot dl = Ni$$

(2.10a)

$$Hl = Ni = F_{core}$$

(2.10b)

Where *N* is the number of turns in the windings and F_{core} is the magnetomotive force in ampere-turn. The magnetic field intensity here is a vector *H*. The flux φ cutting the cross section of the core is given by the integral of the magnetic flux density *B*.

$$\varphi = \int B \, dA$$

(2.11)

As represented in Figure 6 the magnetic field intensity has an almost linear relationship with the magnetic flux density and as soon as certain threshold is reached, the magnetic flux

density levels off as the *B-H* relationship becomes nonlinear. This threshold represents the point at which the core will start to saturate. When saturation is reached there are two very important occurrences to note:

- Increase in the auxiliary field *H* cannot increase the magnetization *B* of the core any further.
- There is a high core magnetic reluctance as μ decreases (Sen,1999)

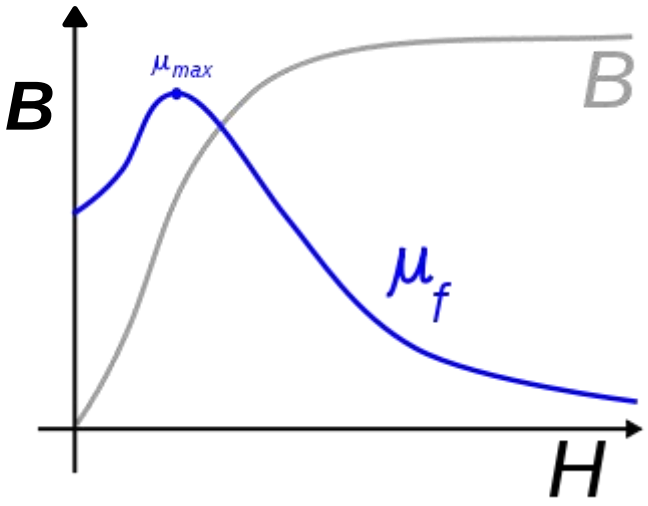

Figure 6: B-H relationship. B is the magnetic flux density in Telsa and H is the magnetic field intensity in ampere turns per meter. the Unlike the ideal transformer whose $\mu \rightarrow \infty$, practically permeability reaches a maximum and the declines when the saturation threshold is reached (Zureks, 2009). μ_{max} is the point of maximum permeability and μ_f is the point representing core saturation or minimum permeability.

In the experimental procedure, the hysteresis loop of the transformer under test (TuT) will be examined to monitor the effect of GIC. A vertical shift in the hysteresis curve will be expected with dc injection as found by Heindl *et al.* (2011) (see Figure 7). It is important to note that half wave saturation of the core is not represented in this diagram. If this was so, there would be an asymmetry either at the top or the bottom of the hysterisis loop.

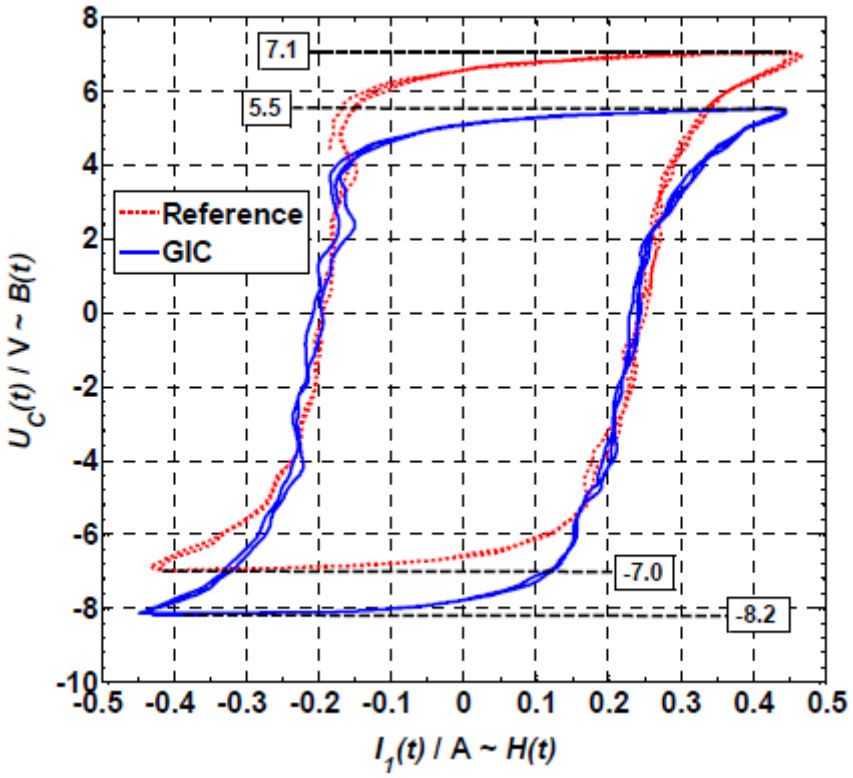

Figure 7: Illustration of vertical shifting of the hysteresis loop with the dc injection of a 30kVA power transformer (Heindl, *et al.*, 2011). $U_c(t)$ is the integrated voltage which is proportional to the magnetic flux density B (t). $I_1(t)$ is the input magnetizing current which is proportional to the magnetic field intensity H(t). The red loop is a representation of the BH characteristic without dc and the blue loop represents the one with a dc flowing in the transformer windings.

In the Heindl *et al.* study, the relationships between the rate of change of flux, secondary induced voltage and current were used in order to generate the hysteresis loop. The same method will be used in the experimental procedure of this i.e. the manipulation of equations 2.2, 2.10b and 2.11.This will involve the practical integration of the primary voltage using an integrating circuit to obtain a value that is proportional to *B(t).*

2.3.7 Transformers with dc (Half cycle saturation)

Figure 8 represents the magnetic response of a transformer core with a direct current component.

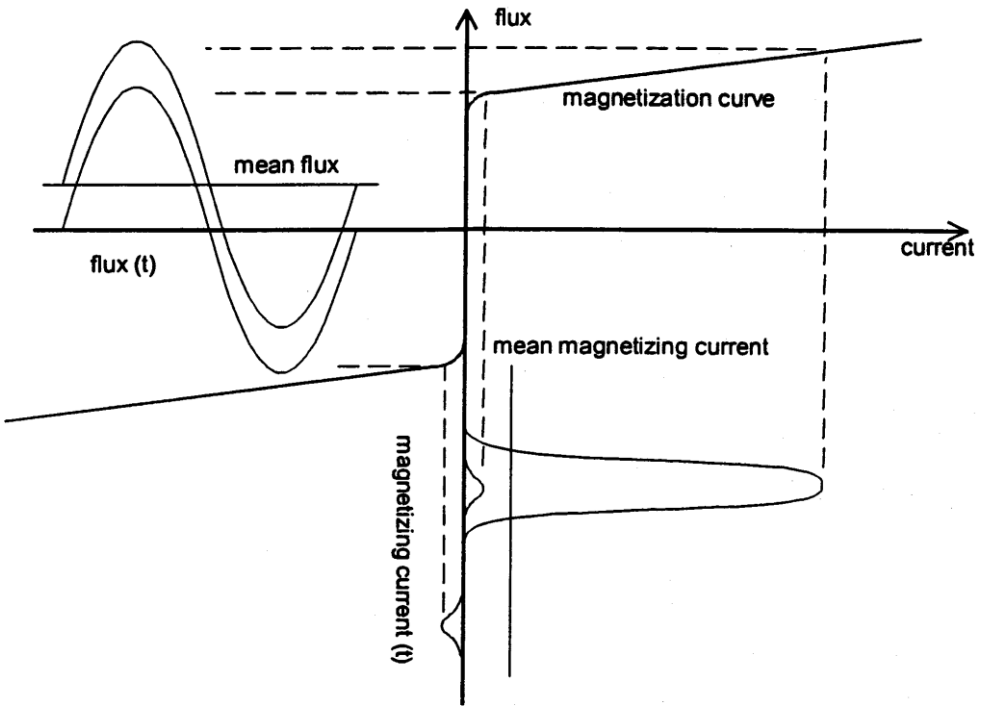

Figure 8: Transformer magnetizing current due to half cycle saturation (Bolduc, *et al*., 2000).

The developed magnetizing flux (left axes) experiences a vertical offset depending on the direction of the dc, and when this is large enough, pushes the core to operate in the saturation region of the magnetization curve. Simultaneously, the magnetizing current increases significantly in the presence of the dc and its peak corresponds to the same operating point in the saturation region that the peak flux is situated. This is known as half cycle saturation and it produces a relatively asymmetrical large magnetizing current lagging the system voltage by 90° and rich in even and odd harmonics (NERC, 2012). This is why there is an increase in the reactive power demand in the presence of GIC.

2.4 Types of transformers

Information from a very large transformer manufacturing plant in the Southern Hemisphere (Powertech transformers) suggests that for large power transformers with a capacity of 60 MVA or more, the most popular core type that is used is the three phase three limb configuration. The three-phase five limb and three phase banks (consisting of a single phase unit per phase) are also used for similar applications in power systems, especially when transportation considerations need to be optimized. For distribution, shell types are commonly used. In general, different applications require different types of transformers. For example, generator step up transformers have a relatively low input voltage, about 20kV, and an output voltage that could range from 132-400kV. Due to the equilibrium that was discussed in section 2.3.1, the current in the primary is normally high meaning that the design of the transformer should be done so as to minimize heat losses. Network

transformers usually stepping down voltage in transmission networks need to be lightly loaded relative to their name plate ratings in order to maintain a secure system. Therefore in the event of one transformer being out of service, some spare built in capacity will kick in (Eskom Holdings Ltd, 1998). In the next section, specific core types of transformers are discussed. Their responses to GIC are then contrasted according to literature reports, paying special attention to contradictions therein that may be tackled in this study.

2.4.1 Transformer Core Types

Two types of cores exist namely (i) the shell type and (ii) the core type. The shell type transformer has both primary and secondary windings on a common limb which is then totally surrounded by outer core plates. The windings have to be highly insulated. Usually a low impedance is required for shell types because close coupling between windings can be achieved readily, making them more efficient than core types. For core types the windings are a wound around the separate limbs of the transformer and these transformers are normally used where a very high capacity is needed (Eskom Holdings Ltd, 1998).

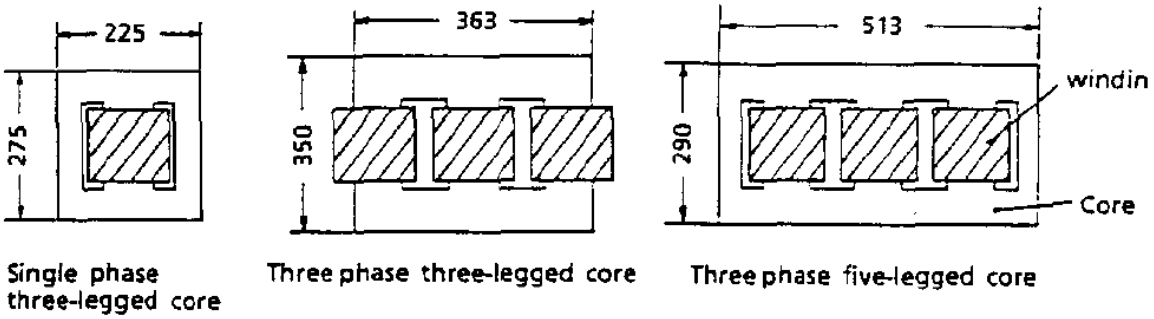

Figure 9: Examples of different bench scale core structures. The dimensions are in mm. (Takasu, *et al.*, 1994).

Typically, three limb single phase and five limb three phase transformers readily offer a dc flux return path through their outer unwound limbs. The response however of the three phase three limb power transformer due to dc excitation differs slightly in the sense that it does not readily offer zero sequence return path for the dc flux as it has windings on every limb. The effects of dc excitation may still occur, though relatively smaller, if the stray flux caused by the GIC is intense enough to dc flux return path through the transformer tank resulting in half cycle saturation.

2.5 Performance evaluation and characterization

The next section is a brief overview of the findings in literature with regards to transformer response to GIC. The susceptibility of different core types is discussed. Possible answers to some of the research questions posed in section 1.3.1. are also addressed.

2.5.1 Takasu et al. (1994)

Transformers have been “studied experimentally on an individual basis” from as early as the 1930s to 1992. Takasu *et al.* (1994) introduced one of the first comparative studies of the core type of the different transformers subjected to dc. Three core types where investigated (i) a three limb single phase shell type, (ii) a three phase three limb core type transformer and (iii) a five limb three phase core type. The following results were generated from their small scale model.

- The three limb single phase shell type transformer was found to be most susceptible core structure to the effects of dc excitation, followed by the three phase five limb and finally the three phase three limb transformer. The latter remained almost unaffected with respect to a rise in its AC peak current and flux leakage.
- While the shell type and the five limb transformers experienced production of even and odd harmonics, the three phase three limb only experienced odd harmonics.

According to this model, three phase three limb transformers are deemed to be insusceptible to the GIC.

2.5.2 Koen and Gaunt (2002)

Koen and Gaunt presented a study on an occurence of the GIC phenomenon and the performance of the Southern African Transmission Network (SATN). After application of a model on the theoretical calculation of GICs in a power network, the authors identified seven substations (see Table 1) in South Africa which had relatively high GICs during the severe storm of 1989 which knocked out an entire power system in Quebec.

Table 1: Substations most susceptible to GICs (Koen & Gaunt, 2002)

Substation	Maximum calculated GIC on 13 March 1989 [A] averaged over 1 minute.
Alpha	108
Hydra	67
Beta	64
Grootvlei	59
Perseus	57
Grassridge	41

A three phase three limb transformer at the Gassridge station was monitored and it was found that between 9 and 10 am on March 31st 2001:

- The transformer current contained higher frequency components whose 2nd and 4th harmonics had a linear relationship which confirms saturation of the core.
- The pronounced 6th harmonic spikes coincided with a relatively substantial GIC dips.
- Reactive power demand of the transformer doubled in that period.

The findings of this three limb three phase transformer appear to contradict the popular belief that such transformers are not affected by GICs as alleged in the study by Takasu *et al*. in the previous sub section. Similar patterns were noted with another transformer on the 6th of November 2001 at the Hydra station. An important result in this study is that there was slight saturation of the core even though the transformer was operating at 10% of its rated value at that time. It was then concluded that load shedding during GIC events may not necessarily prevent saturation of the core. Laboratory testing is therefore necessary in order to verify these findings.

2.5.3 Masoum and Moses (2008)

A detailed nonlinear transformer model was developed by Masoum and Moses (2008) in order to demonstrate the effects of GIC on a three phase three limb transformer. The areas investigated include:

- Different levels of GIC input
- The response of the magnetizing currents
- Transformer additional losses with GIC
- Total Harmonic Distortion (THD) with GIC

It was found inter alia that even under a relatively‘low GIC input’, harmonic losses rose sharply which can stress and overload transformer windings, along with the the magnetizing currents in each phase. These findings once again prove that three phase three limb transformers may be susceptible to GIC damage depending on the level of GIC. For a 1kVA transformer model however, the size of the GICs injected into the neutral (0A, 50A, 100A, 700A) did not appear to be justified considering that the transformer’s full load rated current was 6A/phase. The authors referred to a 50A GIC (approximately 16.7A/phase) as a ‘low GIC input’, which is counter-intuitive given the rated load current. For extremely high GICs flowing into the neutral (>300A), the current THD reached a peak and then fell sharply as the transformer began to operate in its linear air core region above the magnetization curve.

2.5.4 Conclusion

Three cases have been presented in the preceding subsections contrasting findings in literature on transformer response. There are conflicting theories when it comes to the effect of the GIC phenomenon on three limb three phase transformers; saturation being the main variable in question. Moreover, it has been commonly perceived that transformers that are lightly loaded do not get affected by GICs as is the case in the Finnish network (Boteler *et al*., 1998)but Koen and Gaunt’s findings suggest otherwise. These cases will be subjected to testing in the experimental protocol of this study, which is outlined in Chapters 3 and 4. Masoum and Moses present a comprehensive three phase transformer model which brings light to multiple aspects that also require comparison with the laboratory measurements and computer simulations.

2.6 Calculations of Power

The measurement of power is a requires careful consideratrions when dealing with the unbalance and distortion that comes with GICs (Gaunt & Malengret, 2012). All the resulting inefficiences need to be accounted for and the total effect on the system needs to be adequately represented. It has already been pointed in section 2.3.7 that the non-active power demand of transformers increases with GIC and consequently the system efficiencies fall. Some methods of power calculation will therefore be contrasted in this context; namely the conventional power calculation and the general theory of power (Malengret & Gaunt, 2011).

2.7 Computer Simulations

The computer simulations to be performed for comparison with real laboratory measurements will need to be capable of modelling various aspects of transformer core saturation that arises from dc excitation. This requires the accurate modelling of the non-linear characteristics of a practical transformer given the necessary parameters. In their study, Chandrasena, *et al.* (2004), present a hysteresis model that is implemented in an electromagnetic transients program (EMTP) PSCAD/EMTDC. Their work involved the comparison of recorded exciting current waveforms and simulated data in to investigate the losses in a BH loop. Figure 10 shows very good correlation between the recorded and simulated data in PSCAD/EMTDC.

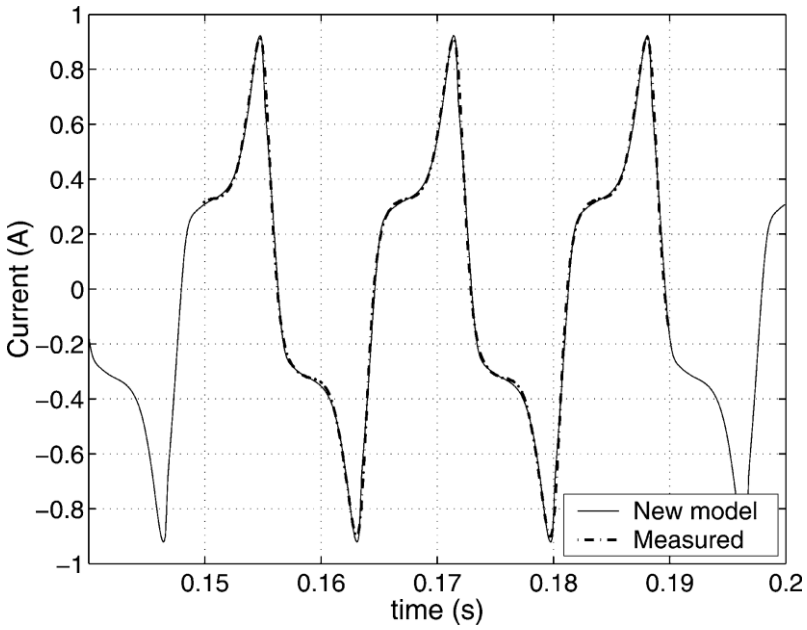

Figure 10: Exciting current of a 3 kVA, 115 V/2300 V, 60-Hz single-phase distribution transformer.

Berge, *et al.* (2011) established a linear relationship between GIC and reactive power in a three phase bank of autotransformers using computer simulations in PSCAD/EMTDC. Measured data was then taken from a Hydro One 230/500kV during a mild geomagnetic disturbance in Canada. Their implanted PSCAD simulation model in was validated by the real measured data. An extension of this work (Marti, *et al.,* 2013) brought about the development of a technique to determine the amount of GIC in a power transformer. This proposed technique was not only found to be consistent with simulations in PSCAD/EMTDC and measured data on a Canadian autotransformer with a dedication GIC monitor during a mild geomagnetic disturbance.

Though no comparisons of measured and simulated data were made in a harmonic analysis study undertaken by Li and Yun (2012), their PSCAD simulation test system

brought about expected results regarding the generation of even and odd harmonics in a power transformer with dc bias.

It is evident from the literature that modelling in the EMTP PSCAD environment has recently impacted research in the understanding of the GIC phenomena. Very few other studies have been undertaken to consistently validate this simulation software especially in the context of GICs and transformers varying in core structure.

This study seeks to develop a simulation protocol in this EMTP simulation software based the laboratory test systems. Real measurements will be recorded investigating various electrical and magnetic responses of transformer with dc and the PSCAD transformer models will implemented based on the laboratory experiments. Consistent results between the real data and computer simulations may lead to more understanding on the GIC phenomenon in transformers of differing core structures and sizes as the validated simulations models may be extended to investigate transformer behaviour that is difficult to test in reality.

2.8 Summary

The literature review on GICs and transformers addressed some of the research questions posed chapter 1. The findings from literature identified the following key points:

- There appears to be a debate when it comes to susceptibility to GIC as a function of core type. Takasu *et al.*'s model (1994) states that three phase three limb is not susceptible to GIC damage but Koen and Gaunt's (2002) findings from a Grassridge transformer prove otherwise. Later on, Masoum & Moses (2008) yielded results from a three phase three limb transformer model that also brought about significant harmonic distortion and saturation of the core.

- There are conflicting ideas between the Boteler *et al.* (1998) study which stipulates that Finland's lightly loaded transformers rarely experience problems from GICs despite its high susceptibility to GMDs, whereas Koen and Gaunt (2002), and later on Li & Yun's (2012) reported from their findings that even a lightly loaded transformer close to no load conditions may be driven to saturation during a geomagnetic disturbance.

- There are two approaches to measuring apparent power and non-active power under non–ideal conditions: (a) the IEEE 1459-2010 conventional approach and (b) the general power theory as defined by Malengret and Gaunt (2011) in their two companion papers. These differences will be investigated in the context of GICs and transformers.

- While there may have been some debate with regards to GIC damage and loading conditions or GIC damage and core type, there has been good agreement in literature with regards to the reactive power absorption of transformers under dc excitation. For instance in 1993, Albertson *et al.'s* study suggested that GIC disturbances increase the reactive power consumption of transformers. Later on, in their studies, Molinski (2002) and Berge *et al* (2011) identified a linear relationship between reactive power consumption and the level of GIC. This relationship will therefore be investigated in the experimental and simulation procedures.

- Thomson *et al*.'s (2010) interdisciplinary study on the present knowledge of the GIC effects and future recommendations points out the need to identify:

  "...the characteristics of power transformers that determine their susceptibility to GICs and therefore determine the extent of damage sustained under different levels of GICs".

  There has yet to be a standard for classifying different magnitudes of a GIC based on the characteristics of a particular transformer. This has resulted in some transformer studies involving levels of GIC imposition that seem to be arbitrary or not properly justified relative to the size of the transformer making it difficult to characterize the response in a way that will be useful to a power utility whose MTS has a transformers of differing core types. Introducing a standard scaling system that relates the magnitude of the GIC, some key parameters of transformers of different core structures, and then generates the expected response may be useful particularly in control centres for mitigation. The experimental protocol in this study seeks to investigate the generation of such relationships.

3 REQUIREMENTS FOR LABORATORY TESTING

It is clear from the literature review that transformers are the major component of power systems affected by GIC, and will therefore be the main focus of the rigorous testing procedure. There are two laboratory environments that will be used in this investigation:

(a) A bench-scale test system involving transformers of differing core structures (900VA, 300VA – 120/230V). This is the platform on which the testing protocol is to be developed and implemented. Most aspects of the investigations in this study will be addressed in this environment.

(b) Based on (a), the developed methodology will then be implemented on a three phase medium scale test system (48kVA). The purpose of this procedure is to test the applicability of the developed protocol on higher capacity transformers. The transformers will be subjected to carefully selected levels of dc according to the protocol, and the results will be used to analyse their response.

However, before the test systems can be developed a knowledge base on the behaviour of different transformers under dc excitation, along with the related research skills needs to be developed. Having done an extensive survey of literature reports (*vide supra* 'Literature Review'), it is apparent that the characterization of transformers by means of laboratory testing is of considerable value in GIC, power delivery and power systems studies. Moreover, the overall behaviour of a power system under GIC attack can be assessed more accurately if the induced level of GIC and corresponding transformer response characteristics are well known. Against this literature review, there will be an attempt to answer the research questions in a laboratory and simulation environment.

Firstly, a rigorous laboratory testing procedure is to be developed for testing transformers with GIC-like currents. This protocol should satisfy the working conditions of the laboratory and will not only be based on generic methods available in open literature, but also on the skills developed during the investigation. A simulation protocol based on the actual laboratory tests will then be developed and implemented for comparison with measured results.

Measurement and calculation methods that are in compliance with the most up to date power calculation conventions are to be used. For instance, in earlier experimentally based studies (Amuanyena & Gaunt, 2002; Dlamini, 2008), the measurement apparatus that was used to measure the reactive power demand and harmonic content in laboratory GIC tests was not clearly documented to have met the criteria set by the *IEEE 1459-2000* standards or *IEC-76* convention. Online calculations along with the post processing of relevant waveform data are to be undertaken in order to rigorously meet not only these standards

but the new method proposed by Malengret and Gaunt (2011). Precise measurements conditions including the details of the models will have to be given.

3.1 Relationship between GIC, Reactive Power and Non-Active Power

One of the most important indicators of the effect of GIC flow in power systems is the increased demand of *Q* power by grounded power transformers. In their studies, Molinski (2002) and Berge *et al.* (2011) reported a linear relationship between absorbed reactive power and GIC in a transformer by means of field measurements, PSCAD/EMTDC simulations and laboratory test systems, respectively. When a transformer is under dc excitation, saturation occurs on one half of the AC cycle causing the draw of relatively large amounts of asymmetrical magnetising current. This I_{mag} lags the system voltage by 90° which causes reactive power losses. This relationship between GIC and the differences between reactive and non-active power are to be investigated. This procedure is described in the following sections.

3.1.1 *Comparison of approaches to Q*

When extreme disturbances such as severe GMDs occur, the threats posed to the power networks are often very complex and measurement conditions begin to play a key part in condition monitoring and mitigation. The methods used for calculating important aspects during such events like apparent power and harmonic distortion have to be compliant with the most up to date IEEE and/or IEC conventions. For this reason, two methods of calculating power were compared namely: (i) the conventional power theory, and (ii) the general power theory.

Gaunt and Malengret (2011) in two companion papers did a rigorous study of the progression and development of all the power theories, and identified their limitations and specific conditions in which adequate power calculations could be obtained or not obtained. A general theory of power was then developed whose formula is derived through the properties of linear algebra and vector space for a system with any number of wires/phases taking into account the losses in the neutral wire (if there is a neutral). Unlike the conventional power calculation where ideal conditions are assumed, and in most cases this may be adequate, the general power theory is applicable to a system with distortion, unbalance and direct current components. The subsequent sections contrast the differences between the two approaches to calculating *Q*.

3.1.2 *Conventional Calculation of Power*

Instantaneous power in to a load is given by the sum of the products of the instantaneous voltages and currents in each phase over one period and is represented by the equation below:

$$p(t) = e_a(t).i_a(t) + e_b(t).i_b(t) + e_c(t).i_c(t) \quad (3.1)$$

Where *p(t)* is the instantaneous power, and *e(t)* and *i(t)* are the instantaneous values of the voltage and current in each phase subscripted *a, b* and *c.* All the instantaneous phase voltages are measured with respect to a common neutral. The real power *P* is given by the average of the instantaneous power *p(t)* over one cycle. The apparent power *S* is then calculated by taking the root mean square (r.m.s) values of the currents and voltages in each phase over one cycle and this is represented by the equation below

$$S = E_1I_1 + E_2I_2 + E_3I_3 \quad (3.2)$$

where *E* and *I* are the r.m.s values of *e(t)* and *i(t)* respectively over a whole cycle. The power factor, which is a measure of efficiency of the transfer of energy along the line, is given by the ratio *P/S*. The angle between the current and the voltage is denote by *φ* ; and this is the power angle. The reactive power is then calculated using:

$$Q^2 = S^2 - P^2 \quad (3.3)$$

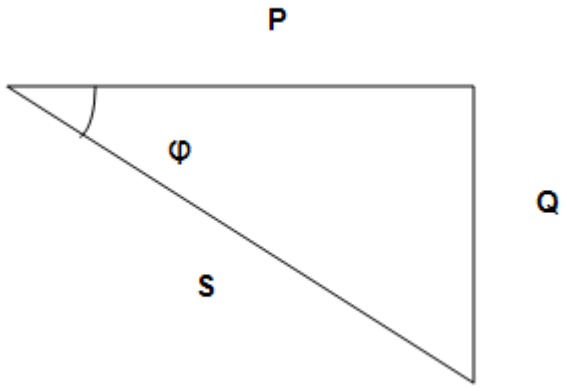

Figure 11: The power triangle representing real power *P*, apparent power *S* and reactive power *Q*.

A study on why we use the term non-active power was done by Gaunt and Malengret (2012); expounding on the concepts of unbalance and distortion with regards to *Q*. This study brings to light the introduction of the distortion power concept as it was realized that the distortion that comes *Q* may be split into two categories: “the reactive power that was associated with inductive or capacitive reactance, and the distortion power with the inefficiency introduced by unbalance and harmonic distortion.” This model of *Q* however does not account for all the non-ideal conditions consistently because the relationship between reactive power and distortion power is not uniquely defined in a mathematical manner.

3.1.3 *General Power Theory*

The work leading up to the general power theory (Malengret & Gaunt, 2008; Malengret & Gaunt, 2011; Malengret & Gaunt, 2011) showed that the components of non-active power can be separated into the part that can be compensated between the wires without energy storage and the part that requires energy storage. These components are not only orthogonal to each other but also are orthogonal to the real power; thus making the apparent power now uniquely defined. Consequently, this brings about a three dimensional power triangle as shown in Figure 12.

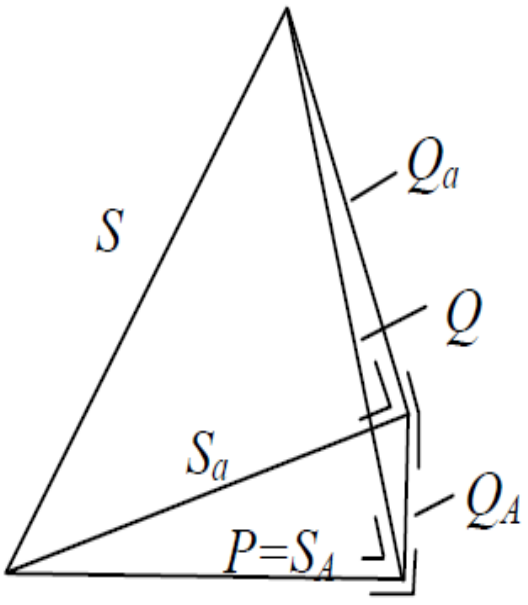

Figure 12: Complete power triangle, in which *Q* = total non-active power, where Q_a is the component that can be compensated without energy storage and Q_A the component that requires energy storage for compensation. S = apparent power without any compensation, S_a the apparent power after compensation without energy storage , and S_A the apparent power after complete compensation so that $S_A = P$ (Gaunt & Malengret, 2012).

Considering a three phase system with a neutral, where the resistances in each phase are equal ($r = r_1 = r_2 = r_3$) and the neutral resistance (r_n) is not necessarily the same, such as the one in the laboratory set up (see Figure 13), the methods of the developed general theory may be demonstrated in equations 3.4 to 3.8 below. Since the losses in all the wires are accounted for, including the neutral, the neutral current is required and may be calculated from the instantaneous values using Kirchhoff's Law:

$$i_n = -(i_1 + i_2 + i_3) \tag{3.4}$$

where i_1, i_2, i_3 are the phase currents and i_n is the neutral current. The first step is to calculate the resistance-weighted square of the currents:

$$||\boldsymbol{i}'||^2 = (i_1^2 + i_2^2 + i_3^2 + \frac{i_n^2 r_n}{r}) \cdot r \tag{3.5}$$

where $||\boldsymbol{i}'||^2$ is the resistance weighted norm of the current. The resistance-weighted reference for the voltages for all the sample points is then calculated using equation 3.6 and from this, the weighted norm of the instantaneous voltages is calculated (equation 4.8):

$$e_{ref} = \frac{(e_1+e_2+e_3)}{3+\frac{r}{r_n}} \tag{3.6}$$

$$||\boldsymbol{v}_2'||^2 = ((e_1 - e_{ref})^2 + (e_2 - e_{ref})^2 + (e_3 - e_{ref})^2 + (0 - e_{ref})^2 \cdot r/r_n)/r \tag{3.7}$$

The apparent power is then calculated using the resistance-weighted norms of the voltages and currents:

$$S = ||\boldsymbol{V}_2'|| \cdot ||\boldsymbol{I}'|| \tag{3.9}$$

The above equation is implemented by integrating the sampled values over an integral number of with $||\boldsymbol{V}_2'||^2$ being the average over one cycle of $||\boldsymbol{v}_2'||^2$ and $||\boldsymbol{I}'||^2$ that of $||\boldsymbol{i}'||^2$. The delivered real power P does not change and may be calculated using the conventional approach or by taking the product of the instantaneous voltages and currents. The total non-active power *Q* may be calculated using the same Pythagorean relationship described in equation 3.3.

3.2 Purpose of Study

Above is a detailed description of some of the important aspects involving power calculations under conditions with distortion, unbalance and dc components of current such as those imposed by GIC. Overall, this study seeks to investigate/address the following key subject matters:

1) Ensure adequate measurement of voltages and currents for online and offline processing (electrical response)
2) Developing a testing method and characterizing the transformers specifically to the aspects of investigation.
3) Based on 2) determination of adequate levels of dc injection in the context of core saturation studies, along with a rigorous determination of simulation parameters.
4) Recording and monitoring of the electrical and magnetic response of the various test transformers.
5) From 3) developing a simulation protocol in an adequate simulation environment for testing transformer models comparable to the laboratory transformers for the effects of dc excitation.
6) Based on 4) and 5) interpreting the results, discussing the relevance of the findings, and drawing conclusions based on these findings.

Having surveyed literature it was found that reported transformer tests often lacked detailed methodologies, the justifications for the sizes of the GIC inputs, the magnetization parameters of the transformers in question and so on; with the emphasis of the studies being mainly on findings and conclusions. This limitation unfortunately makes it difficult to rigorously compare some reported transformer responses against others. For instance, it is possible to compare the response of two transformers of a similar core structure but having completely different rated voltages and capacities by putting the important parameters (which will be brought to light in this report) into the per unit domain. Doing this gives a much clearer picture on the effect that the relative imposed GICs have on particular transformer types; but all these important parameters need to be known and clearly defined.

It is the relationship between reactive power and GIC that is often reported in literature when characterizing the electrical response of power transformers. However, it is clear that the non-ideal conditions introduced by GIC make it necessary to consider how the non-active power demand may differ from the conventionally calculated reactive power. This difference may have significant implications with regard to the perception energy transfer capacity across power networks.

4 LABORATORY PROTOCOL

A preliminary investigation into the effects of GICs on transformers was undertaken at a bench-scale level using a system of three phase banks of single phase shell type units. Having developed a suitable test protocol based on system, more laboratory tests ensued with comparable transformers of differing core structures. An additional application of the protocol will be demonstrated in a system of 48kVA LV transformers that were available in the UCT laboratory.

4.1 Introduction to Laboratory Protocol

The bench scale test system involved two three-phase transformers with three single-phase units each. This is commonly referred to as a three phase bank or a bank of three phase transformers. A three phase variable power source was connected to the source transformer which supplied power to the load transformer. The harmonic profile of the supply voltage was checked for compliance with the IEEE Std. 579-1992 convention (Blooming & Carnovale, 2006) to ensure that it did not have a THD that exceeded 5%. The source transformer was chosen to be significantly larger than the load transformer so that the dc injection levels based on the load transformer characteristics would have a negligible effect on its magnetization characteristics.

The transformer nameplate ratings were as follows:

- Source transformer: 900VA (300VA per phase), 120/230V
- Load transformer : 300VA (100VA per phase), 120/230V

Further information was needed before the commencement of the experimental procedure as all that was known about the transformers at the time was their nameplate ratings (above). Test certificates from the manufacturer were not available. Various basic transformer tests were then done in order to generate important parameters that were relevant to the investigation. These tests will be described in subsequent sections.

4.2 Purpose of experiments

In the development of the protocol, the purpose of the laboratory test system was to emulate a GIC event that occurs in archetypal high voltage power transmission networks. Such a system typically involves a generator step-up transformer, transmission lines and a load transformer connected to the resistive load. In this protocol, it was important for the source transformer to be significantly over-rated in terms of capacity (VA rating) and voltage so that the dc that would be injected as a function of the much smaller load transformer characteristics would have a negligible effect on its magnetization characteristics. This way, the test transformer of the system would automatically become the smaller load transformer.

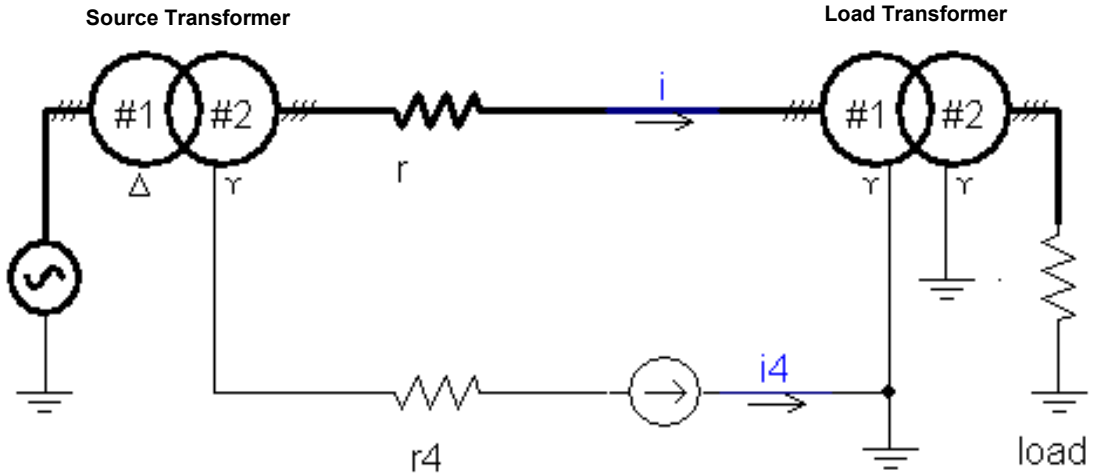

Figure 13: Simplified single phase diagram of the conceptual laboratory arrangement. Direct current is injected in the load transformer neutral. The load transformer is the test transformer.

4.3 Magnetization Curve

The nameplate voltage ratings of the transformers were 120/230V. In order to accurately model the actual laboratory set-up in a simulation environment a better understanding of the relationship between the nameplate ratings and the regions of the magnetization curve was needed. Therefore, a brief procedure of basic tests was undertaken: Having ensured a clean or 'low distortion power supply (Blooming & Carnovale, 2006), the applied voltage was slowly varied from zero to 120% of the name-plate rating at no load and the corresponding input current *i* and output voltage *v* values were recorded for each transformer. These *v* and *i* values were then used to plot the magnetization curves for the transformer cores of each transformer. Figure 14 shows the magnetization curve of one single phase transformer in the three phase transformer bank.

The knee point voltage of each transformer was selected to be the point where a straight line drawn from the origin is tangent to the curve at it knee, representing maximum

permeability, as defined by McLyman (2004). This point defines the 'true' linear region of the transformer core steel. Using this method, the knee point voltage of each transformer, V_{knee}, was then determined. V_{knee} for the load transformer is at 33.3% below the name plate rating with a magnetizing current, I_{mag}, of 55 mA (See Figure 14). Perhaps for economic reasons, these transformers were designed to operate close to and into their saturating region and hence their name plate ratings were found to represent over-excitation. The new transformer ratings were chosen based on the magnetization curve of each transformer (see Table 2).

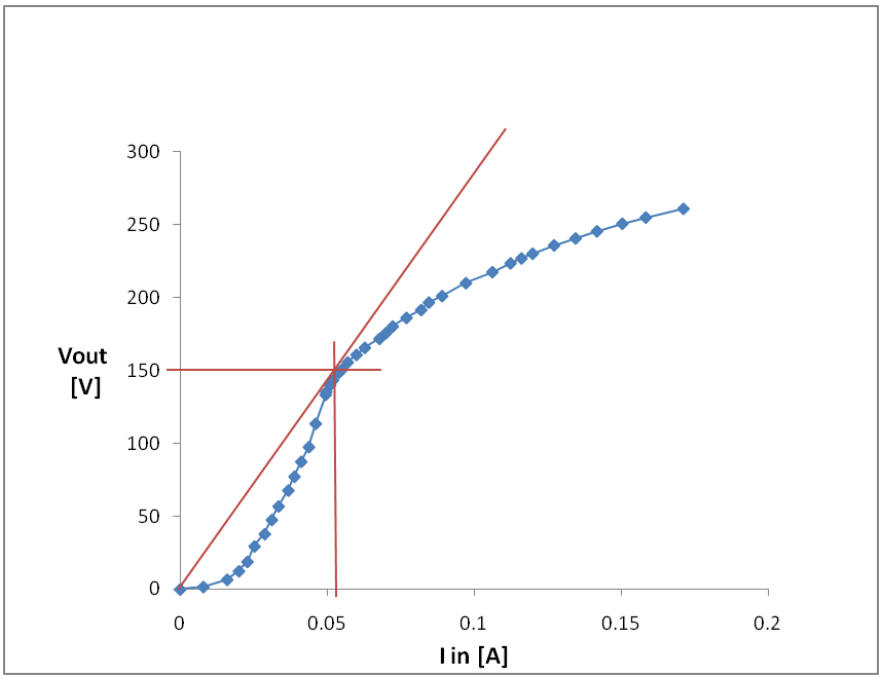

Figure 14: Magnetization curve of the load transformer core (one phase). The knee point voltage appears to be 0.66 p.u. of the nameplate rating.

Table 2: New transformer ratings (per phase) based on the transformer's knee point voltage

Transformer	New voltage rating per phase	Operated as
Source	80/150 V	42/80 V
Load	80/150 V	80/150 V

A very important result from the curve above is the value of the magnetizing current I_{mag} at V_{knee}. This value (approximately 55mA for the load transformer) which effectively separates the linear region from the non-linear region was then used as a guideline for the amount of dc to inject into the neutrals of the transformers to monitor pre- and post-distortion conditions in the load transformer.

4.4 Open and Short Circuit Tests

As can be seen in Figure 14, the nameplate rating of these transformers represented over-excitation. Therefore it was important to establish a new rating for the transformers (see Table 2). An open circuit (O.C.) test was used to determine the shunt resistance and inductance elements R_c and X_c, while a short circuit (SC) test was used to determine the series impedance elements R_L and X_L. These tests and their underlying principles are discussed in detail in Sen(1997). The modeling of the test system was then done in PSCAD using these parameters. The parameters generated from the O.C. and S.C. tests can be found in Appendix *A1*.

4.5 Varying Load Tests

The effect of applied voltage at different loading conditions on reactive power had to be verified in the preliminary tests. This was done by varying the load at a constant voltage and monitoring the response of the transformer. Graphs of input power P_{in}, applied voltage V_{in}, absorbed reactive power Q_{in} versus a varying loading condition, represented by R_{load}, were plotted and examined .On the same axis, a graph of the output conditions was also plotted and examined (P_{out}, V_{out}, Q_{out} versus R_{load}).

After a series of tests it was shown that the increase in Q_{in} absorbed by the transformer is a function of the applied voltage and is independent of the resistive loading conditions. Below is a per unit graph of the transformer response at a 1.0 p.u. voltage (80/150 V based on the magnetization curve). R_{load} is varied as a percentage of the maximum loading condition R_{load} max i.e. varied from approximately 55% to 100% of the full load (based on its name plate VA rating of 300VA or 100VA per phase).

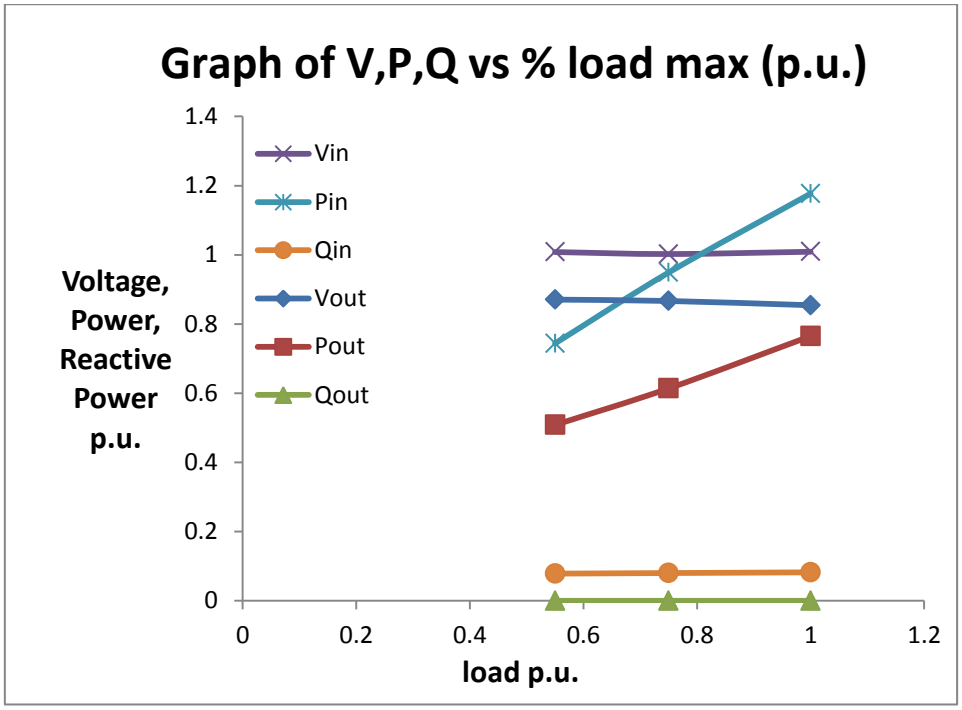

Figure 15: Per unit graphs of voltage, power and non-active power against varying load conditions. Please note that an input voltage V_{in} of 1 p.u. is applied here resulting in an absorbed reactive power Qin of about 0.1 per unit.

4.6 Setting up of dc injection circuit

The purpose of the injection circuit was to simulate the quasi-dc GIC that typically flows in an HV power transmission network (PTN). The question of dc injection magnitudes was approached with extreme caution and careful consideration. The magnitudes of dc injection were chosen so as to start injecting a small percentage of I_{mag} of the TuT and increase it in small steps, while monitoring the response. Such small magnitudes of dc could easily be realized by using a 1.5V torch cell as the dc source, though careful considerations would have to be made in terms of the level of neutral current and the impedance of the torch cell.

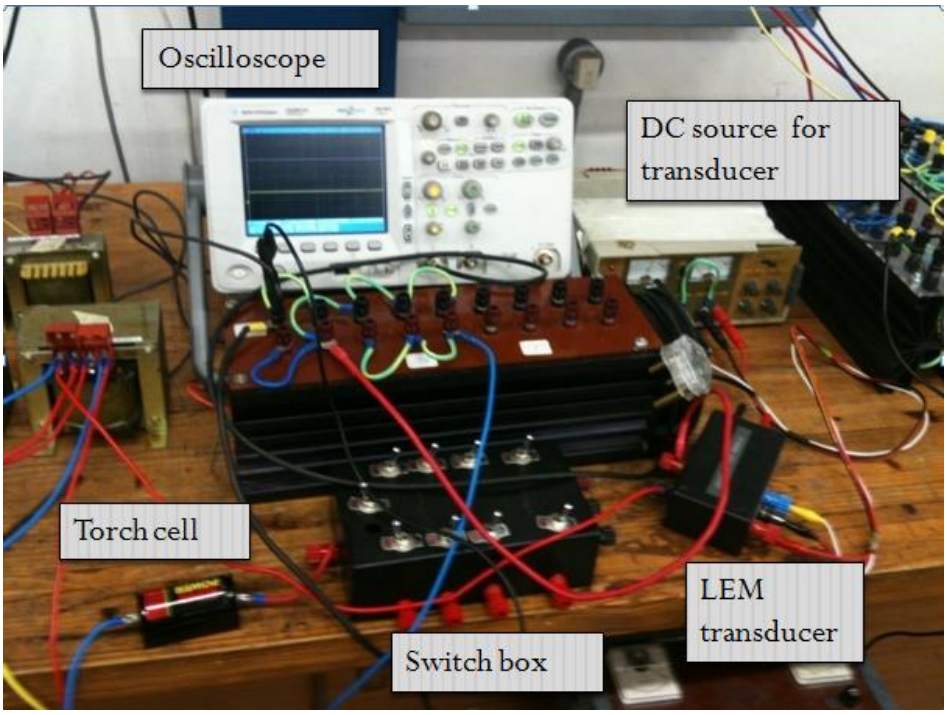

Figure 16: Laboratory set up of DC injection circuit

It was suspected that should there be a significant unbalance in the three-phase neutral as a result of the dc injection, there may be a relatively large AC component that would flow through the non-rechargeable torch cell bringing about detrimental effects. It was reasoned that should this neutral current be above a certain threshold, which is a function of the batteries physical properties and chemical composition, then the AC components might aggravate the battery and eventually damage it. After a series of tests, and careful monitoring of the neutral currents, it was however realized that the circuit was adequately balanced with a very small neutral AC component in the presence of dc.

Another important consideration in the circuit was determining the impedance of the battery. Realizing that the torch cell's internal impedance would contribute to the neutral resistance R_n implied that it had to be quantified. It was imperative to keep track of the neutral resistance as two power calculation theories would be contrasted in a brief comparative study later in the study: (a) The Conventional Power Theory which does not take into account losses in the neutral, and (b) The General Power Theory (Malengret & Gaunt, 2011) which takes into losses in the neutral.

Table 3: Presented are the values of the resistances used for the voltage divider to act on the torch cell in order to achieve different levels of dc in one of the test systems. R1 includes the battery impedance and R_{eq} represents the Thevenin equivalent impedance as seen by the transformer neutrals. The total neutral resistance denoted by R_n.

Experiment	R1 (Ω)	R2 (Ω)	R_{eq} Thev DC(Ω)	DC/phase (mA)	Rn(Ω)
DC0	--	--	1.1	0	1.1
DC1	5.3	1.4	1.2	20	1.2
DC2	5.3	2.7	1.8	30	1.8
DC3	5.3	5	2.7	40	2.7
DC4	3.6	5	2.2	54	2.2
DC5	2.7	5	1.9	64	1.9
DC6	2.2	5	1.7	72	1.7
DC7	1.7	5	1.4	82	1.4

A voltage divider was used to vary the voltage across the neutrals of the transformers, effectively varying the amount of dc injection. Since the neutral resistance was important in the power calculation comparative study, the Thevenin equivalent resistance of the torch cell and the voltage divider as seen by the transformer neutrals was used to determine a value for R_n. This value was then used to account for losses in the neutral wire when calculating apparent power according to Malengret and Gaunt (2011) (see Table 3). The Thevenin equivalent resistance as seen by the transformer neutrals is also given in the same table. An important aspect to note in this table is that R_n was smaller than each transmission line resistance r so as to mimic most real HV systems.

4.7 Laboratory set up

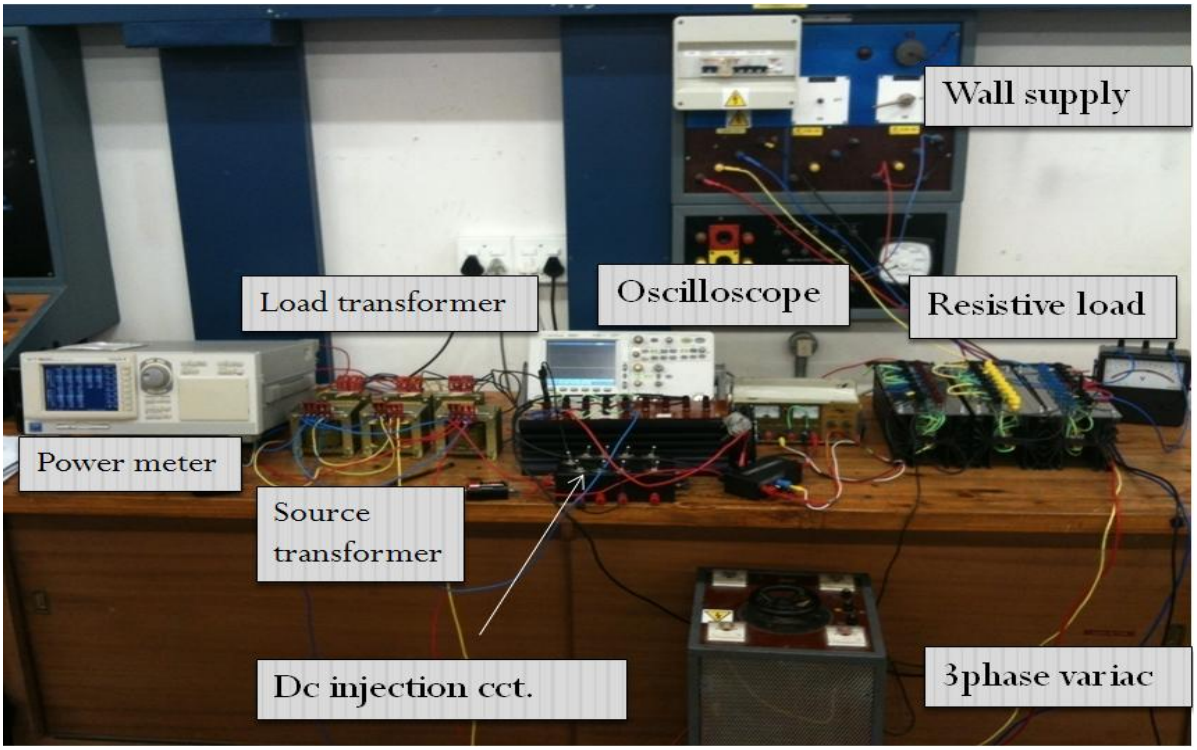

Figure 17: Full laboratory set up

Figure 17 shows the full laboratory test system that was used for the preliminary investigations. Voltages and currents were measured by an IEC76-1 (1976) compliant Yokogawa WT1600 Digital Power Meter. The meter is capable of performing online measurements and also has a facility whereby the instantaneous values of the voltage and current waveforms can be recorded and stored for post processing. Fast Fourier Transforms were done up to the 10^{th} harmonic (500 Hz). Samples were taken over two and a half cycles within a resolution of 1002 readings (20.04 kHz), more than satisfying the Nyquist criterion. The neutral current could easily be calculated by application of Kirchhoff's laws during post processing. Other measurements required external circuitry and were monitored using a

high resolution Agilent 6000 series oscilloscope. The transformers supplied power to a balanced bank of power resistors for each loaded experiment. The supply voltage to the source transformer was a 6kVA, 380 V three phase variac from the wall supply. It was ensured that the supply voltage was compliant with the IEEE Std. 519-1992 on harmonic limits. This convention defines a ‘clean’ or ‘distortion-less’ voltage supply as one having a total harmonic distortion (THD) of less than 5%.

5 TESTING PROCEDURE AND SIMULATION PROTOCOL

The work leading up to the end of the previous chapter brought about the development of a rigorous knowledge base that enabled further testing of the bench transformers for their electrical and magnetic response.

The laboratory test system conditions were as follows:

- Clean three phase wall supply
- Source transformer name plate rating 120/230V, 900VA, delta-star
- Load transformer (TuT) name plate rating 120/230V, 300VA, star-star
- 1 p.u. is 80/150 V with a corresponding VA base of 200VA for the load transformer. The same load current as per the name plate rating will still be delivered to the load.
- Resistive load representing 70% of the full load capacity of load transformer
- Yokogawa power meter for measurements for ac voltage, ac current, power, apparent power and reactive power, dc current.
- dc injected as a percentage of the magnetizing current of the load transformer
- Both source and load transformer were grounded at a common neutral point

As previously mentioned, the transformers were set up in such a way that the source transformer would never operate in the region that represents saturation. This was to be verified in more detailed investigations involving analytical definition of saturation, harmonic distortion and the nature of the hysteresis loops of each transformer.

5.1 Bench Transformer Test A – *A Preliminary Investigation* (0-2 p.u. dc injection)

The injected dc levels were a function of the magnetising current I_{mag} of the load transformer based on the rationale outlined in *Chapter 4.* The source transformer (mimicking a generator step-up transformer) was deliberately over-rated in the sense that as it supplies power to the load transformer not only will it be three times its VA rating but it would also be operating well below its knee point voltage. This way, the injected dc should have a negligible effect on its magnetization characteristics whose operation point will be well below its knee point. It was important to verify the immunity of the source transformer by means of an analytical method when the system was subjected to various dc levels (section 5.1.1).

5.1.1 *Analytical Determination of Saturation*

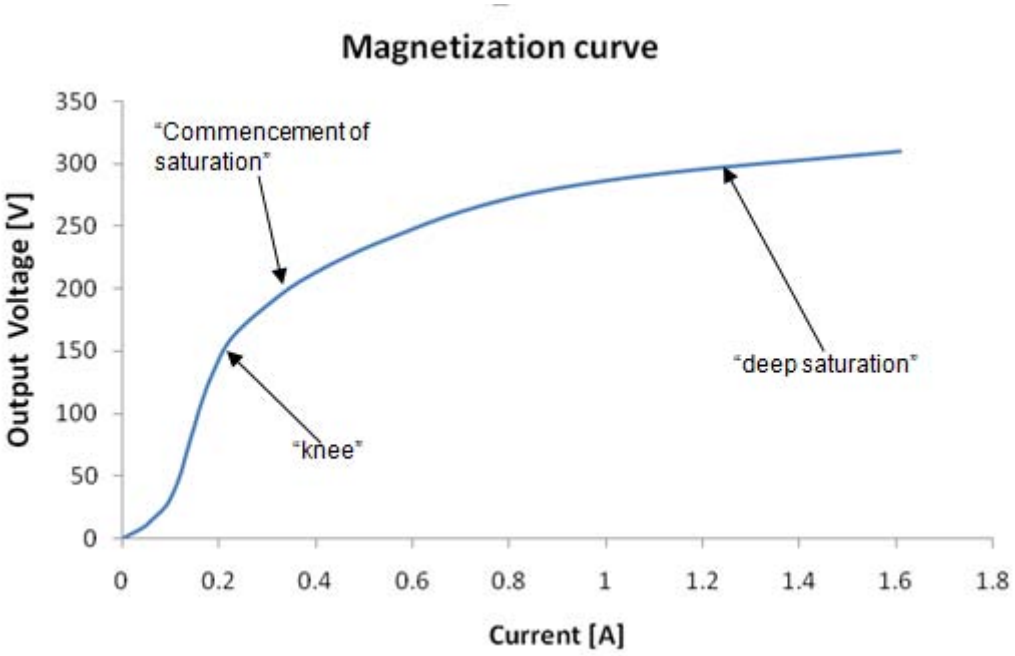

Figure 18: Diagram representing the different levels of saturation based on the source transformer's magnetization curve (measured from the laboratory)

On the issue of saturation it is important to consider the differences between the linear region, the commencement of saturation and 'deep' saturation (see diagram above). The 'knee' is chosen as explained in chapter 4, and the commencement of saturation is chosen analytically as will be described in this section. The concept of 'deep' saturation will be discussed later in the context of extreme levels of dc injection. Using several unique points on the *BH* loop and arriving at a rigorous analytical solution, McLyman (2004) concluded that:

"Saturation occurs when the peak exciting current is twice the average current."

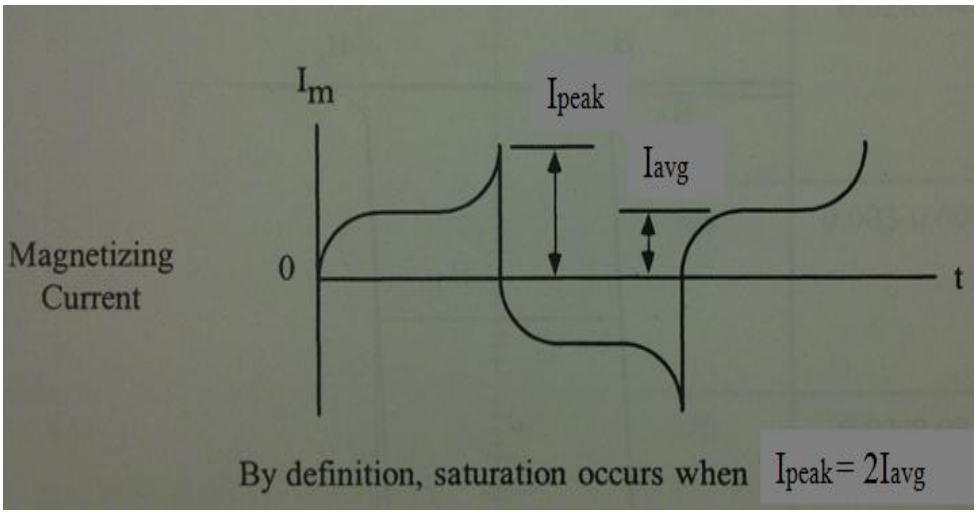

Figure 19: Diagram illustrating how saturation can be calculated using the exciting current waveform (McLyman, 2004).

Figure 19 may be summarized using the following formula:

$$I_{peak} = 2 \cdot I_{avg} \tag{5.1}$$

Where I_{peak} is the peak exciting current and I_{avg} is the average exciting current. This equation signifies the point at which saturation *starts* to occur and not necessarily full saturation or 'deep' saturation.

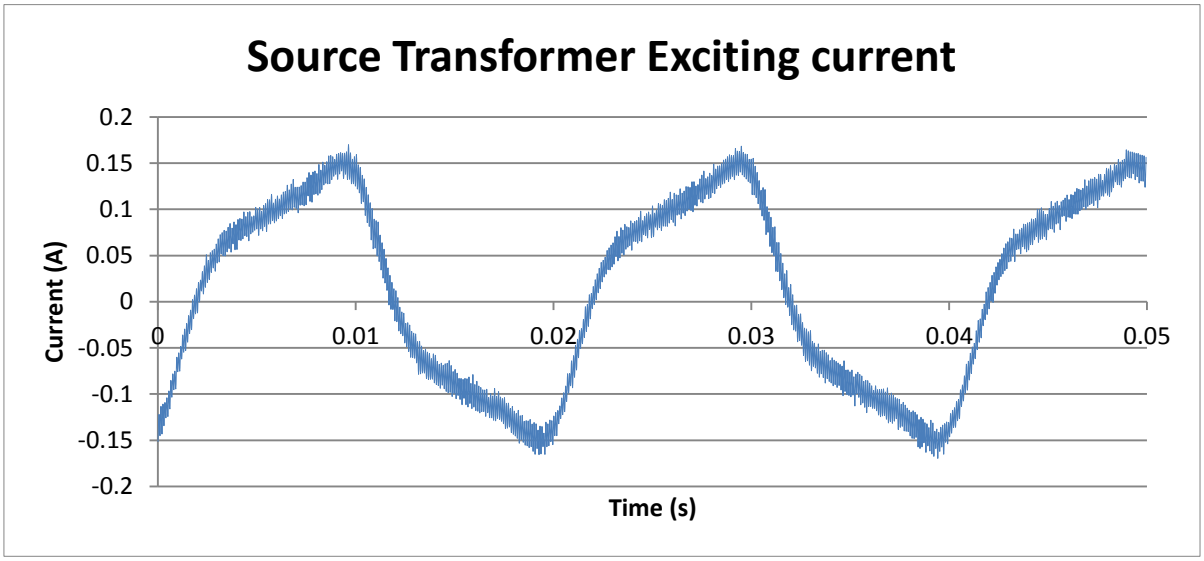

Figure 20: The exciting current waveform of the source transformer in the red phase measured by the Yokogawa power meter. The numerical waveform data is used to calculate I_{peak} and I_{avg}.

Practically, this theory was applied by taking the numerical waveform of the source transformer's magnetising current (see Figure 20 above) for each instance of dc imposition, and then calculating the average exciting current using equation 5.2:

$$I_{avg} = \frac{(I_0 + I_1 + I_2 + \cdots + I_n)}{n} \quad (5.2)$$

Where *n* is the last sample point at or just before the zero crossing of the positive half cycle. The peak magnetizing current was then calculated by means of a 'max' function for the *n* sample points. Finally a condition statement was used to determine whether the criterion in equation 5.1 had been reached or not. Results from a varying dc injection test are tabulated in Table 4. Dc levels ranged from 0 -1.3 per unit of I_{mag} denoted DC0 – DC7. It can be seen from the table that saturation did not occur in the source transformer at any time as expected.

Table 4: Table indicating whether saturation occurs or not in the source transformer.

Exp	I_{avg} (A)	$2*I_{avg}$(A)	I_{peak}(A)	Saturated?
DC0	0.093	0.186	0.160	no
DC1	0.097	0.194	0.178	no
DC2	0.100	0.200	0.195	no
DC3	0.103	0.206	0.194	no
DC4	0.105	0.210	0.202	no
DC5	0.113	0.226	0.223	no
DC6	0.130	0.260	0.256	no
DC7	0.138	0.276	0.273	no

The generation of the magnetization curves of the source transformers revealed that their nameplate ratings represented over-excitation. This was further validated by use of McLyman's rule of thumb at the transformers knee voltage (80/150 V) and nameplate voltage (120/230 V). The results are shown in Table 5 below.

Table 5: Table showing whether saturation had occurred or not in the transformers at V_{knee} and V_{rated}

Transformer	Voltage	I_{avg} (A)	$2*I_{avg}$ (A)	I_{peak} (A)	Saturated?
Source	V_{knee}	0.093	0.186	0.162	no
Source	V_{rated}	0.210	0.420	0.461	yes
Load	V_{knee}	0.058	0.117	0.113	no
Load	V_{rated}	0.125	0.250	0.295	yes

5.1.2 *Effect of Applied Voltage on Q*

A series of tests concluded that the reactive power, absorbed by the TuT is a function of the applied voltage and is independent of the resistive loading condition (see section 4.5: *Varying Load Tests*). For this reason, the experiments that were then to be conducted would be at an arbitrary loading condition of 70% of the full load (resistive). The aim of the experiment in this part of the protocol was to verify the power curve relationship between applied voltage and the reactive power, alongside varying levels of dc. Therefore the following procedure was undertaken:

- Using a 70% resistive load, vary the applied voltage from 0.4-1.5 per unit
- At each applied voltage level inject a range of dc values from 0-1.5 per unit of I_{mag}
- Record values for Q
- Plot the *Q*-*V* curves for each level of dc injection on the same axis
- Determine whether the transformers exhibit the expected power curve characteristic ($Q \propto V^2$)

5.1.3 *Power Calculations*

In preparation for the experiments that were to be carried out during the study, whereby non-ideal conditions were expected, a power calculation comparative analysis was undertaken in order to determine the most adequate method for calculating power. Chapter 3 discussed the differences between the terms reactive power and non-active power as identified by Gaunt and Malengret (2012). An experimental procedure was then undertaken to contrast the two approaches to calculating power. Using the set-up in Figure 13 and the measurement conditions described in chapter 4, the two power theories were contrasted. The injected dc ranged from 0*Imag - 1.6*I_{mag}. Numerical waveform data for three voltages and three currents from the primary side of the load transformer was recorded for each experiment varying in dc levels of injection. These data were then processed off-line to calculate the conventional reactive power conditions (described in section 3.1.2), and the non-active power (section 3.1.3).

5.1.4 *Hysteresis Loops and theory*

In section 5.1.1, two very important results were observed: (a) the source transformers imperviousness to dc levels relative to the test transformer's I_{mag}, and (b) the chosen knee point voltage did not represent distortion conditions. In this section, the hysteresis loops of the transformers will be studied under various conditions.

The permeability *μ* of a magnetic material is defined by the ratio of the flux density *B* to the magnetizing force *H*. The relationship between *B* and *H* is non-linear because the permeability varies as the Weiss Domains align themselves along an external field. This non-linear *B-H* relationship may be analysed in a hysteresis loop.

When a current *i(t)* flows through the primary windings of a transformer of *N* turns and a geometric length *l*, an auxiliary magnetic field *H(t)* is generated (Sen, 1997).

$$H(t) = \frac{N_1}{l} \cdot i(t) \tag{5.3}$$

Faraday's law stipulates that when there is a changing magnetic field in the secondary windings of a transformer, then the induced voltage $V_2(t)$ isproportional to the rate of change of flux *φ* and the number of turns N_2 in the windings:

$$V_2(t) = N_2 \frac{d\varphi}{dt} \tag{5.4}$$

Where *φ* is the product of the magnetic flux density *B(t)* and the cross section area *A* of the core. *B(t)* can therefore be determined by integrating both sides of equation (5.4), and practically by tapping off the induced voltage $V_2(t)$ and integrating it with an *RC* circuit *(R>>1/ωC)*. This is how the measurements of the BH loops were done in the laboratory.

Considering an initially unmagnetized core, if *H(t)* is increased by increasing the current with time, the flux density will change according to the magnetization curve to the point *a* (see Figure 21). If *H(t)* is slowly decreased, the BH curve follows a different path to B_r where *H(t)* is zero and the core has residual flux density. If *H(t)* is now reversed in polarity the flux in the core decreases for a particular value – H_c (coercive force) and the residual flux B_r will have been brought to zero. Further increasing *H(t)* in the reverse direction causes B(t) to increase in the reverse direction. If *H(t)* is decreased to zero and then increased to the point H_1, the BH curve will follow e, f, g, a'. After a few cycles of magnetization the loop closes and it is called a hysteresis loop. The size of the loop is proportional to the hysteresis losses that occur during a cycle of variation of H(t).

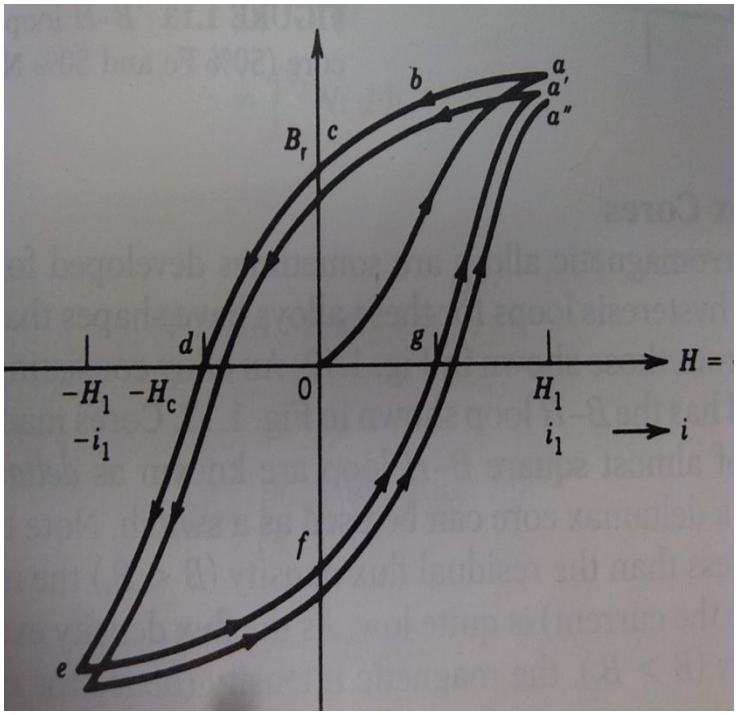

Figure 21: Magnetization and hysteresis (Sen, 1997).

The hysteresis loop that is plotted using *i(t)* and the integral of $v_2(t)$ is not a direct representation of the actual magnetic state of the transformer core. It is however a good approximation of the hysteresis loop obtained through data that are proportional to the magnetic flux density and magnetic intensity.

5.1.5 *Harmonic Analysis*

It is important to distinguish between voltage harmonics and current harmonics (Blooming & Carnovale, 2006). For voltages the levels of distortion are represented by the Total Harmonic Distortion (THD). After a series of tests with dc as a fraction of the magnetizing current, it was seen that the voltage waveforms of the TuT were unaffected by this moderate dc. It was ensured that the initial conditions were as close to ideal as possible in terms of the levels of distortion and balancing the voltages. The tests performed on the load transformer were at no load.

Therefore for current waveform analysis at a light loading configuration, total demand distortion (TDD) is preferred to indicate the measure of distortion as opposed to total harmonic distortion (THD). The rationale behind this is TDD is a function of the maximum load current, while THD is a function of the actual fundamental current and could exaggerate the distortion levels when the transformer is lightly loaded and this difference is shown in equations 5.5 and 5.6 (Blooming & Carnovale, 2006; Berge, *et al*., 2011).

$$THD = \sqrt{\sum_{h=2}^{N}(\frac{I(h)}{I(1)})^2} \quad (5.5)$$

$$TDD = \sqrt{\sum_{h=2}^{N}(\frac{I(h)}{I_{rated}})^2} \quad (5.6)$$

where *h* represents the order of the current harmonic *I(h)*, *I(1)* is the fundamental component and I_{rated} is the rated load current.

5.2 Bench Transformer Test B (2-50 p.u. dc injection)

This part of the experimental procedure looks into the voltage and current response in two very special cases: (a) imposition of extreme levels of dc on the transformer; (b) the effect of reducing the operating voltage for mitigation. The tests were performed in the laboratory using the 3p-3s transformer systems.

5.2.1 Effects of extreme GIC levels

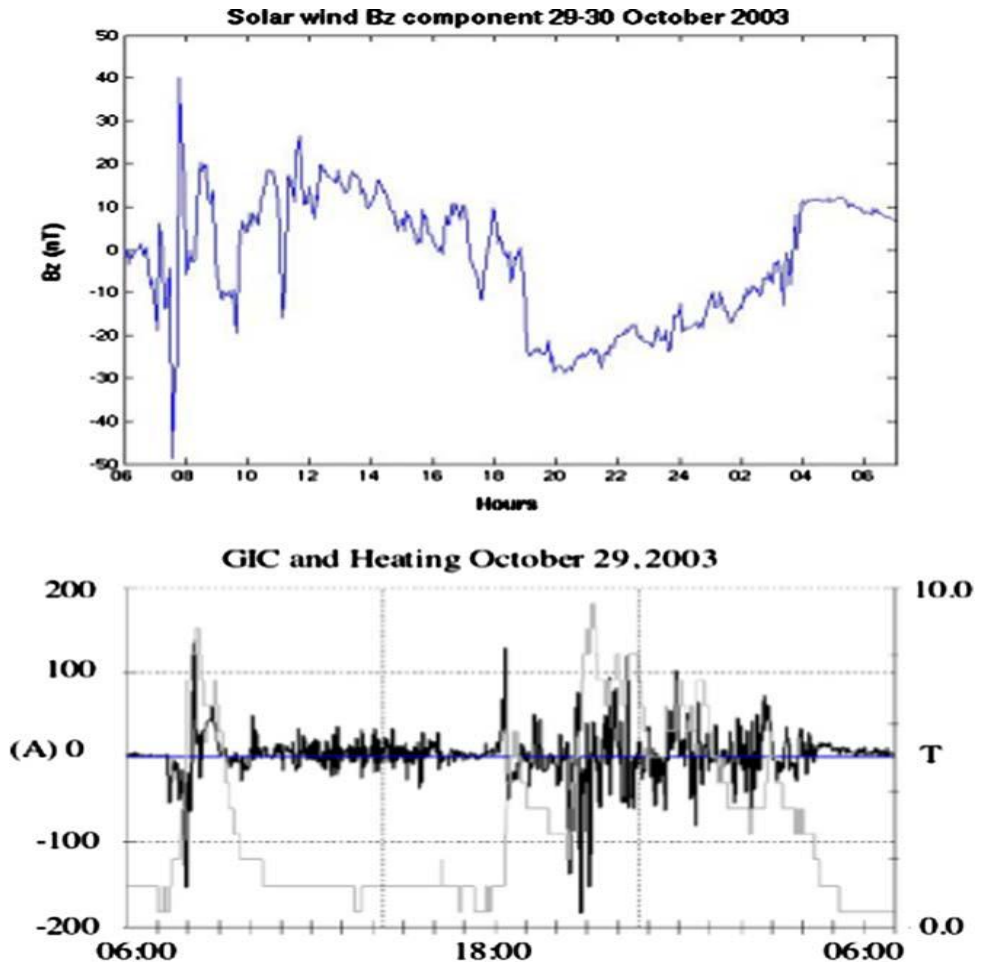

Figure 22: Correlation between the orientation of the solar wind magnetic field Bz component with the measured GIC (black) and heating of the transformer tank due to stray flux (grey) during the Halloween storm of 2003. The Bz component is a component of the earth's magnetic field that has been reported to correlate well with GIC activity (Lundstedt, 2006).

When CMEs are blasted from the surface of the sun, they will reach the earth's near space environment within a matter of days (Kappenman & Albertson, 1990). The porlarity of these charged particles is important because the earth's protective magnetosphere is northward bound. Therefore, if these solar flares are orientated northwards, the GMD that occurs as a result of the CME-magnetosphere coupling may not be so severe. If the particles are, however, southward orientated then the effect of the coupling will be much more unrelenting as the charged particles pass right throught the magnetosphere. Figure 22 illustrates this relationship by means of a magnetic field *Bz* component contrasted with measured GIC and temperature values during the Halloween storm of October 2003 (a severe GMD) in a Swedish transformer (Lundstedt, 2006). This intense coupling then results in the flow of very large ionospheric currents which cause large variations in the earths magnetic field; and ultimately very large quasi-dc induced currents flow in electrical systems (it can be seen in Figure 22 that large magnitudes of GIC correlate well with a southward *Bz* component).

When relatively high levels of GIC flow in power transformers, they have been known to cause myriad problems that ultimately have detrimental effects on power system reliabillity and stability. During the two most recent and severe disturbances, namely the GMD in 1989 and the Halloween storm, the tripping of power lines, voltage collapse and black-outs were reported (Kappenman & Albertson, 1990; Lundstedt, 2006).

5.2.2 Procedure

This section will investigate the response of the bench-scale test system to levels of dc injection that are in the order of up to 50 p.u. of the magnetising current.

It was reported in a very early experimental study (Hock-Chuan & Swift, 1984) that when a "very high GIC" was imposed on a transformer, the voltage and current harmonic contents actually diminished because the "air-core" or saturation region of a transformer core steel has a "straight line" (linear) behaviour. This was because the transformers developed flux was forced into the linear air-core region by the large dc offset resulting in a decrease in distortion. In a later study, Masoum and Moses (2008) produced a three phase transformer model which was tested for "very large GIC inputs"; and this resulted in a similar response of the transformer core steel from a qualitative perspective. These characteristics of the bench transformers were therefore investigated.

The laboratory set-up was an upgraded version of the setup in Figure 17: Full laboratory set up. The experimental procedure and conditions are outlined below:

- In order to ensure that the transformer was heavily loaded, the nameplate rating of the load transformer was used i.e. 120/230V. The source transformer therefore stepped up an applied voltage in the order of 63/120V.

- Approximately 90% of the rated full load power delivered to the resistive load.
- 80% of full load rated current flowing through the primary and secondary windings
- dc was injected from 0 to 50 per unit of I_{mag}, i.e. 0 - 2.7 A per phase.
- Measurements were taken in the transmission line (primary of load transformer) and at the load side – six voltages and six currents in total.
- The dc injection periods were kept just a little over the transformer time constant response (approximately 5-6 seconds) so as not to damage the units that were already operating well beyond their current carrying capacity.

5.2.3 Voltage reduction in the presence of dc

It was shown that transformer saturation is a function of its relative VA capacity and operating voltage (*vide supra* section 5.1.1: *Analytical Determination of Saturation*'); where the source transformer was immune to the dc that was much smaller than the current flowing in its windings. The purpose of the following experiments was to investigate the effect of voltage reduction in the presence of a moderate level of dc. The dc injection was held constant at 1.3 p.u. of the magnetization current which was known from earlier experiments to push the transformer into saturation, and the voltage was varied from 0.6 -1 p.u. of the knee voltage V_{knee}. Three different loading conditions were considered for each experiment: (a) no load, (b) 50% load and (c) 70% load. In each experiment, the *B-H* loops, *Q,* and harmonics were measured alongside the implementation of the analytical determination of saturation.

5.3 Bench Transformer Test C – Differential core type response (0-2 p.u. dc injection)

Having performed multiple transformer tests with the bench scale system (three phase bank consisting of single phase units), the next step was to test transformer systems that were comparable in terms of voltage and VA ratings but differing in core structure (three phase three limb and three phase five limb). In order to maintain consistency with the former system, the new transformers were industrially fabricated by the same transformer company that had made the single phase units.

At this point in the project, the setting up of 10kVA isolated power supply had been completed and commissioned. This supply consisted of four machines that were coupled in such a way that the three phase output power was completely isolated from the building's supply (schematics of this set up can be seen in Appendix B). This ensured that the experiments were immune to any system disturbances that could have been experienced at points of common coupling (PCC's) within the building supply. This may include voltage dips, harmonics, dc components, etc. Having verified a clean, balanced voltage supply according to the *IEEE Std. 519-1992*, the next step was to characterize the transformer cores.

5.3.1 Characterization of the transformer cores

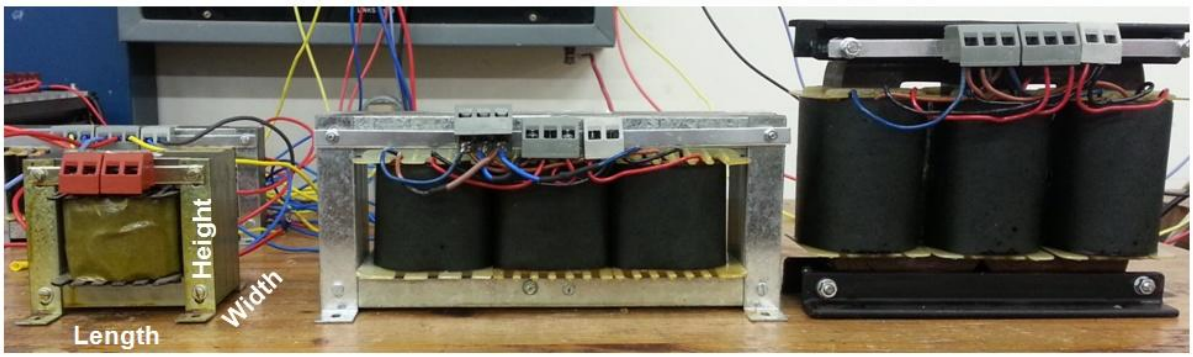

Figure 23: Bench-scale source transformers of differing core structure - Single phase three limb (left), three phase five limb (centre) and three phase three limb (right).

Table 6: Nomenclature used to distinguish the different core configurations subjected to dc excitation

Core Configuration	Abbreviation
Three phase bank	3p – 3s
Three phase three limb	3p – 3L
Three phase five limb	3p – 5L

Figure 23 shows the different core configurations of the same voltage and capacity ratings that were under consideration. It was remarkable to notice the difference in height and width between the three phase five limb (*3p-5L*) and the three phase three limb (*3p-3L*) transformers having similar ratings. Due to transportation considerations *3p-5L* power transformers are often preferred because of their relatively shorter height compared with *3p-3L's.* The capacity is however compensated for in their widths and the inclusion of two outer limbs; which effectively makes them more stable throughout the shipping procedures (Eskom Holdings Ltd, 1998). It was important to individually test these core configurations in order to check their responses against literature; but before any tests could follow each transformer core had to be individually characterized according the protocol applied to the *3p-3s.*

5.3.2 Magnetization curves

Tracing the *v-i* curves was done by energizing each limb of the transformer cores separately so as to exclude the effects of mutual inductance in the case of the 3p-3L and 3p-5L transformers. In a three phase transformer that is wound in each limb, the magnetising current in one phase is a function of the fluxes that arise in all three phases, or conversely the flux in one limb is a function of the currents in all three phases (see equations 6.1 and 6.2). Owing to the different reluctance paths that the flux arising in each limb sees, the corresponding *v-i* responses for each limb are not necessarily the same. An averaging technique was therefore used to locate the knee point of the transformer cores based on the individual limb responses. This is different from the case of the 3p-3s whereby magnetising currents in each single phase unit are a function of solely their self-inductances.

$$i_a(t) = g(\varphi_a(t),\ \varphi_b(t),\ \varphi_c(t)) \tag{6.1}$$

$$\Phi_a(t) = f(i_a(t), i_b(t),\ i_c(t)) \tag{6.2}$$

5.3.3 Open Circuit and Short Circuit tests

The OC and SC tests for the test transformers were performed by the manufacturer and the results are found in Appendix A. These results were important for determining the series and shunt admittance elements of the transformers for inputs in the simulation software.

5.3.4 Sizing of the load and determination of VA base

Since the transformers had the same VA ratings, similar resistive loading configurations were used to tests the differing core structures. The three-phase three limb *(3p-3L)* load transformer was slightly under-rated in terms its voltage ratings owing to a manufacturing discrepancy. But since the transformers' response was to be compared based on their relative magnetising currents and knee point voltages while maintaining the same VA base, this minor difference did not bear any significant implications. On average all the (name plate rated 300VA) bench transformers appeared to have a knee point voltage that effectively de-rated their VA rating by about 60-66%. A 200VA base was therefore used for per-unitizing all the transformer systems' investigations that ensued. Two aspects of the system conditions under dc excitation are investigated for comparison purposes namely: (a) reactive and non-active power demand, and (b) generated harmonics.

5.3.5 Differential Q due to dc excitation

The different approaches to calculating apparent power have been discussed in great detail in *Chapter* 3. Reactive power, which will be denoted by Q_{MVar}, was calculated using the conventional method while non-active power, which will be denoted by Q_{MM}, was calculated using the method proposed by Malengret and Gaunt (2011). The general power theory algorithm for calculating Q_{MM} has been made available online (*Electric Power Systems Research* website) in the form of an excel spread sheet. Required inputs include instantaneous voltages and currents, the resistances of the wires and conventional measured results from the data acquisition tools for comparison with the new method.

Each transformer test system consisted of a deliberately over-rated source transformer, immune to the effects of the injected dc, and a smaller load transformer of the same core structure. All the measurements for on-line measurements and post-processing were once again taken by the *IEC-1992* compliant Yokogawa Power Meter whose specifications were given in section 4.7.

Having established the effect that dc excitation has on transformers of differing core structures, some measured results from literature of power transformer response are contrasted on a per unit scale with the bench units.

5.3.6 Differential Harmonic Current Analysis

In this part of the procedure, the harmonics generated when moderate levels of dc are imposed on the transformers of different core structures were measured. Only the current harmonics were of interest to the investigation because no notable voltage distortion was observed (for up to 2 p.u. dc). Experiments were performed under the exact measurement conditions as those used in section 4.7; the only exception being the use of an isolated generator as a voltage supply.

5.4 Simulation Protocol

PSCAD/EMTDC v4.2.1 Educational, an Electromagnetic Transients Program (EMTP), is the simulation environment that was used to model the various transformer systems under investigation. Given the necessary transformer saturation parameters, in addition to the O.C and S.C parameter, transformer saturation can be adequately represented in this environment as reported in literature. The purpose of the simulation protocol is to investigate the modelled transformer response for comparison with measured results. Inherently, two transformer models are represented in PSCAD/EMTDC: (a) the Classical Approach and (b) the Unified Magnetic Equivalent Circuit Model (UMEC) approach (Manitoba, 2005).

5.4.1 The Classical Modelling Approach

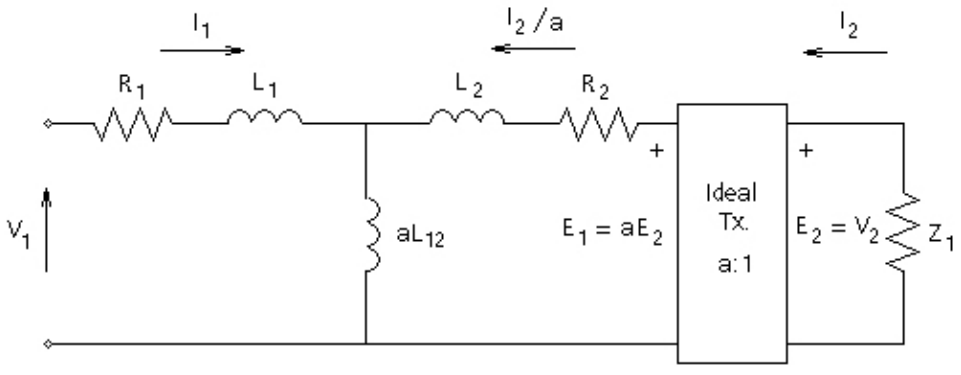

Figure 24: EMTDC's equivalent circuit of two mutually coupled transformer windings

Table 7: Description of transformer Data

Parameter	Description	Unit
T_{MVA}	Transformer single-phase	MVA
f	Base frequency	Hz
X_1	Leakage reactance(primary)	p.u. of S_{BASE}
N_{LL}	No load losses	p.u. of S_{BASE}
V_1	Primary winding voltage (RMS)	kV
I_{m1}	Primary side magnetising current [%]	% rated current
V_2	Secondary winding voltage (RMS)	kV
I_{m2}	Secondary side magnetizing current [%]	% rated current

Figure 24 is a representation of the electrical equivalent circuit employed in the EMTDC software, and Table 7 is a description of the corresponding transformer data. The S_{base} of the transformer is taken from the MVA rating and is then used to calculate the primary and secondary current bases using equation 5.7, where I_{base1} is the primary current base and I_{base2} is the secondary current base. The no load losses N_{LL} and the primary leakage reactance X_1 are calculated from the open and short circuit tests. The corresponding primary and secondary impedance bases $Z_{base1,2}$ are given by equation 5.8.

$$I_{base1} = \frac{S_{base}}{V_{base1}} \ , \qquad I_{base2} = \frac{S_{base}}{V_{base2}} \tag{5.7}$$

$$Z_{base1} = \frac{V_{base1}^2}{S_{base}} \ , \qquad Z_{base2} = \frac{V_{base2}^2}{S_{base}} \tag{5.8}$$

The primary and secondary side magnetizing currents I_{m1} and I_{m2} are then given as a percentage of the rated base currents (see equation 5.9).

$$I_{m1} = x\% * I_{base1}, \qquad I_{m2} = x\% * I_{base2} \tag{5.9}$$

A representation of how the saturation properties of a transformer may then be adjusted is shown in Figure 25. The three parameters that shape the degrees of freedom of the core saturation characteristic are the following:

1. Air core reactance, which is estimated to be twice the leakage reactance X_1 by the software
2. The effective knee voltage defined to be 1.0 p.u.
3. Magnetizing current corresponding to the effective knee voltage

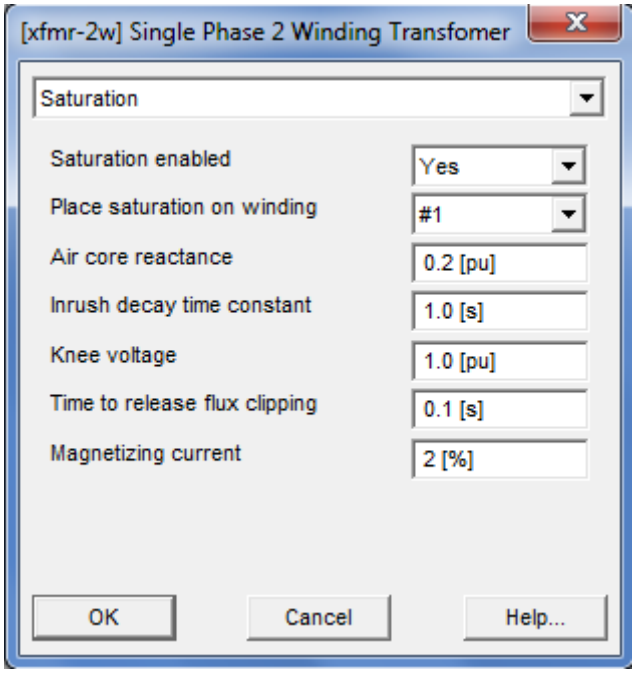

Figure 25: Saturation properties of a single phase shell type transformer in PSCAD/EMTDC.

The example of the inputs above shows some of the parameters that PSCAD requires. From the experimental protocol the knee voltage and corresponding magnetizing current can be readily provided. The software manual provides clear definitions of other unknown parameters (inrush decay time constant, time to release flux clipping, etc.) and suggests default parameters that are suitable for the size of the transformer being modelled. The classical modelling approach is more of an approximation of the core saturation characteristics and is useful in situations where there is limited transformer data, which is often the case when power utilities are referred to.

5.4.2 The UMEC Approach

The magnetic coupling between windings of different phases is not taken into account in the aforementioned classical approach. The more detailed UMEC approach, which takes into account magnetic coupling between phases in addition to coupling between windings of the same phase, is briefly described in this section. The following transformer core structures can be represented using the UMEC model:

- Single phase units
- Three phase, three limb units
- Three phase, five limb units

The underlying theory behind the UMEC transformer model can be found in Enright *et al.* (1997). The incorporation of mutual inductance in a three limb transformer (with windings in each limb) is comprehensively described in the PSCAD/EMTDC Master Libray Models. Figure 26 shows how some transformer parameters are entered. The software uses a

combination of the transformer core aspect ratios and information from its piece-wise magnetizationcurve as measured in the laboratory or as specified by the manufucturer or power utility.

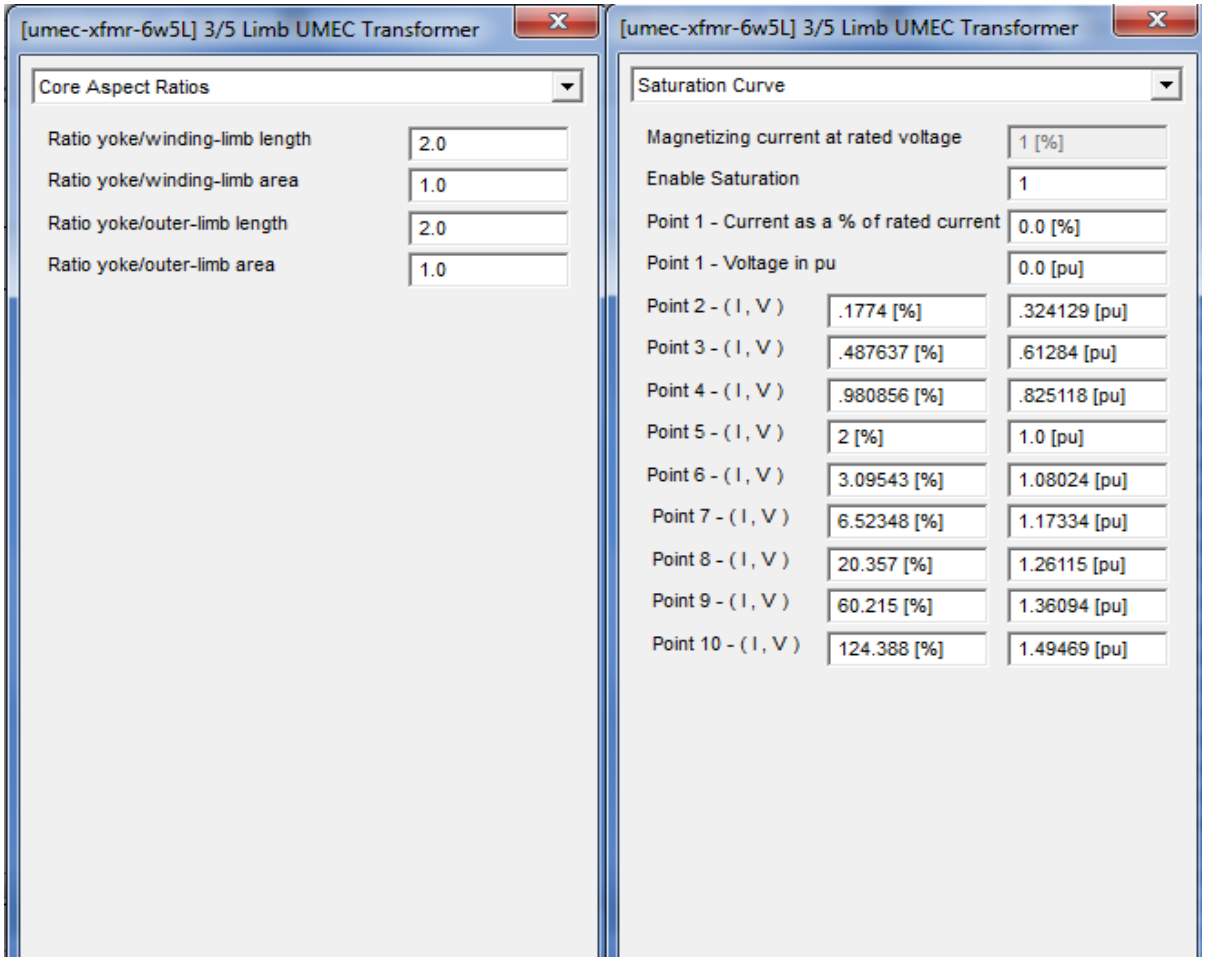

Figure 26: Some of the parameters required by EMTDC to model a three phase, five limb transformer

5.4.3 PSCAD/EMTDC transformer models: Summary

The two primary transformer models in PSCAD/EMTDC have been briefly described above. The classical model can only be used to represent single phase, double wound units. The UMEC models differ from this approach by considering inter-phase coupling and core geometry. In the classical models, the non-linear characteristics are approximated based on the 'knee point', the corresponding magnetizing current and the 'air core reactance'; whereas non-linearity in the UMEC model is entered directly as a *v-i* curve. Both these models will be investigated in the context of the laboratory based dc excitation experiments.

5.4.4 Procedure

The focus of the simulation protocol was on transformer response with regard to the conventionally calculated reactive power Q_{Var}, and non-active power Q_{MM} calculated using

the general power theory developed by Malengret and Gaunt. The objectives that aided the development of a comprehensive PSCAD test system are described in the subsequent sub-sections:

.

5.4.4.1 Transformer selection and parameterization

Based on the actual laboratory set up, the applicable transformer models were to be selected from the PSCAD/EMTDC master library. The chief parameters in the selection criterion were the core structure and the transformer model (either Classical or UMEC approach). The Classical approach offered single phase shell type transformers that could be arranged into three phase banks of any winding configuration. In addition to single phase units, the UMEC approach offered three phase three limb and three phase five limb transformers. Having selected the required transformer type and modelling approach, the necessary parameters were carefully entered. Figure 27 is an example of the 'configuration' input parameters for a single phase transformer.

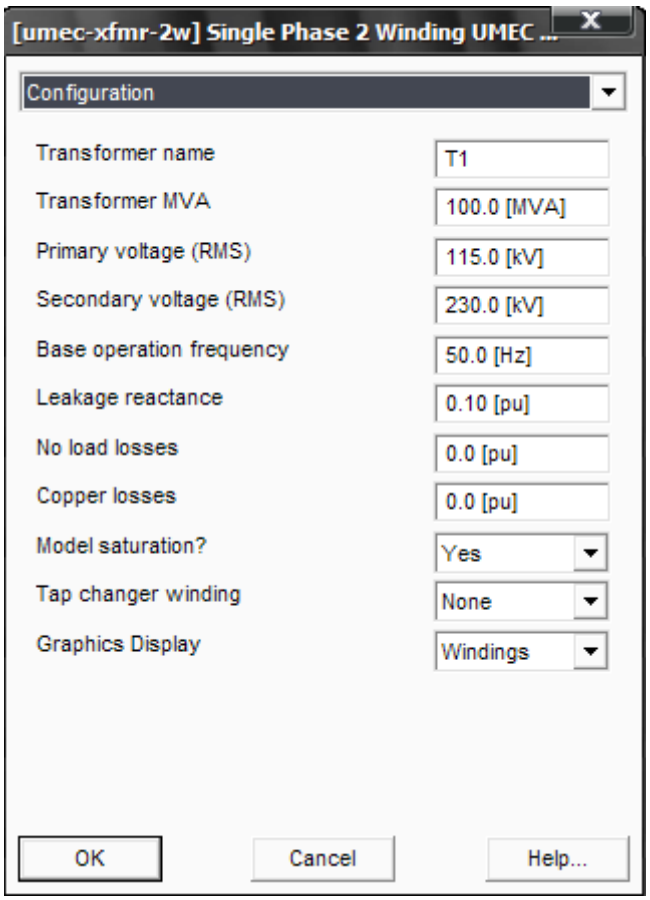

Figure 27: Example of input parameters for a single phase shell type UMEC transformer model in PSCAD. The parameters above a for an default PSCAD power transformer and have no relation to the bench scale protocol.

5.4.4.2 Open Circuit Test System

The fully parameterized transformer models were then subjected to the open circuit simulation test system in Figure 28. The transformer model was energized at the McLyman knee point voltage (linear operation). The phase output voltages and magnetizing currents, open circuit power and reactive power were recorded and checked for consistency with measured results.

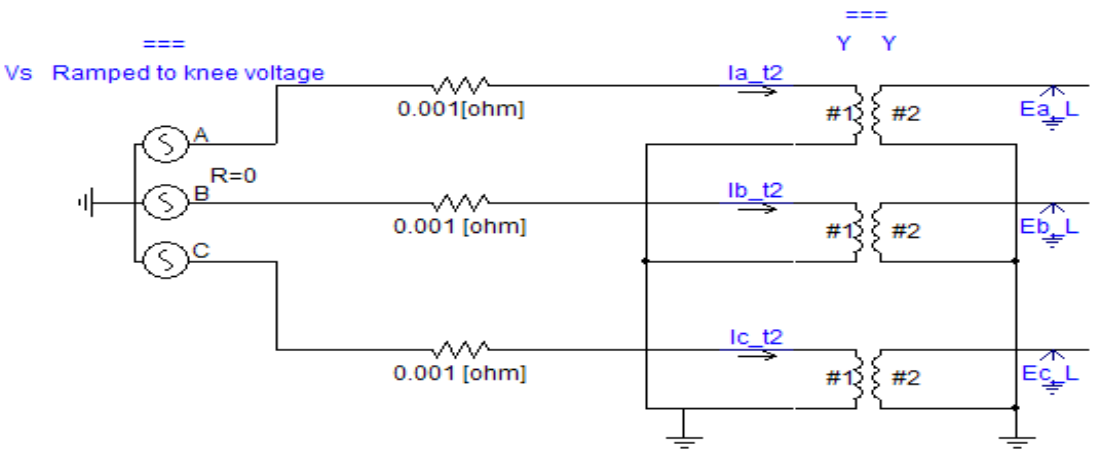

Figure 28: Transformer open circuit test system

5.4.4.3 Loaded transformer test system

After the verifying the expected performance of the transformer model at no load, the next step was to apply a resistive load to the test system. Once again the *V, I, P, Q* characteristics of the transformer model were recorded and compared against measured results.

5.4.4.4 DC injection scheme

GIC was modelled with a dc current source; and similar to the laboratory set-up, the dc was to be injected into the neutral of the load transformer where it would then be expected to split into three equal currents flowing through the 'transmission line' (line resistances being r_1=r_2=r_3). The dc return path would then be the source transformer's neutral. It was also important to ensure that the dc injection scheme was capable of injecting varying levels of dc at the desired time i.e. before start up or some time after start up. Since the 'transmission line' resistances were equal, the same amount of dc must to flow in each phase. The method that was used to verify this was to run a Fast Fourier Transform (FFT) for each of the line currents and then measure the value of the dc component. Ideally the dc in the 'transmission line' i_{dct} should be 1/3 of the dc injected into the neutral i_{dcn}. Figure 29 illustrates the dc injection set up that was employed in PSCAD.

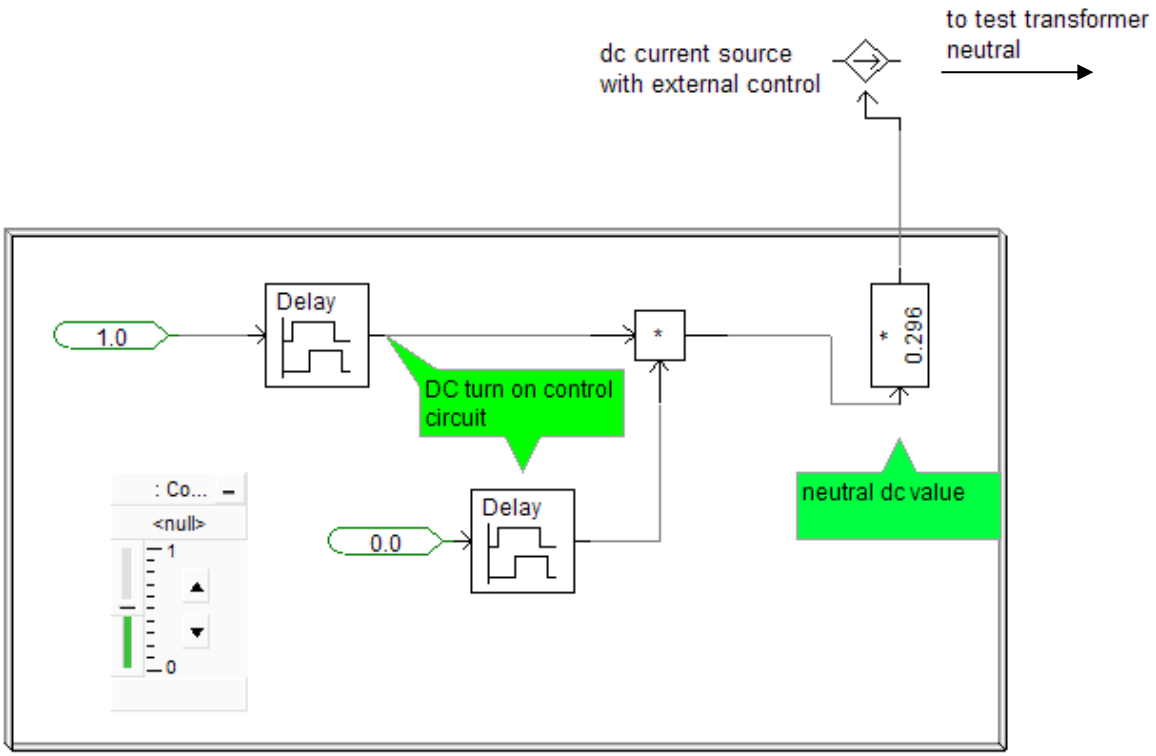

Figure 29: Dc injection scheme consisting of a dc current source with an external control.

5.4.4.5 Voltage and Current Measurements

The master library possesses different kinds of measurement apparatus depending on the purpose. In the laboratory set-up, the measurement scheme was limited to measuring only six voltages and six currents simultaneously. The simulation environment however was not limited in this manner. The PSCAD apparatus that was used to measure the different aspects of the voltages and currents included the following:

- Volt-meters and ammeters
- Multi-meters
- Power meters
- Online frequency scanners (FFT processing blocks)
- Interpolated integrators (practically an RC circuit was used to integrate the voltage for BH loop measurements)

Some readings were monitored on-line while the relevant instantaneous waveform data was stored for post-processing. The conventional power measurements done by the PSCAD apparatus were checked for consistency against off-line processed data. Similarly PSCAD FFT results were compared against their corresponding data sets run through an FFT algorithm in Matlab.

5.4.4.6 Results

The procedures described in the preceding sub-sections ensure the adequacy of the simulation model to run tests based on the actual laboratory set up. The final step is to energize the system and inject varying levels of dc in order to monitor the response of the transformers first for the (banks of single phase) classical model transformers and then for the multi-limb UMEC transformers. Measurements are to be processed and finally the simulations results are compared against measured results.

6 RESULTS AND DISCUSSION

This chapter displays the results from the experiments described in the previous chapter and then discusses the implications of each outcome. Firstly, the procedure outlined in section 5.1: *Bench Transformer Tests A* is investigated whereby the effect of varying the applied voltage on *Q* at different levels of dc is shown. Then the difference between reactive and non-active power in the presence of dc is investigated. The measured results of the transformers' *BH* loops under levels of dc are then displayed; and lastly the measured harmonics will be analysed.

Secondly, the outcomes of the procedure outlined in *section* 5.2: *Bench Transformer Tests B* where the effect of extreme dc is explored in detail, followed by the effect of reducing the voltage for mitigation.

Thirdly, the differential core type response is investigated as outlined in section 5.3. This part contrasts the response of three different core structures of transformers to relatively similar magnitudes of dc imposition, under the same operating condition.

Finally the simulation procedure from section 5.4 is investigated alongside a comparison against with the corresponding measured results.

6.1 Laboratory Electrical and Magnetic response

This section shows the results of some preliminary investigations that were undertaken to verify the conventional understanding of transformer behaviour.

6.1.1 V-Q Relationship under Varying Levels of dc

In Figure 29, the expected power-voltage relationship ($Q \propto V^2$) is observed. Also, an expected proportional upward vertical shift with increasing dc is demonstrated. An interesting finding from these experiments was the gradual tendency of the *Q*-*V* curve to become more linear with increasing dc. Table 8 shows that when each curve's trend line is generated in the quadratic form $y = ax^2 + bx + c$, the magnitude of the x^2 component tends to decrease while that of the x component increases with increasing dc. This association between the level of dc and this *Q*-*V* characteristic is unclear and is therefore not considered as important in this research for characterising the transformer response. Further comments on these observations are made at the end of this section (6.1.5: *Discussion*).

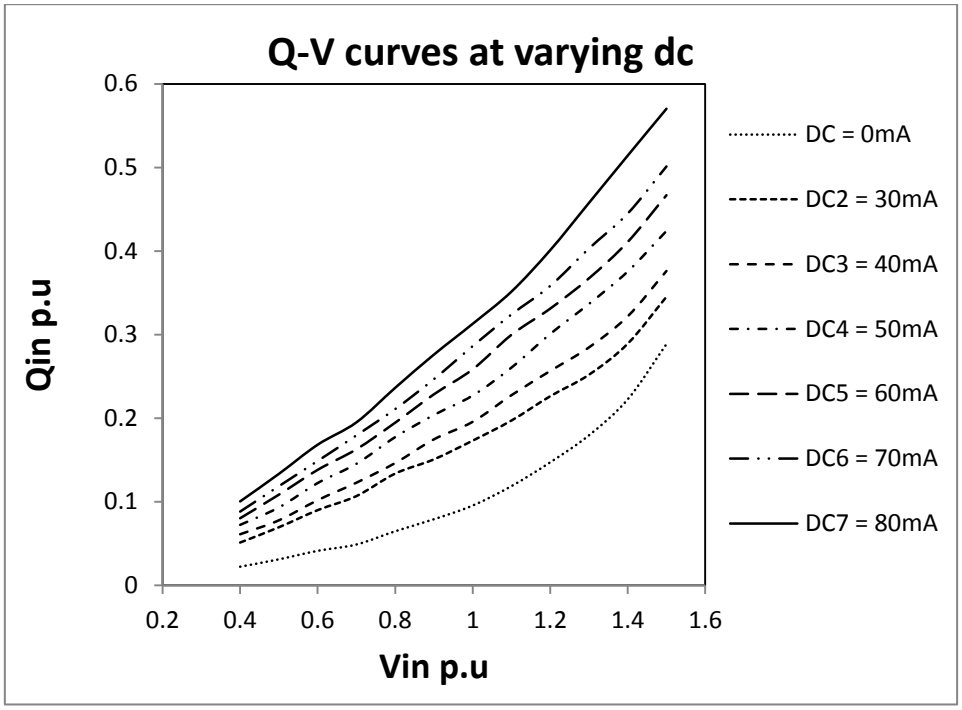

Figure 30: ***Q-V*** **graphs at different levels of injected direct current. The dc is a percentage of the magnetizing current of the load transformer. The per unit bases for V and Q are calculated from the data.** I_{mag} **= 55mA.**

Table 8: Parameters for $y = ax^2 + bx + c$ **representing each V-Q curve's trend-line**

DC [mA] per phase	a	b	c
0	0.222	-0.202	0.076
30	0.112	0.035	0.024
40	0.104	0.077	0.015
50	0.102	0.118	0.011
60	0.094	0.161	0.004
70	0.093	0.19	0
80	0.147	0.14	0.025

6.1.2 *Laboratory Power Calculations*

The results for the different approaches to calculating *Q* under conditions with distortion, unbalance and dc components of current, in the experimental procedure described section 5.1.3, are presented in this section.

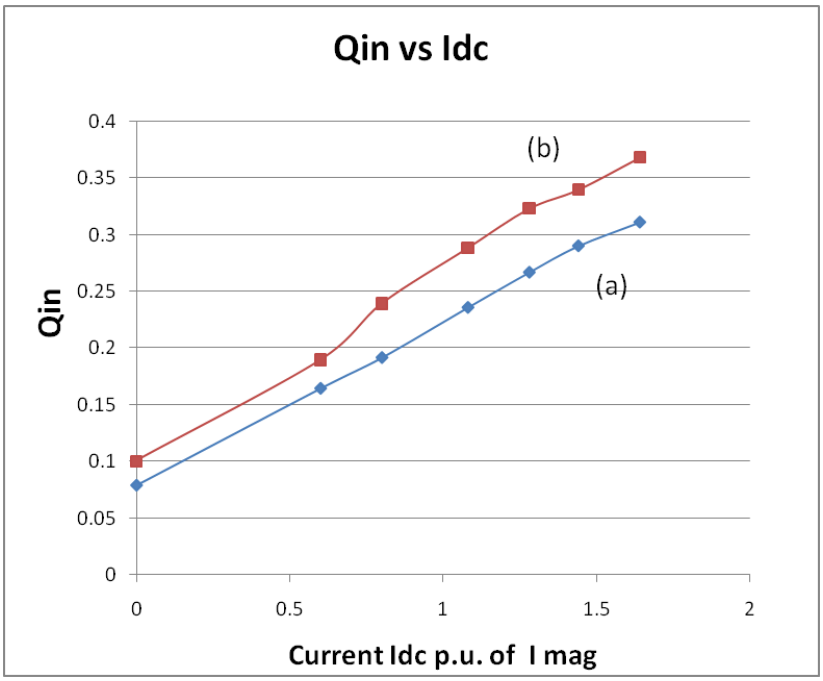

Figure 31: Absorbed *Q* associated with varying levels of dc in the load transformer in per unit. (a) Conventional (b) General power theory

It is clear from the graphs in Figure 31 that the conventional reactive power increases linearly in order to fulfil the magnetization characteristics as reported in literature (Molinski, 2002; Berge, *et al.*, 2011; Marti, *et al.*, 2013), when calculated using the conventional approach. In contrast, calculations using the general power theory, which includes losses in the neutral, show that the total non-active power at the same operating conditions is higher than is indicated by the conventional method. For this reason, the rest of the apparent power calculations in the dc injection experiments were done using the general formula; so as not to underestimate the conditions in the transformer.

6.1.3 *Hysteresis loops (laboratory measured)*

The voltage across the capacitor of the integrator circuit $V_C(t)$ and the instantaneous magnetizing current *i(t)* were then recorded using the Agilent oscilloscope as shown in Figure 32. The *x* and *y* axes, though not labelled, represent the scaled magnitude and the times respectively. The corresponding hysteresis loop was then traced in an XY plot to investigate the characteristics of the BH loop (see Figure 33, left diagram).

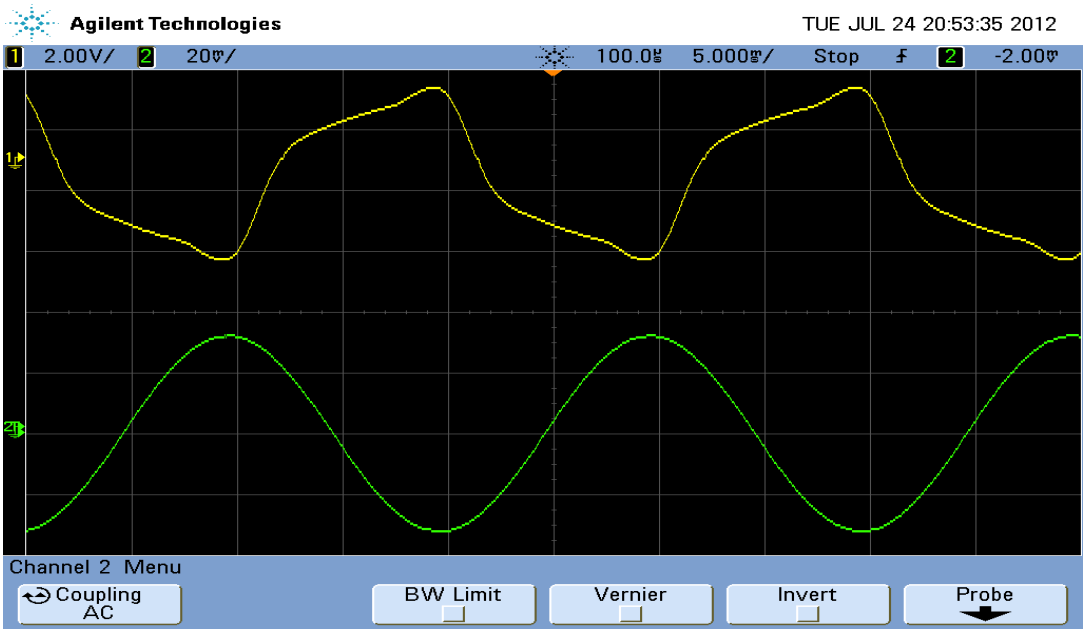

Figure 32: Wave- traces of the magnetizing current *i(t)* (top) and the integrated voltage $V_C(t)$ (bottom) of the load transformer recorded by the oscilloscope (Voltage = V_{knee}, Current = I_{mag}, Open Circuit).

The level of dc injected here is 1.3 p.u. of the load transformer's I_{mag}. The transformer is operating at V_{knee} (80/150V). It can be seen from the diagrams below that under normal operating conditions, a classic *B-H* loop is observed. When a dc is injected into the neutrals of the transformer, the loop shifts vertically upwards and there is a flattening of the top part of the loop as the load transformer will now be operating in the saturation region (see Figure 33). The distortion of the *B-H* worsens with increasing levels of dc. A study by Li, *et al*. (2010) reported a *B-H* characteristics response.

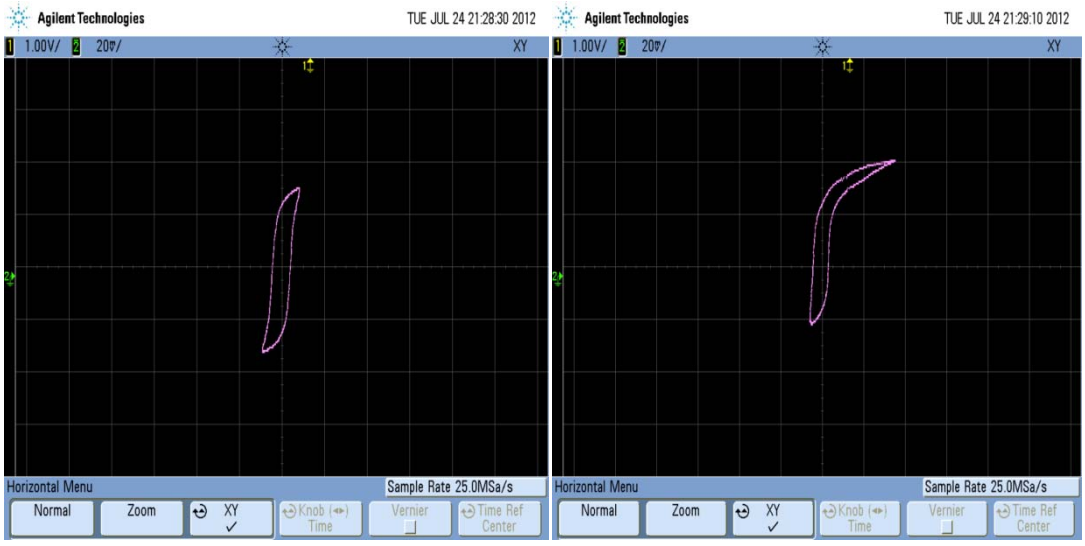

Figure 33: Hysteresis loop of the load transformer at V_{knee} , 0 dc (left) and 1.3 p.u. (69mA) dc injection (right)

The hysteresis loops shown in Figure 34 represent the conditions of an over-excited transformer without dc (left) and with dc (right). The image on the right side indicates that the transformer was experiencing 'deep saturation' because of the extreme distortion of the loop. This operating condition is also characterized by excessive harmonic distortion as will be discussed in the next section.

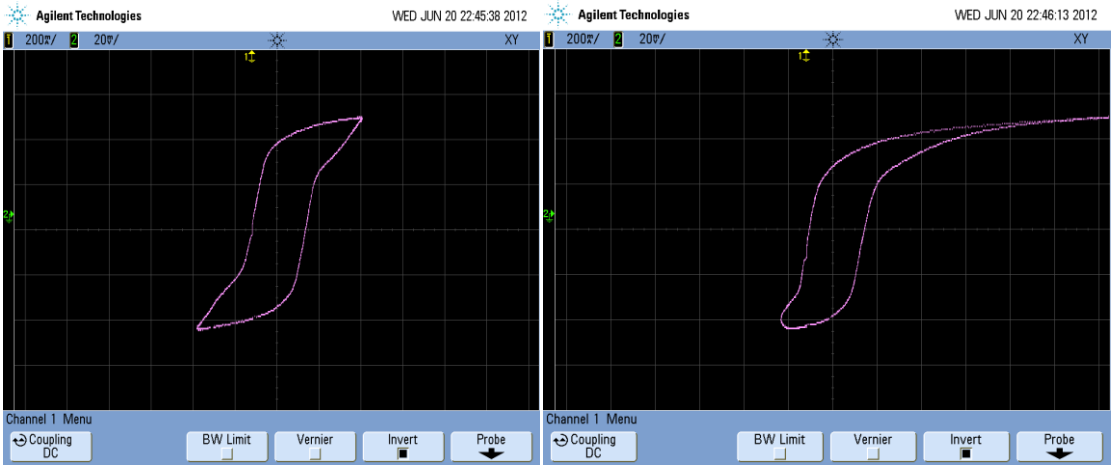

Figure 34: Hysteresis loop of the load transformer at the nameplate voltage (120/230V) without dc (left) and with a dc of 1.5 p.u. – 80mA (right), illustrating 'deep' saturation.

6.1.4 Harmonics

It can be seen from Figure 35 that the voltage source virtually had no harmonics in and out of the presence of dc up to 1.3 p.u. A very small characteristic 5^{th} Harmonic may be seen coming from the wall supply which is what was used as the supply at this stage of the project. Figure 36 shows the current harmonics generated by the TuT at different levels of dc injection. Since the three phase system was balanced, with each phase having virtually the same response, only the red phase is shown here.

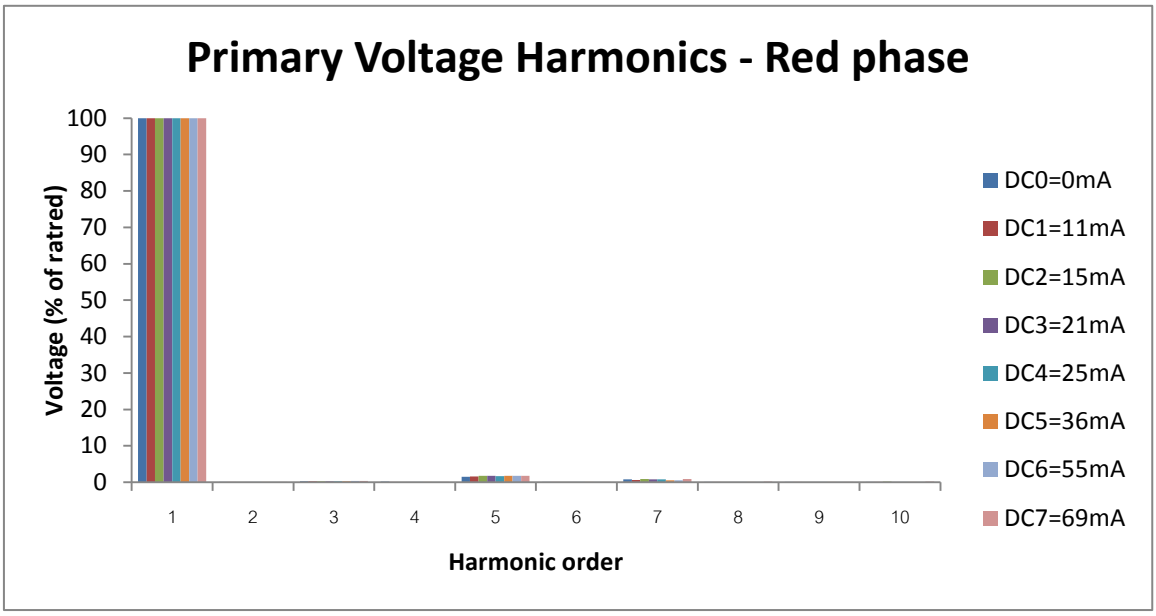

Figure 35: Voltage harmonic profile at various levels of dc showing that the voltage waveform remained the same throughout experiment. A very small 5th harmonic is seen which is characteristic of the utility wall supply. THD was <3% which was below the recommended harmonic distortion limits applied by utilities according the IEEE Std. 519-1992 (IEEE Std. 519-1992, 1993). I_{mag} = 55mA.

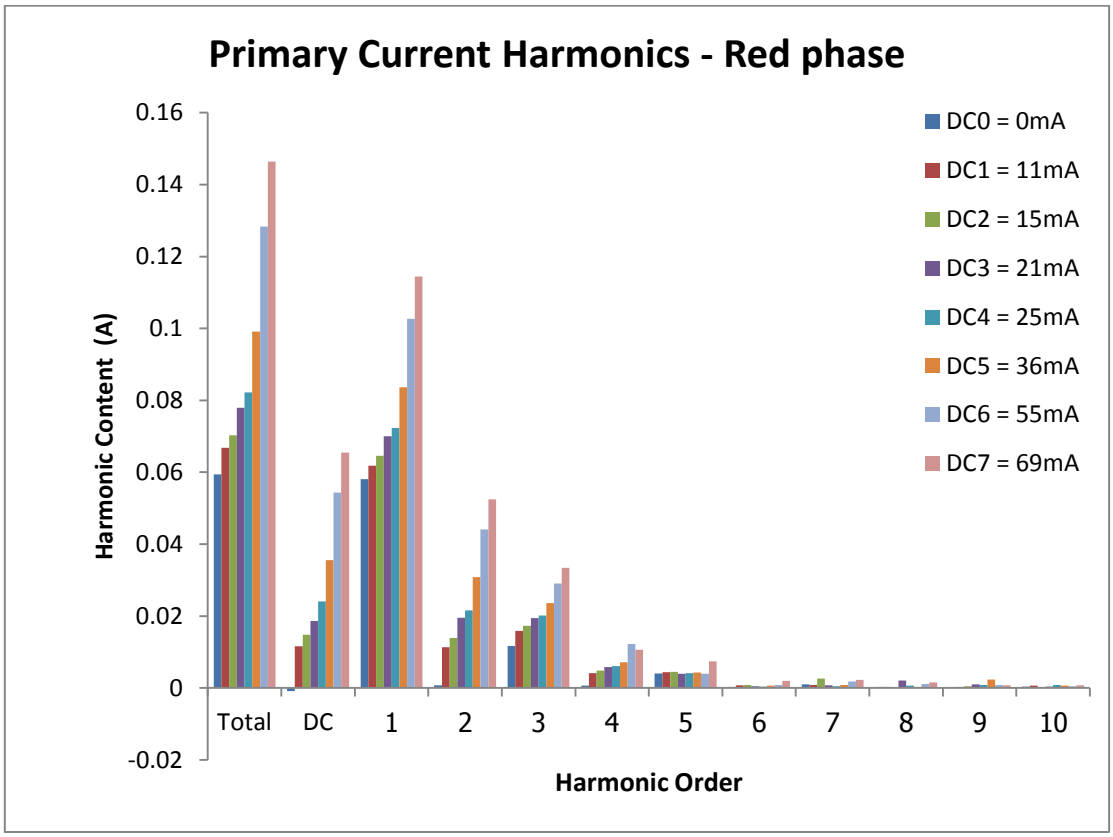

Figure 36: Current harmonics generated in the load transformer at varying levels of dc injection. I_{mag} = 55mA. Applied voltage is 80/150 V = V_{knee} = 1 p.u.

Harmonics were recorded up to the 10th order since higher order harmonics were very small. At no dc, the only harmonics present are the 3rd and 5th harmonics due to the I_{mag}. With the injection of just 11mA of dc, there is the sudden appearance of 2nd and 4th harmonics though they are of smaller magnitudes compared with the 3rd harmonic. As dc is increased beyond 36mA, the 2nd harmonic becomes significantly larger than the 3rd harmonic indicating commencement of saturation. The fundamental RMS component increases considerably with increasing dc owing to the significant increase in the asymmetrical exciting current drawn by the transformer which lags the system voltage by 90 degrees, leading to non-active power losses in the system. The same effect is reported by Kappenman & Albertson (1990) and Malengret & Isumbingabo (2010). Figure 37 shows the measured linear relationship between the TDD of the transformer and increasing levels of dc injection similar to modelled results in a recent study (Berge, *et al*., 2011).

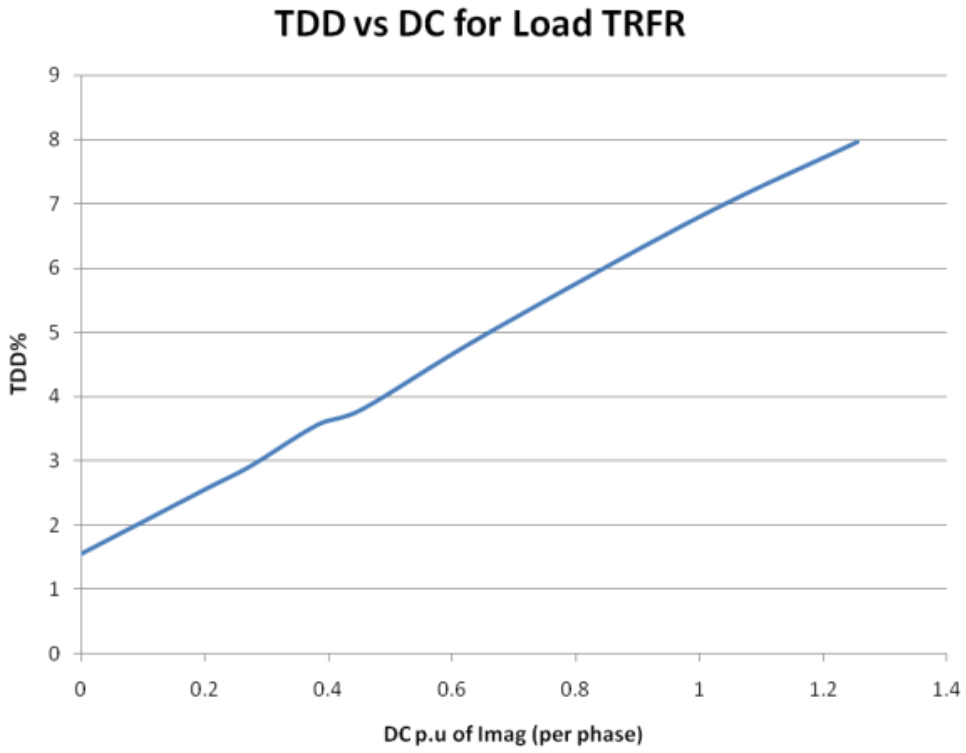

Figure 37: Representation of the input current total demand distortion (TDD) and increasing levels of dc injection when the transformer is heavily loaded.

6.1.5 Discussion

The expected relationship between applied voltage and reactive power in the presence of varying levels of dc was demonstrated. It was however noticed that the shape of the Q-V curve changed with each level dc in the sense that the linear *x* component increased and the x^2 decreased with increasing dc. No clear implications were identified from this result therefore further investigation may be warranted.

The differences in the methods of calculating *Q* were investigated and this was useful in determining the standard that would be used in this study.

The Hysteresis loops may be used as an indicator of not only the presence of GICs but also as a measure of the linearity of the transformer operation (under-excited or over excited; see section 6.1.3). This was seen in the resulting type of distortion that loop faces when compared to its healthy state.

Dc injection resulted in significant harmonic content increase namely the 2^{nd}, 3^{rd}, and 4^{th} harmonics for the three phase bank transformer system. Further analysis on current harmonics due to dc with varying transformer core types is discussed later in the report.

6.2 Effects of Extreme GIC levels

6.2.1 Voltage harmonics and waveforms

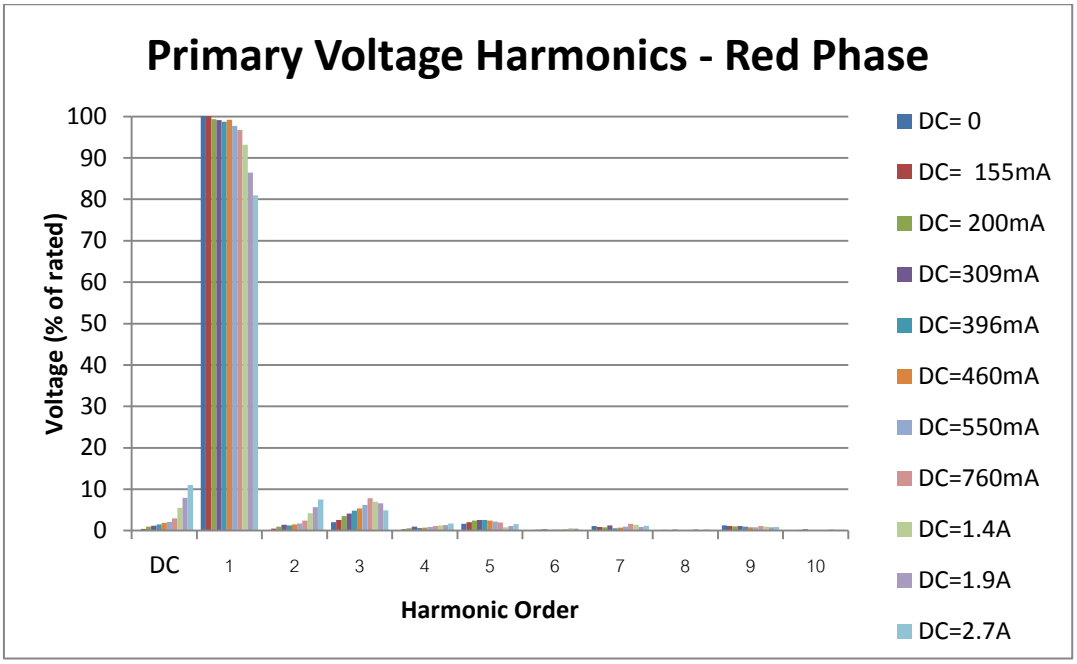

Figure 38: Voltage harmonic content of the primary side with excessively increasing DC. Above is the harmonic spectrum of the red phase. I_{mag} = 55mA.

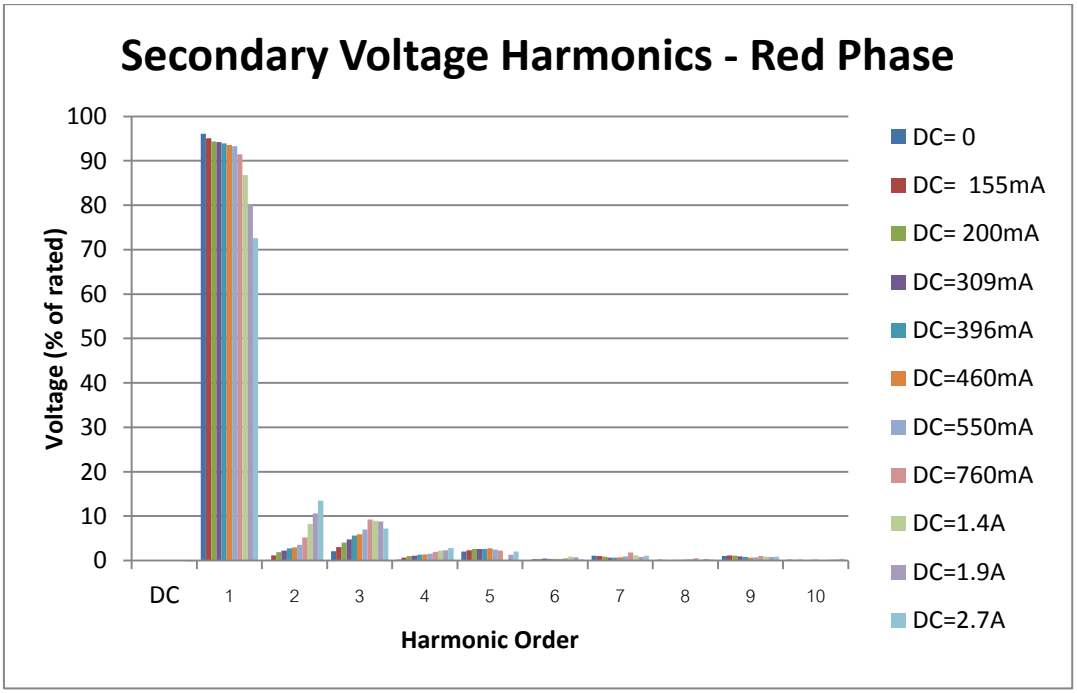

Figure 39: Voltage harmonic content of the secondary (load) side with excessively increasing dc. Above is the harmonic spectrum of the red phase. I_{mag} = 55mA.

Figure 38 and Figure 39 show the harmonics generated by the load transformer in the primary and the secondary (load side) respectively. The size of the maximum injected is about 50*I_{mag} which is 3.4 times rated full load current. From previous tests where dc levels were comparable with magnetizing current, the voltage waveform of the TuT was virtually immune to effect of dc levels comparable with I_{mag}. With very large dc levels, much higher

than I_{mag}, the voltage becomes distorted with the generation of both even and odd harmonics. Figure 40 shows the effect of a very large dc on the voltage waveform.

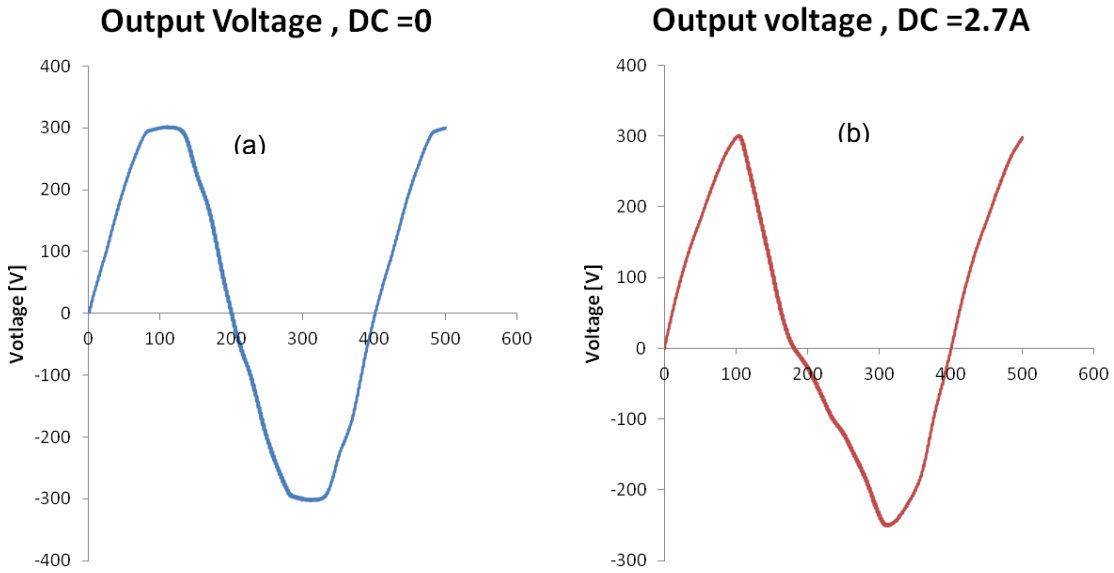

Figure 40: Output voltage waveforms of TuT: (a) at the name plate rating, no dc, and (b) at the name plate rating with a very large dc injection 50*I_{mag}. The x-axis represents the sample number which corresponds to a point in time during the snapshot.

6.2.2 Current harmonics and waveforms

Since current close to rated full load current was flowing in the transformer windings, THD was used to represent the level of distortion as this would be similar to the total demand distortion TDD (see Equations 5.5 and 5.6). It can be seen in Figure 41 and Figure 42 that there is a significant increase of the current harmonic presence in the load transformer as expected, particularly the 2^{nd} and 3^{rd} harmonics. The fundamental component also increases with increasing dc. There is a sudden appearance of 2^{nd} and 3^{rd} harmonic in the load side though the magnitudes are much lower than the primary side harmonics. There is a gradual decrease of the load current fundamental with dc. More details on this observation will be discussed in the subsequent section.

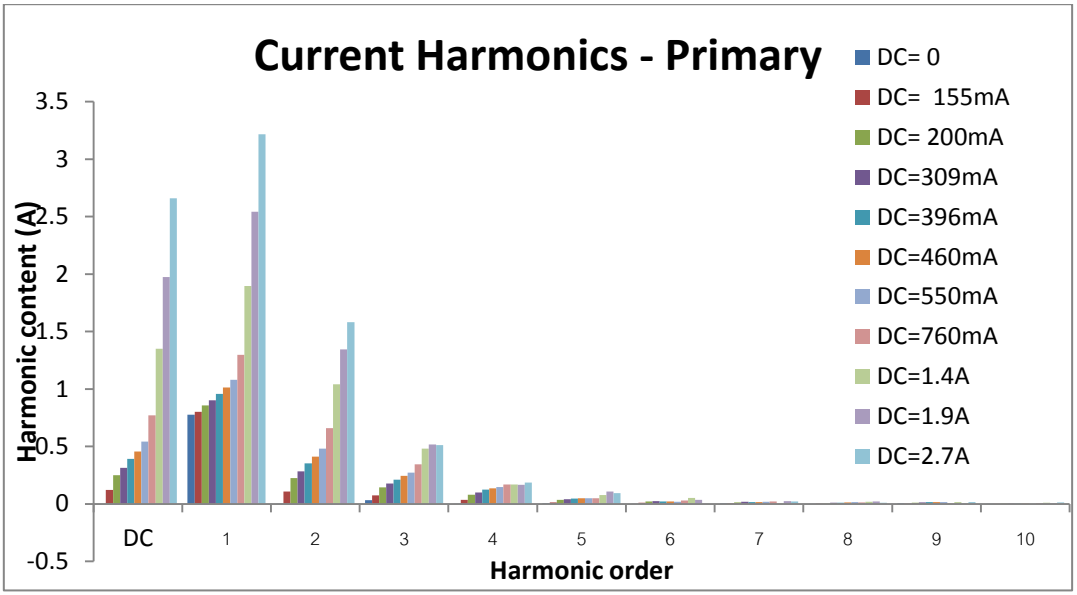

Figure 41: Current harmonics recorded on the primary side of the load transformer.

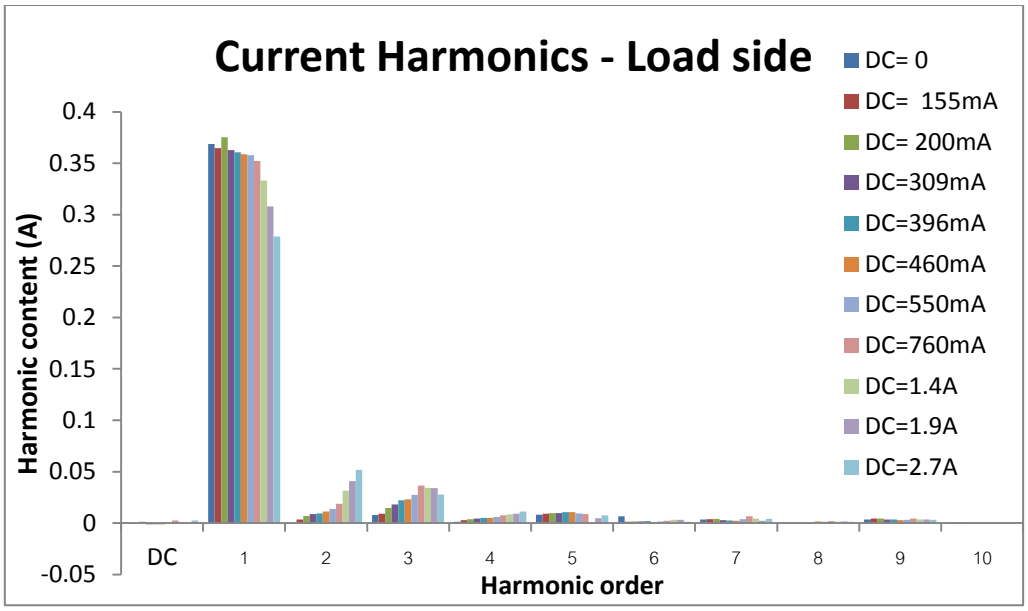

Figure 42: Current harmonics on the load side.

Figure 43 shows how the primary line current becomes distorted with high levels of dc injection. The high current peaks are due to the spike in magnetising current as a result of the dc offsetting the magnetization characteristics of the transformer, as illustrated in Figure 9. The peak current at the highest dc level (2.7A dc) is 10.4 A at an R.M.S. value of 4.7 A (approximately 5.6 times the rated load current). A report by Zhang, *et al*. (2011) had similar results with regard to the increasing magnitude and distortion of the line current with increasing dc.

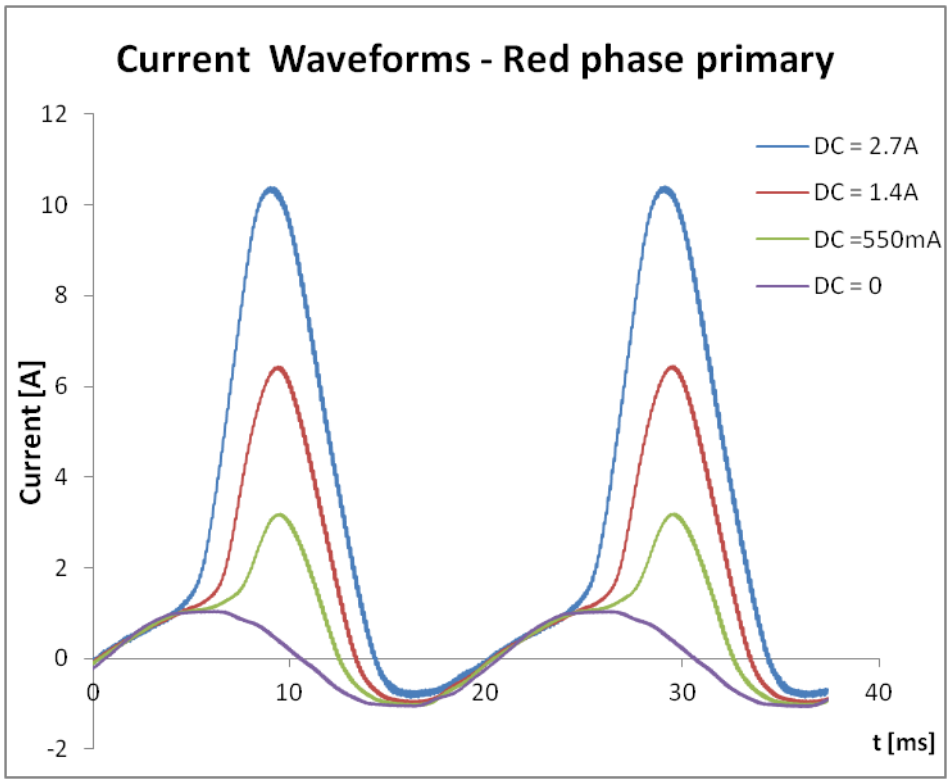

Figure 43: Primary line current waveforms with excessively increasing levels of dc. Maximum peak current was recorded at 10.4 A.

6.2.3 Electrical response with very large dc

The electrical response of the transformer was measured and recorded. The response of the voltages, currents, apparent power and power factor as a function of the injected dc were plotted and may be seen in Figure 44. The bases that were used to calculate the per unit values are represented in Table 9. All apparent power calculations were done using the general power theory.

Table 9: Bases for all units used in experiments

Measurement	Per Unit Base
S, P, Q	300VA
V	120/230 V
$I_{dc,injected}$	0.055 A (I_{mag})

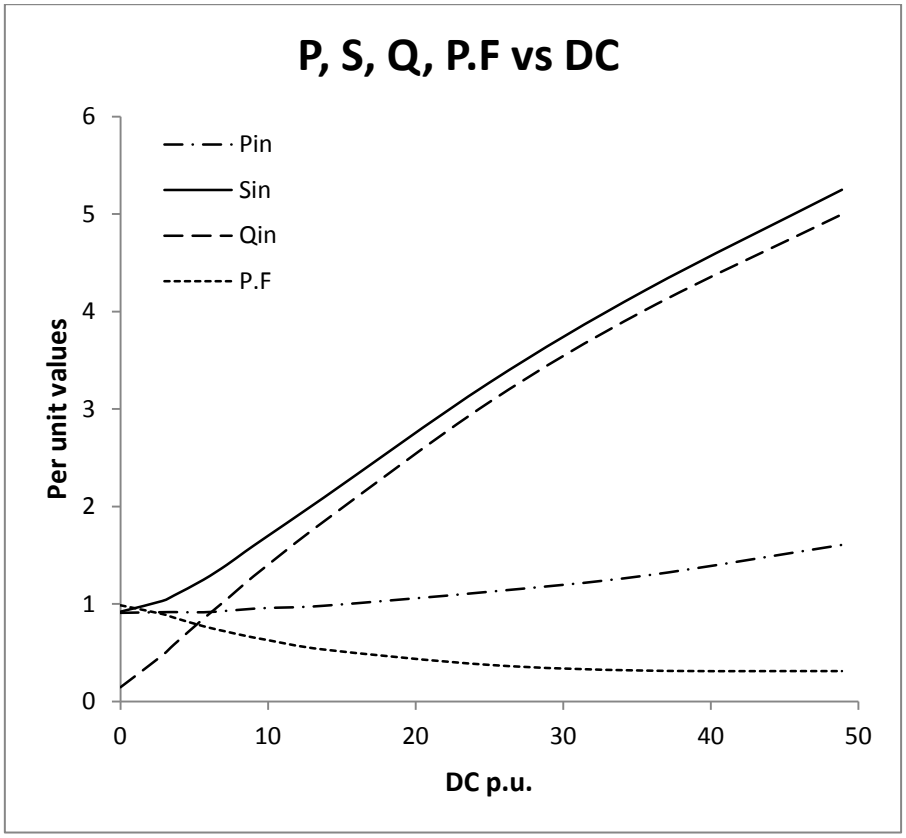

Figure 44: Measured results of the input power P_{in}, input apparent power S_{in}, non-active power Q_{in}, and power factor as a function of excessively increasing direct current.

Figure 44 clearly shows that that the apparent power and Q increase linearly with dc. It is also important to note that the input power requirement also increases as the dominant dc current largely contributes to I^2R losses. There is a substantial drop in the power factor which implies a significantly reduced level of efficiency in energy transfer from the source transformer to the load transformer. The output conditions may be seen in Figure 45 and Table 10.

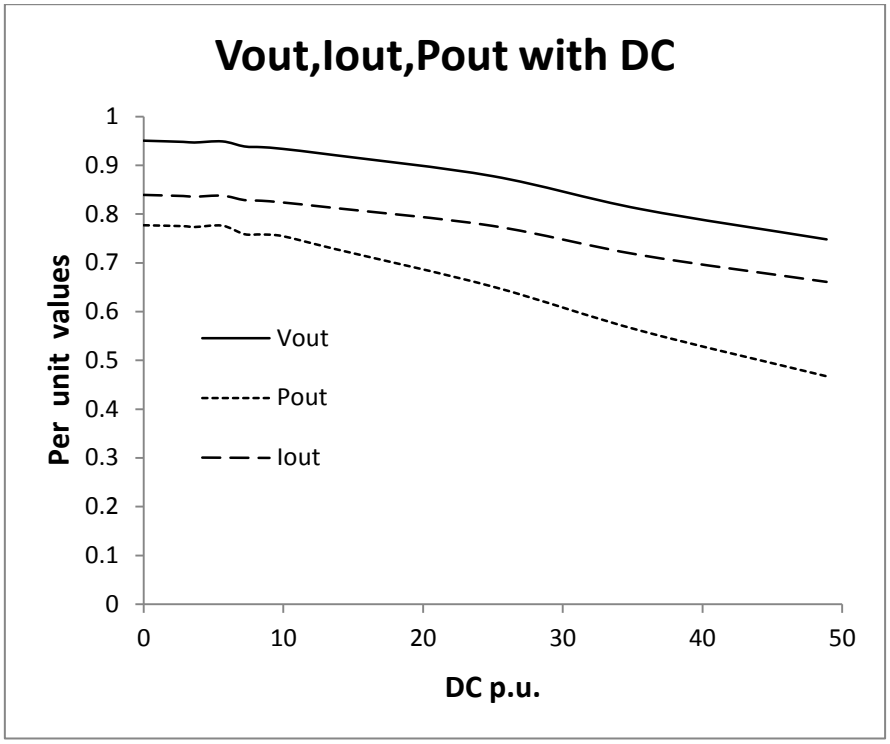

Figure 45: Variation of output parameters with excessively increasing dc impositions

Table 10: Table showing the variation of the transmission line power factor, and output parameters with dc. The initial condition is without dc and the final condition is a dc of 8.1A injected into the transformer neutral (2.7A per phase).

dc/phase [A]	P_{out} % drop	P.F. T_{line} % drop	V_{out}% drop	I_{out} %drop
2.7	**39**	**68**	**21**	**21**

It can be seen in Figure 46 that the current distortion rises sharply up to a certain point, which corresponds to approximately 25 p.u. dc, after which it begins reduce. This is because the extremely large dc levels push the transformer's operating point above the knee of the *B-H* characteristics resulting in linear transformer behaviour. The primary and secondary voltage THDs rise less aggressively than those of the current and seem to level off after 13 p.u. dc. The dc was limited to 2.7A per phase so as not to damage the heavily loaded transformers that were operating well beyond the rated current condition.

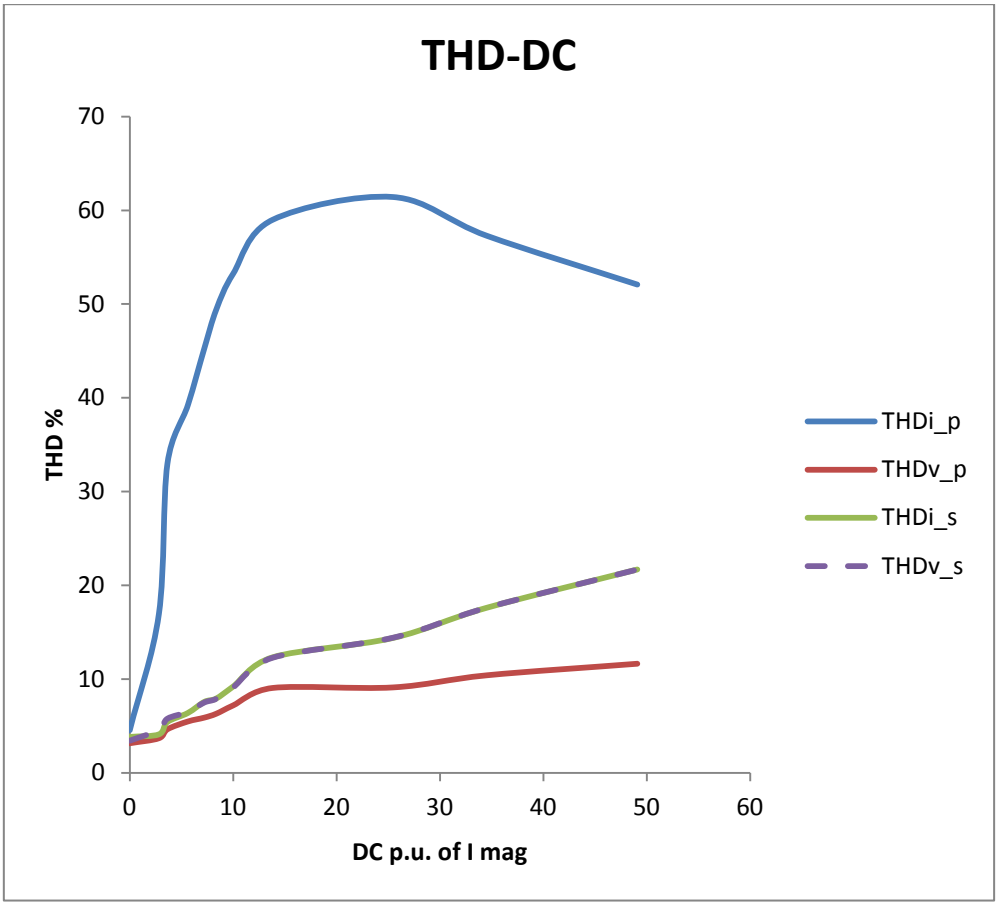

Figure 46: THD response of the primary and secondary sides of the test transformer.

In the literature survey, it was found that a study by Masoum & Moses (2008) investigated the impact of extremely large direct currents in a three phase three limb transformer model (after Hock-Chuan & Swift (1984) had found that a laboratory transformer operated linearly under extreme dc bias conditions). The transformer model investigated in this report is of a different core structure to the bench scale units therefore it is not directly comparable with their response measured for the bench units in this study. However the authors reported the reaching of a maximum THD at a certain large dc which then "dies out" as the dc gets even bigger.

6.2.4 Discussion

The ‘air core region’ investigation yielded some enlightening results with regard to the electrical response (*S, P, Q, I, V*) of the bench transformers when a large dc is imposed on them. This showed the complexity of the non-ideal conditions under which the system was in. The THD-dc response of the output voltage and current waveforms overlaps as expected since they are tied together with the resistive load (see Figure 46). The way in which the dc affects the primary voltage and current (transmission line side) is significantly different. This is because the component of the line current that is mainly affected by the dc is the non-sinusoidal magnetising current, which increases greatly with high values of dc until its maximum is reached. Since the primary side voltage has its own distortion characteristic with the high level of dc, the secondary voltage (two times the primary voltage) must also exhibit the same distortion characteristic. Finally, since the resistive load is connected to an already distorted supply it draws a current whose distortion is a function of this voltage.

6.3 Effect of reducing the operating voltage in the presence of dc (Laboratory experiments)

The effect of reducing the voltage in the presence of dc comparable with I_{mag} was investigated in the laboratory. The next sections show the measured results.

6.3.1 No load tests

6.3.1.1 Measured *B-H* loops

The diagrams below show the effect of reducing input voltage of the transformer without dc from V_{knee} to about 0.6 p.u. of V_{knee}.

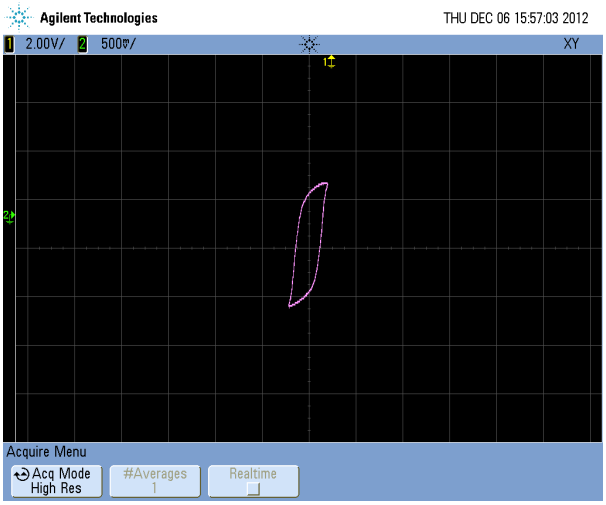

(a) 1 p.u.

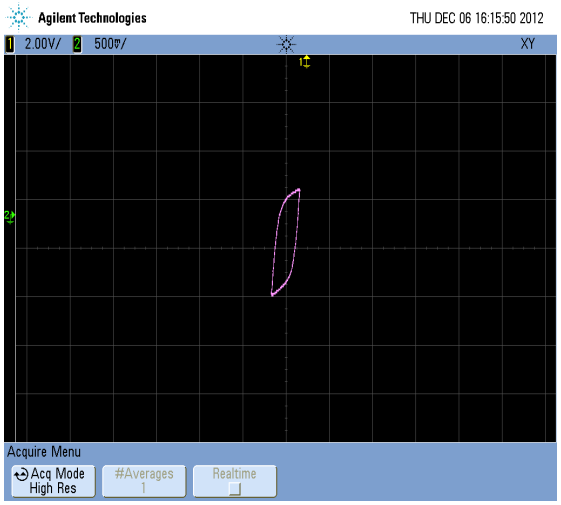

(b) 0.88 p.u.

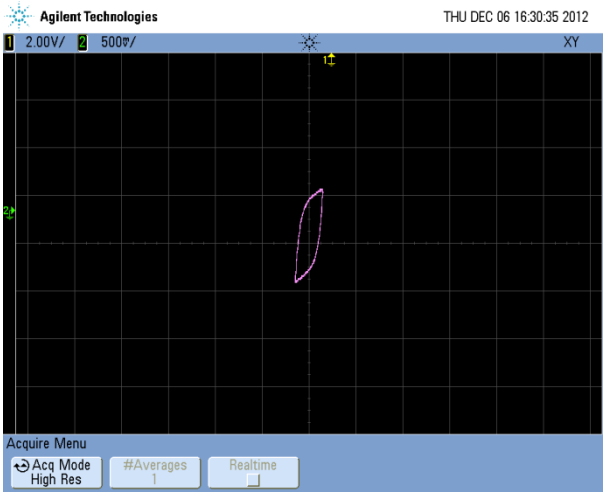

(c) 0.75 p.u

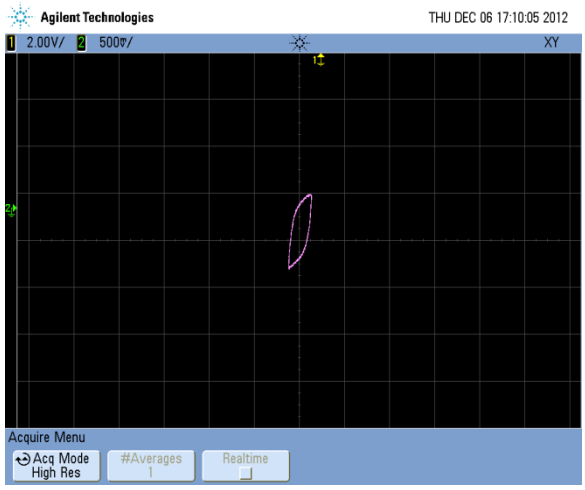

(d) 0.6 p.u

Figure 47: The diagrams (a) to (d) above show the effect of reducing the input voltage from V_{knee} 80 V to 50V under no load and no dc component conditions. The BH loops become smaller as the voltage is reduced along the linear operating region.

A constant dc was then injected into the transformer system and the voltage was decreased in the same steps as measured above.

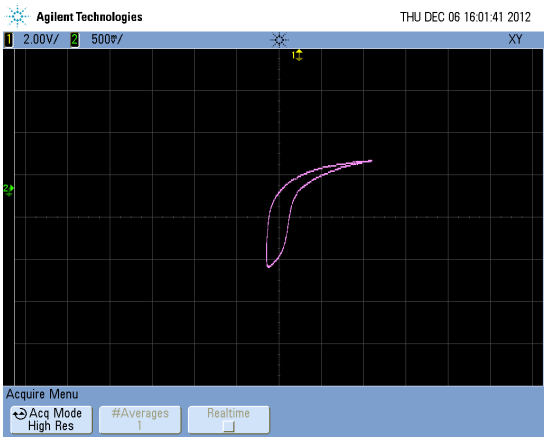

(a) 1p.u.

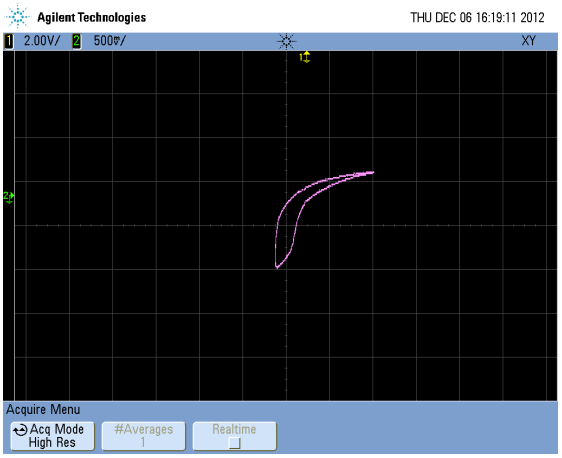

(b) 0.88 p.u.

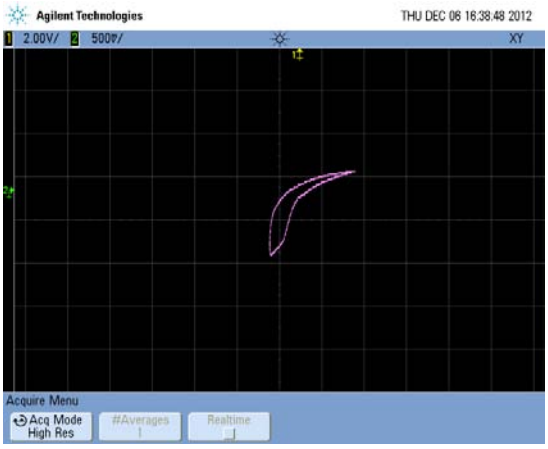

(c) 0.75 p.u.

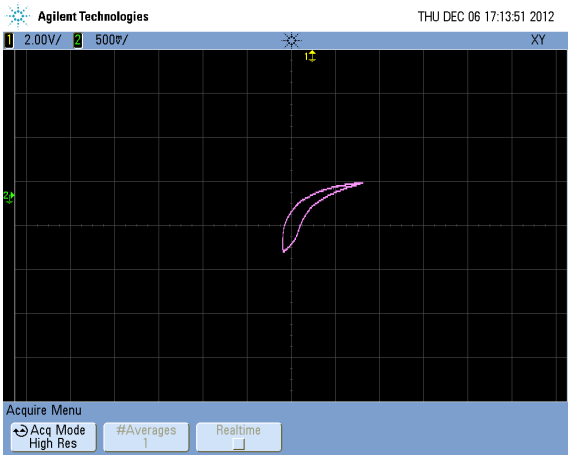

(d) 0.6 p.u.

Figure 48: Diagrams (a) to (d) above show the effect of voltage reduction in the presence of a moderate dc injection.

6.3.1.2 Non-active power

At no load the non-active power absorbed by the transformer was calculated using the general power theory (Malengret & Gaunt, 2011). Figure 49 shows the effect of varying the operating voltage of the transformer from 0.6 p.u. to 1 p.u. when there is no dc component, and when a dc is circulating in the system.

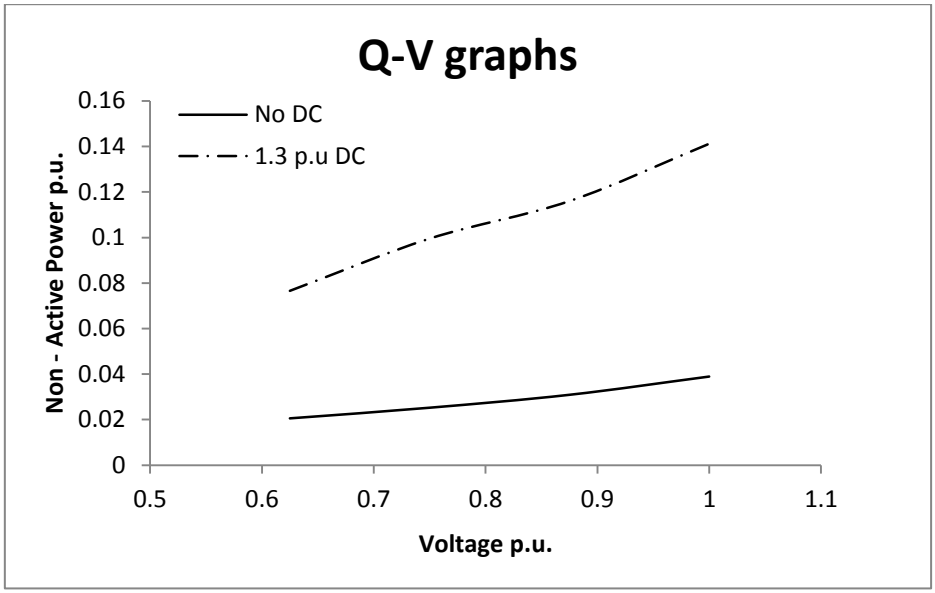

Figure 49: Q-V graphs showing effect of operating voltage with and without dc at no load.

6.3.1.3 Harmonics

The harmonics represented in this section are the current harmonics as these were the ones most affected by the level of dc injected in the experiments.

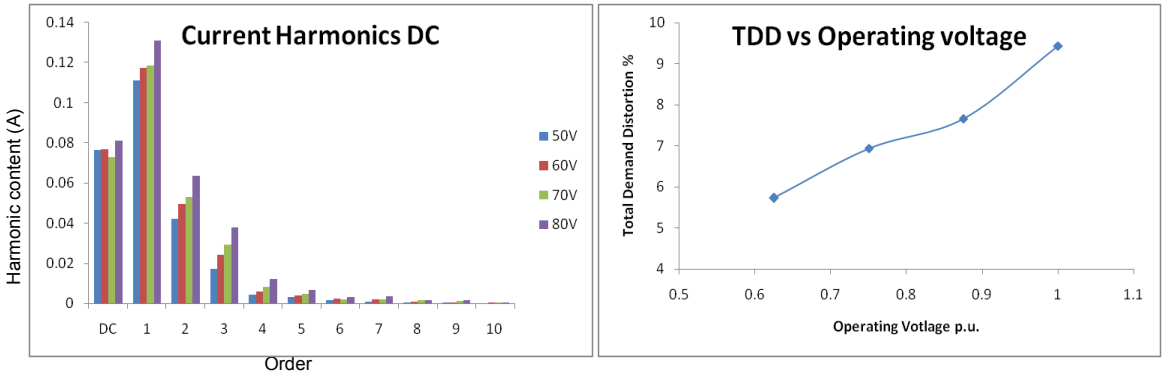

Figure 50: Current harmonics (left) and the corresponding TDD (right)

The diagrams above show the effect of operating voltage on the current harmonics when the transformer is subjected to a dc current. Generally as the voltage is increased at a constant dc in the no load configuration, the order of increase in harmonics seems to follow this expression:

$$H^{2nd} > H^{3rd} > \cdots > H^{th} \tag{5.10}$$

Where H^{th} is the magnitude of the highest harmonic order. The maximum measured TDD was 9.4% (Recommended harmonic limits for such a system are set to a maximum of 5% TDD according to IEEE Std. 1459-2010).

6.3.1.4 Saturation Test

Using McLyman's (2004) rule of thumb (see equation 5.1), the magnetizing current waveform of the transformer was taken at each voltage level. It was found that at a DC injection of 1.3 p.u. of the magnetizing current, saturation had started occurring even at a voltage approximately 40% below the knee point voltage of 80 V (about 60% below the name plate rating of 120 V – see Table 11).

Table 11: Table showing the application of McLyman's formula to the transformer exciting current at different voltage levels in the presence of a dc. V_{knee} = 80V = 1 p.u.

VOLTAGE (V)	AVG (A)	PEAK (A)	2*AVG (A)	SATURATED?
80	0.164	0.440	0.328	YES
70	0.155	0.399	0.310	YES
60	0.169	0.371	0.338	YES
50	0.147	0.329	0.294	YES

6.3.2 50% load tests

Using the same operating voltage and dc injection configuration, the transformers were loaded to approximately 50% of their capacity. The non-active power and harmonics were recorded and are presented below. The *B-H* loops were monitored online giving similar results as the no load condition, as expected.

6.3.2.1 Non-active Power

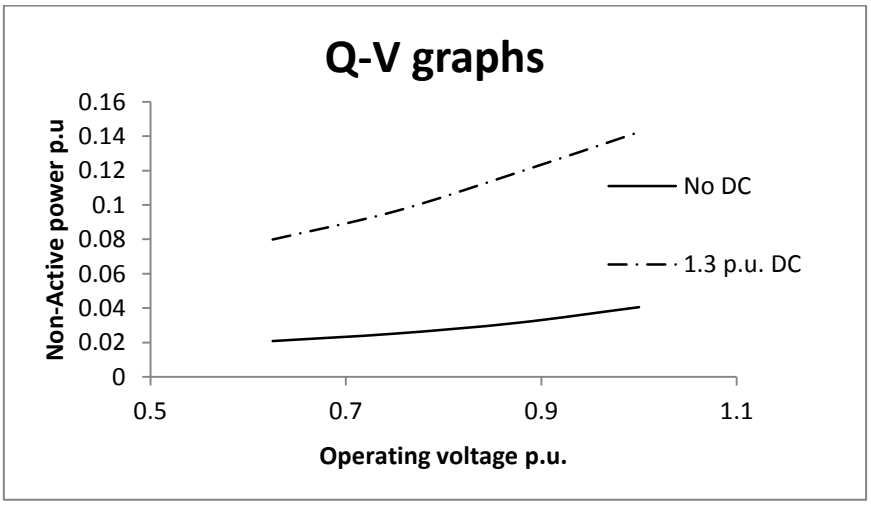

Figure 51: Q-V graphs showing effect of operating voltage with and without dc at 50% load.

As expected the absorbed non-active power is similar to that in the no load experiment where Q is a function of operating voltage and dc.

6.3.2.2 Harmonics

The diagrams below show the current harmonics and the TDD that occurs at different operating voltages under constant loading and dc conditions. The size of the harmonics appears to be the same as those for the no load test. The 5th harmonic appears to have a higher magnitude with increasing dc than the fourth harmonic, which was not the case for the no load condition. This implies that loading the transformer to half of its capacity while a dc is circulating in the system introduces an increase in the 5th Harmonic. The maximum TDD that was measured was 8.2%.

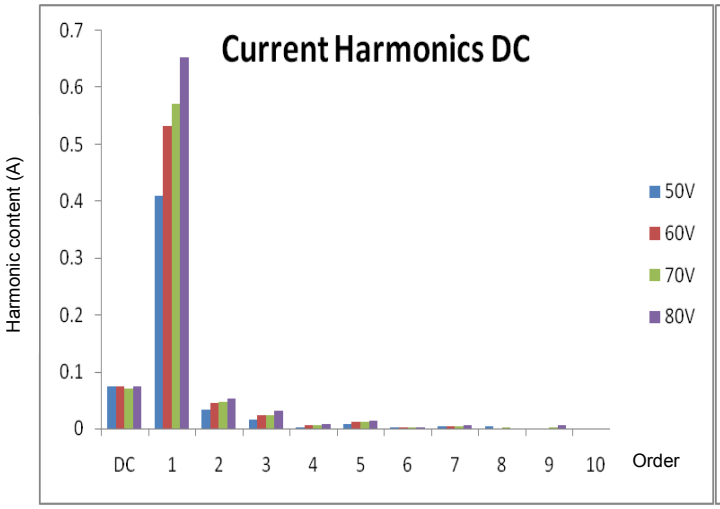

Figure 53: Current harmonics with a 50% loading configuration at different voltages in the presence of a constant dc.

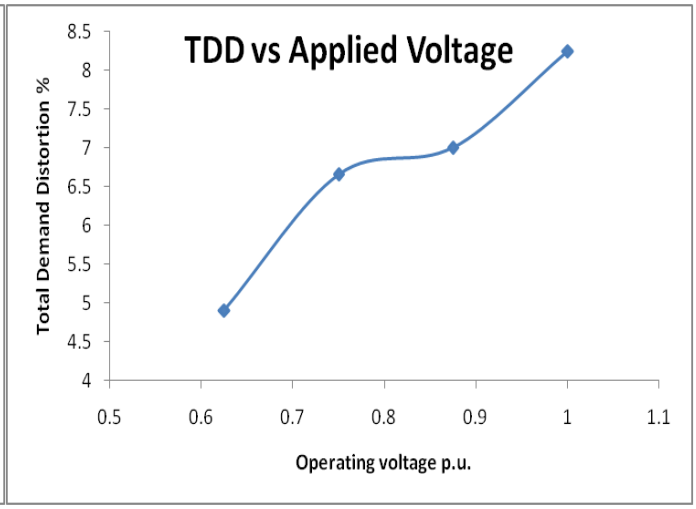

Figure 52: TDD against operating voltage in the presence of a dc

6.3.3 70% load tests

Finally the transformer was loaded to 70% of its capacity and similar tests were performed. The shapes of the BH loops resembled those for the previous two experiments, as expected.

6.3.3.1 Non-active Power

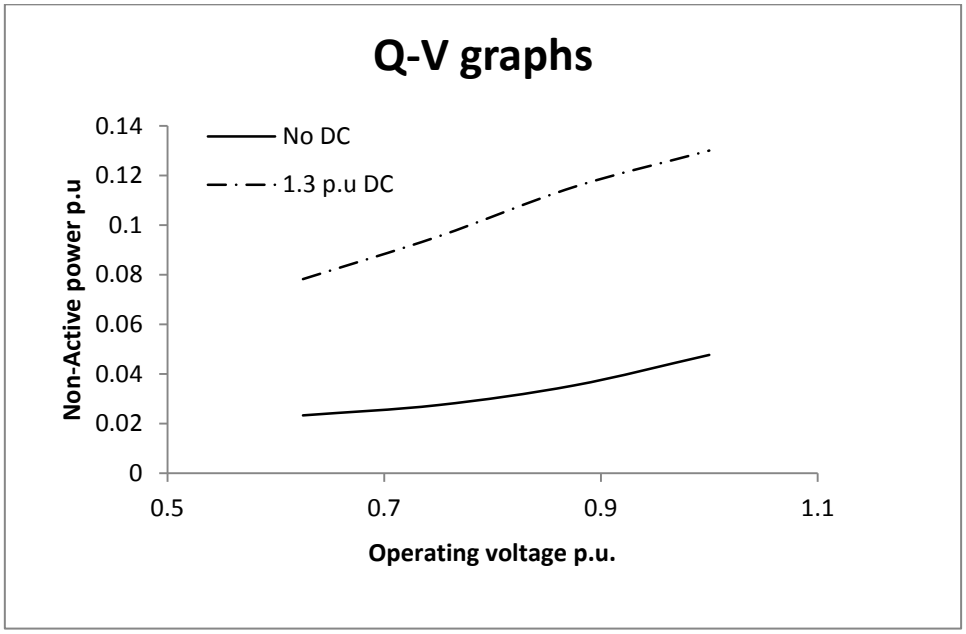

Figure 54: Q-V graphs showing effect of operating voltage in and out of the presence of DC at 70% load

As expected the absorbed non-active power is similar to that in the no load experiment as Q is a function of operating voltage and dc.

6.3.3.2 Harmonics

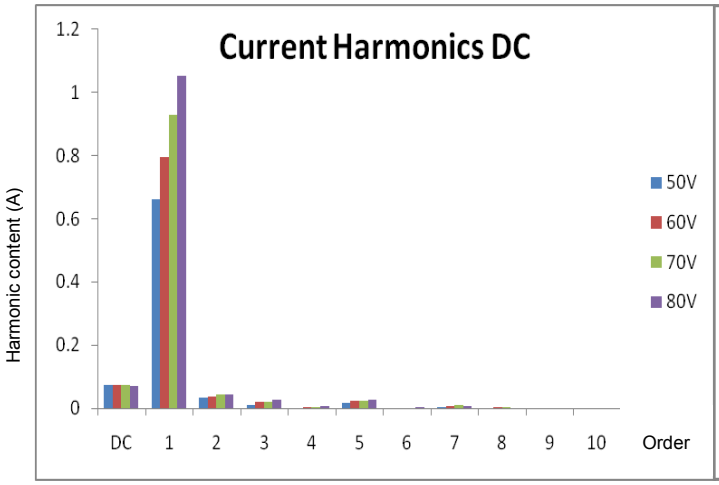

Figure 55: Current harmonics with a 70% loading configuration at different voltages in the presence of a constant dc.

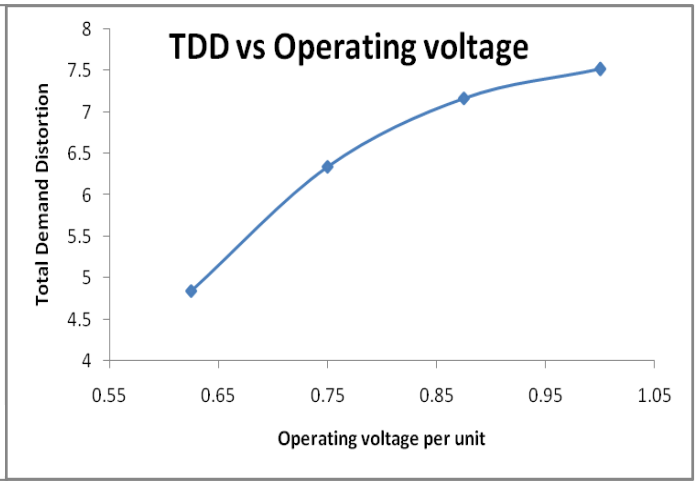

Figure 56: TDD against operating voltage in the presence of a dc

The diagrams above show the harmonic distortion in the transformer .A similar increase in harmonics is seen as before. There is an overall increase in the harmonics with a particularly larger increase in the 5th harmonic when there is a 70% load. The maximum TDD that was measured was 7.5%.

6.3.4 Variation of harmonic component magnitude with load

The harmonic patterns that are generated as a function of the operating voltage and the loading condition are not easily identified just by looking at their spectra. This is because the load current fundamental is relatively large when compared with the individual harmonics. The size of each harmonic was then analysed against the varying loading and voltage conditions. In earlier no load experiments, the harmonics that were used to indicate saturation were the 2nd, 3rd, and 4th harmonics since higher order harmonics were increasingly small. The results from the experiments presented here revealed that as the load increases in the presence of a dc, the 5th harmonic starts behave in a rather counter-intuitive manner (see equation 5.10).

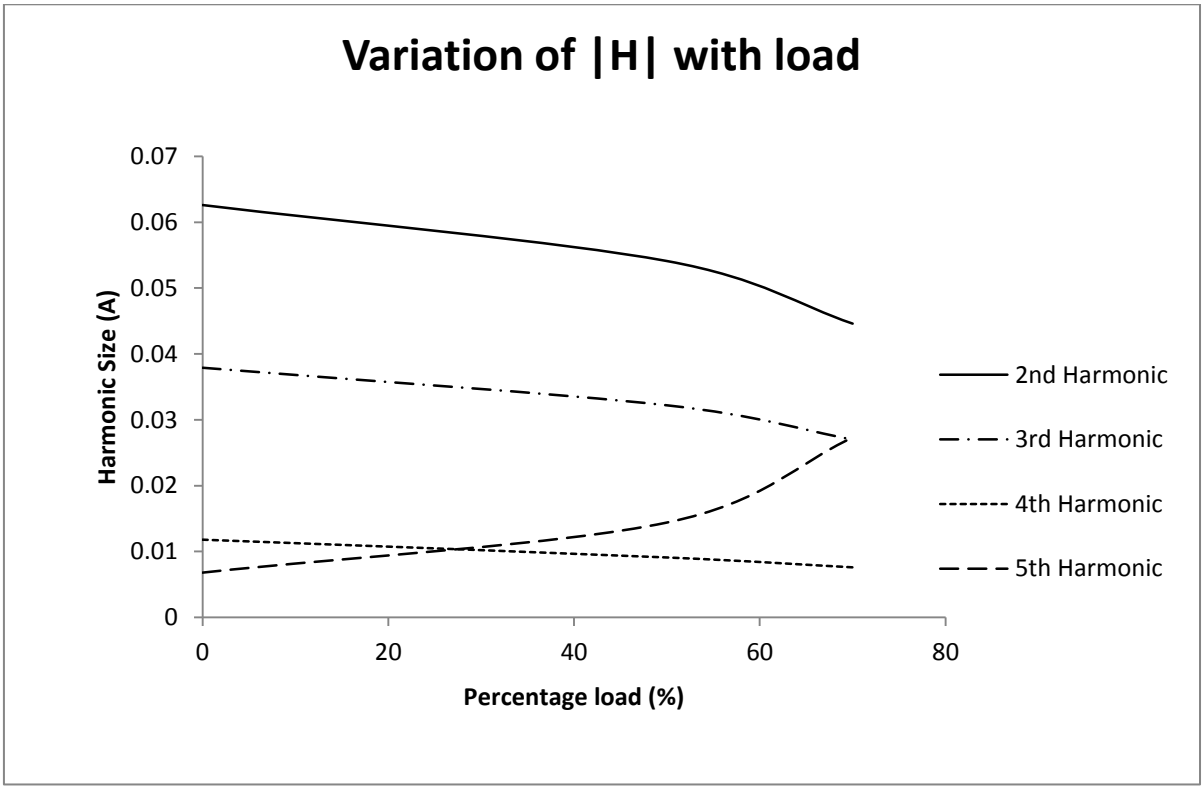

Figure 57: Graphs showing the variation of the harmonic magnitudes |H| with increasing load at 1.0 p.u. voltage (80V) and a constant dc.

Figure 57 shows that (at a constant dc and voltage) as the load is increased the 2nd, 3rd and 4th harmonics steadily reduce as the 5th harmonic suddenly increases. The 5th harmonic is smaller than the 2nd, approaches the 3rd and is larger than the 4th at the maximum loading configuration.

6.3.5 Discussion

The distorted B-H loop indicates the presence of dc however this is not enough to make conclusions on effect of reducing voltage.

A resistive load tending to full load causes the distortion levels to decrease owing to a dominant load current (though not significantly).

Reducing operating voltage reduces *Q* in the presence of dc. However if the dc is big enough the transformer will still go into saturation.

The transformer was observed to go into saturation when dc comparable with its I_{mag} was imposed on even when the applied voltage drastically reduced (well below the 10% specifications of QOS). Therefore the use of a significantly over-rated power-transformer (like the source transformer in the test system) with a very large core to withstand the half-cycle saturation would be required to guarantee a sizeable amelioration of the system conditions; which is not economically feasible, as also reported by Kappenman & Albertson (1990).

6.4 Different core structure response

This section presents the results of the tests described in section 5.3: *Bench Transformer Test C – Differential core type response*. Even though the transformers might not be completely comparable, the laboratory measurements and computer simulation (section 6.5) do indicate a consistent direction of response in the range tested. Completely comparable results require a deeper analysis of transformer design beyond the scope of this dissertation, but the testing protocol that has been developed offers a useful and consistent approach to testing different transformers.

6.4.1 Magnetization Curves

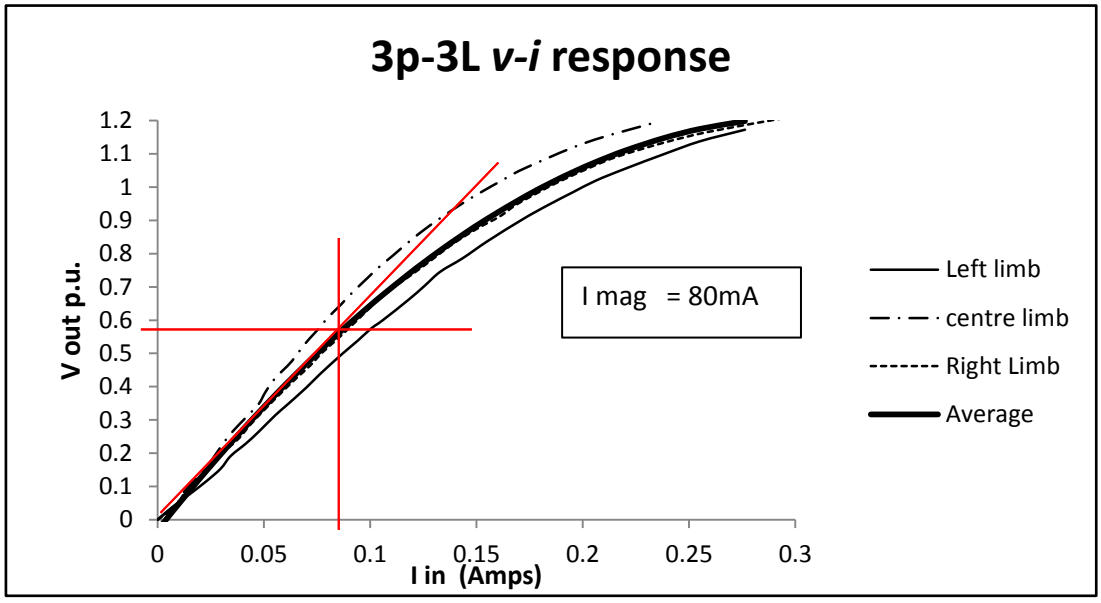

Figure 58: Magnetization curves of the *three phase three limb* load transformer. The knee point of the curve is defined to be at approximately 0.56 p.u. of the rated voltage with a corresponding magnetising current of 80mA.

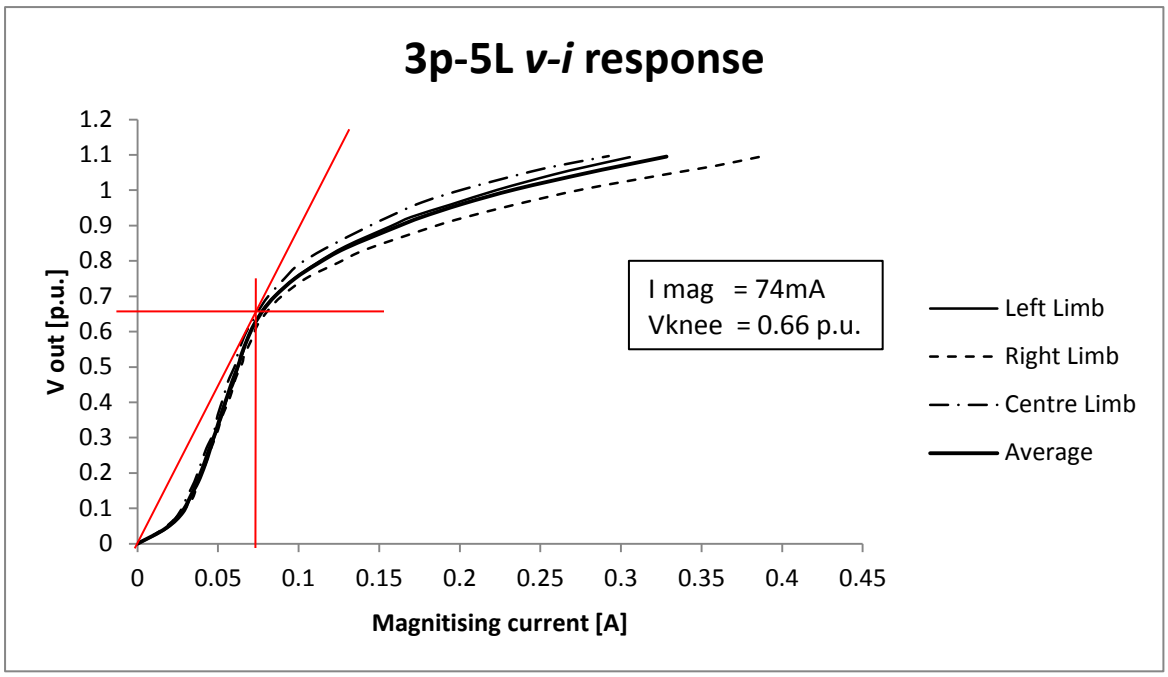

Figure 59: Magnetization curves of the *three phase five limb* load transformer. The knee point of the curve is defined to be at approximately 0.66 p.u. of the rated voltage with a corresponding magnetising current of 74mA.

The *v-i* responses of the two different load transformers can be seen in Figure 58 and Figure 59. The *3p-3L's v-i* response seems to be quite uncharacteristic in comparison with typical transformer cores. This may be attributed to the fact that for commercial purposes, these isolation LV transformers are not required to have a very high efficiency in most applications. The 3p-5L transformer appears to have a very similar response to that of the 3p-3s with a knee point voltage 33% below the name plate rating - see *Figure 14: Magnetization curve of the load transformer core (one phase).*This point (of maximum permeability) separates the linear operating region from the saturated region and denotes the commencement of saturation.

6.4.2 Q-dc investigation

This section illustrates the Q-dc response of the different core structures of transformers. First each core type's response is discussed, then the results are compared on the same graph using the per unit system.

6.4.2.1 Three phase bank transformer system (3p-3s)

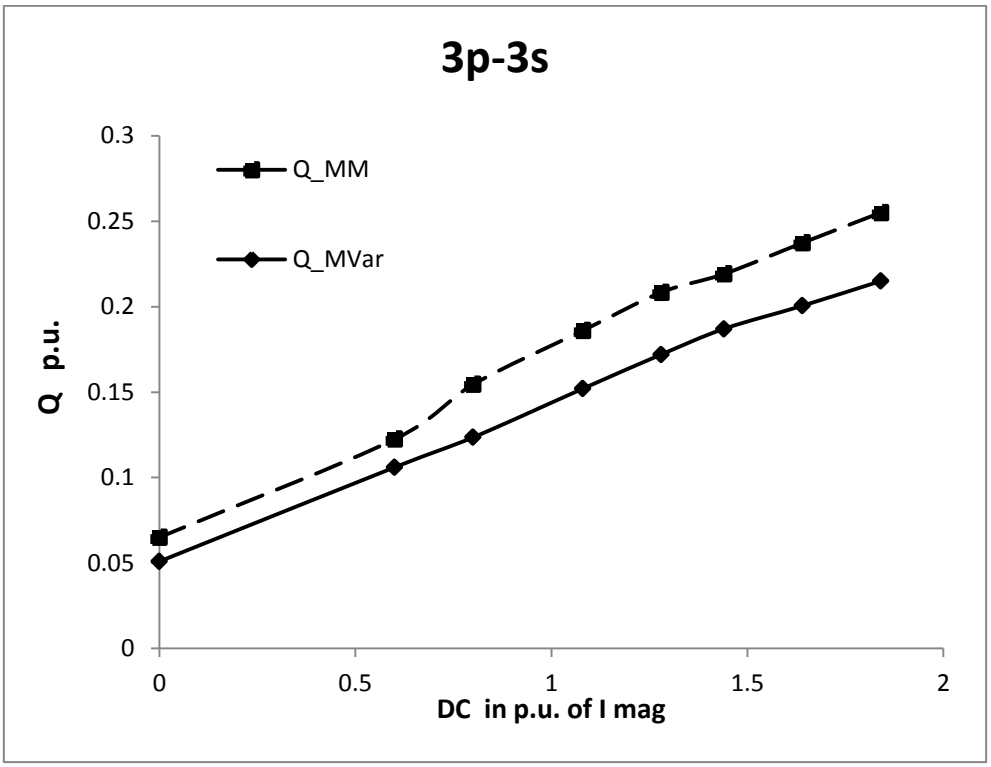

Figure 60: Q-dc response of the 3p-3s transformer system on a 200VA base.

The differences that come with the two methods of calculating power are once again represented in **Error! Reference source not found.**. The reactive power Q_{MVar} has a very linear relationship with dc as widely reported in literature whereas the non-active power Q_{MM} appears to slightly diverge from a strict linear path as the levels of dc approach 1 p.u. of the knee point magnetising current.

6.4.2.2 Three phase five limb transformer system (3p-5L)

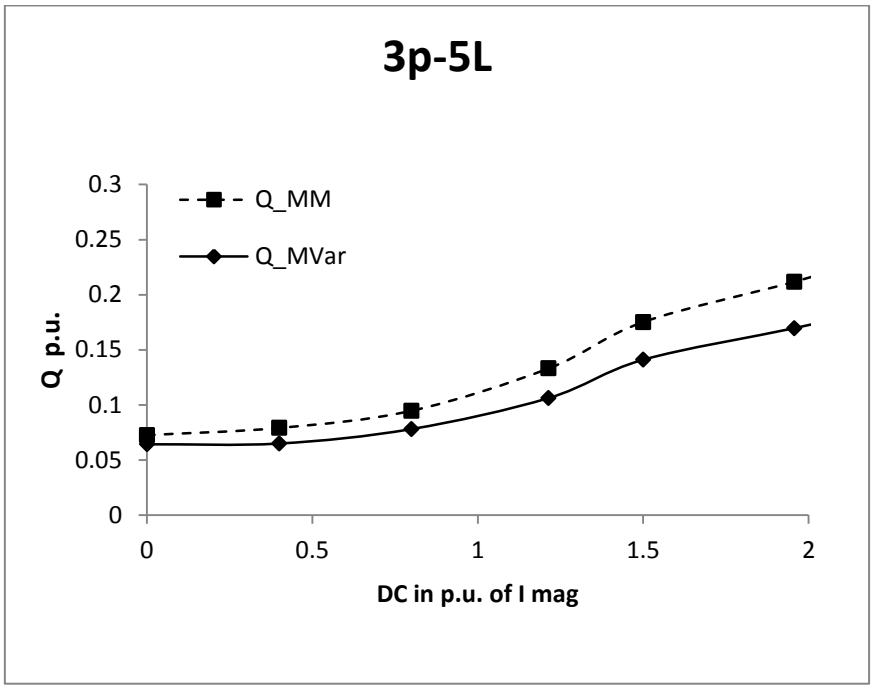

Figure 61: Q-dc response of the 3p-5L transformer system on a 200VA base.

Non-active power Q_{MM} yields a higher calculation than that of reactive power Q_{MVAr} as the dc increases. The shape of both curves does not appear to be strictly linear as their slopes change after 1 p.u. dc. This may be a characteristic of the core structure

6.4.2.3 Three phase three limb transformer system (3p-3L)

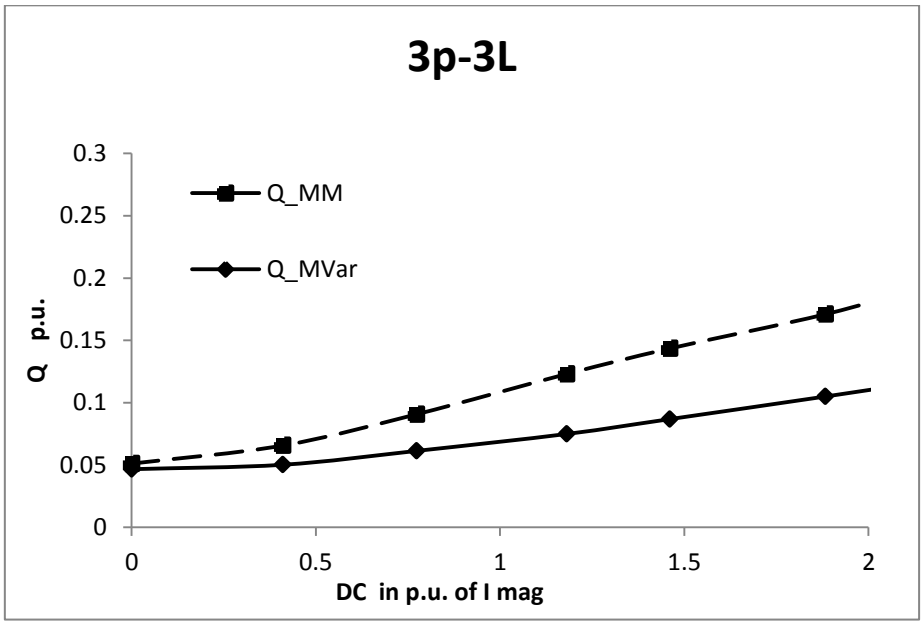

Figure 62: Q-dc response of the 3p-3L transformer system on a 200VA base.

Figure 62 shows that the differences between Q_{MM} and Q_{MVar} become quite significant as the dc is increased with the 3p-3L core structure.

6.4.2.4 Non-active Power

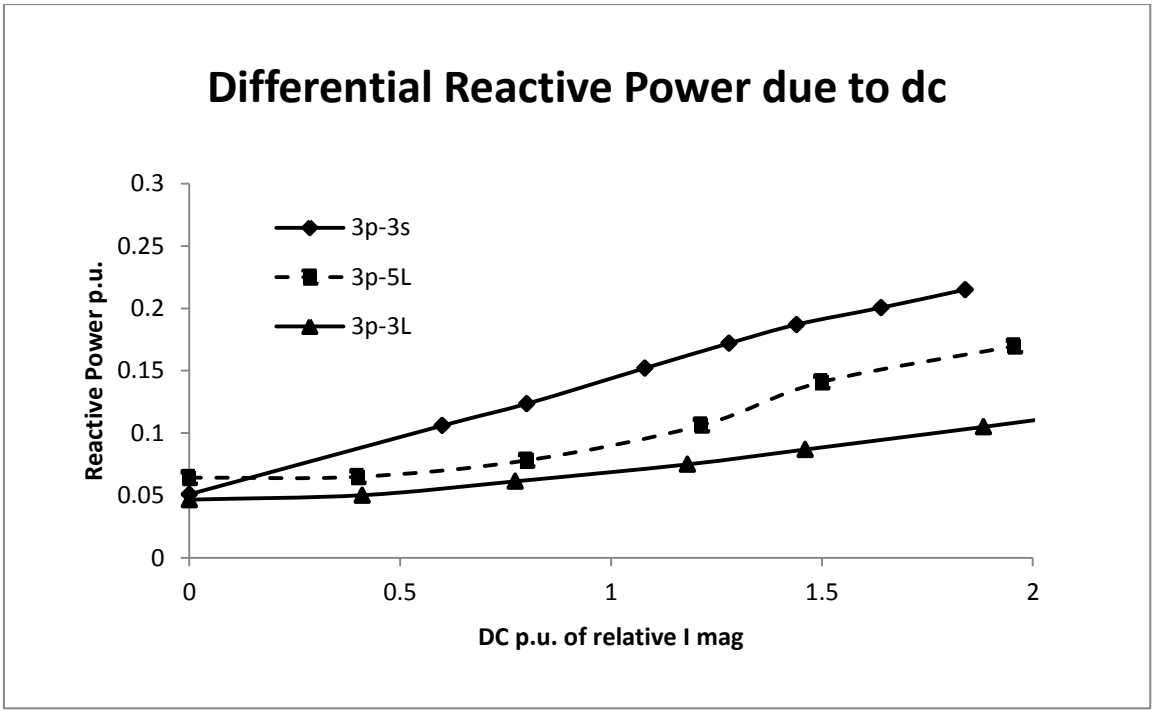

Figure 63: A representation of the reactive power of each transformer core type when imposed with the same amount of dc under the same relative conditions of voltage and resistive loading.

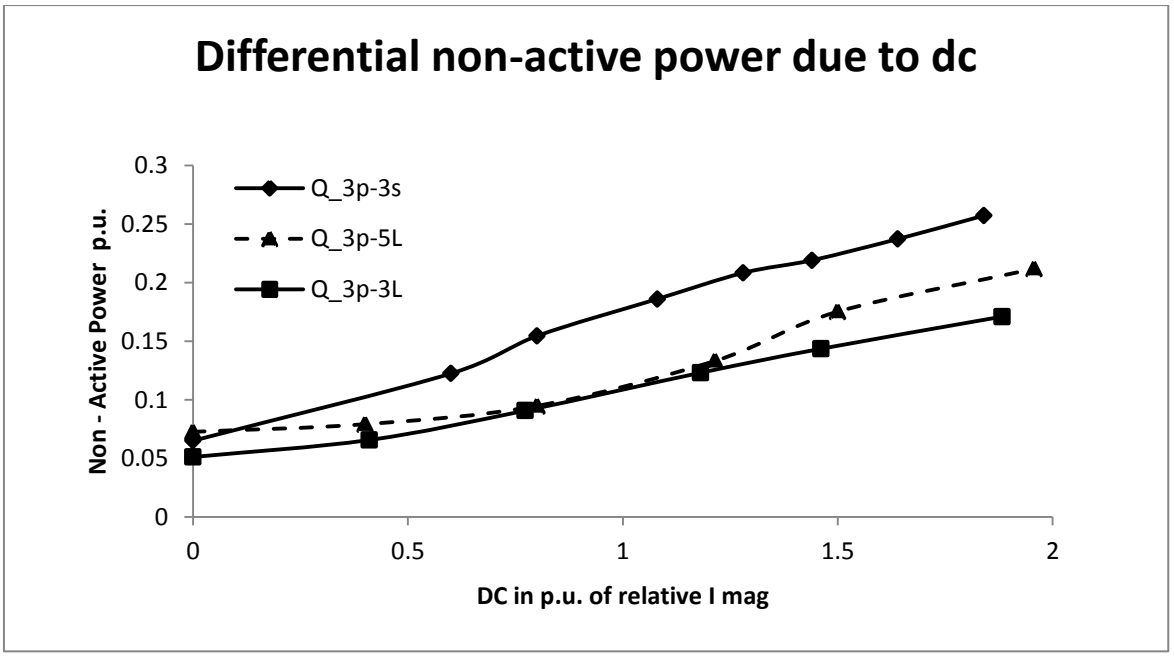

Figure 64: A representation of the non-active power of each transformer core type when imposed with the same amount of dc under the same relative conditions of voltage and resistive loading.

As represented in Figure 63 and Figure 64, the core-type measured to absorb the highest amount of *Q* under the dc excitation is the 3p-3s followed by the 3p-5L which is followed by

the 3p-3L. A higher Q_{MM} is generated for all types of transformers as the dc excitation is steadily increased.

6.4.3 Comparison of Q with power transformers (MVA range)

Having investigated the Q-dc responses of the bench transformers, the next activity probed into how the response of typical power transformers would compare against the tested bench transformers. As already discussed in the literature survey, it was found that early investigations into the core-type susceptibility function of power transformers to GIC effects yielded conflicting conclusions among researchers. For instance, the conclusions on specific core-type responses due to dc excitation brought about a lengthy dialogue (Takasu et. al, 1994, -discussion) on the issue of a *three phase three limb transformer*. Kappenman who was not in full agreement with the notion that this type of transformer was immune to dc excitation, presented some field test results that showed evidence of harmonics generation and significant reactive power demand in not only a *single phase shell type* (where the general consensus was that this type of transformer was very vulnerable to GICs), but also in a *three phase three limb auto-transformer*. The transformer ratings provided by the author are shown in Table 12.

Table 12: Power transformer ratings for the field tests performed by Kappenman (1989).

Core - structure	Voltage	Capacity
Three Phase Three limb	230/115kV	187 MVA
Single Phase Shell Type	500/230kV	187 MVA

While the Q-dc curves presented by Kappenman conveyed a very clear picture of how these large transformers (6 X 10^5 times bigger than the UCT bench transformers) responded, very little information was given that could be used in the developed protocol (Chisepo, *et al.,* 2013). In particular the *v-i* characteristics that would provide the magnetising current at the knee point voltage was necessary to establish a per unit base for the dc. Approximations were therefore made for each transformer whereby the knee voltage was assumed to be at 1.0 p.u. with a corresponding magnetising current of 2% of the rated load current. This magnetizing current was then used to per-unitize the dc that was given in Amperes per phase. The bench-scale results that were used to compare against the power transformers were on the same per unit bases as those in the preceding sections. Since Kappenman calculated the reactive power absorbed by the power transformers, only the Q_{Mvar}-d*c* response is contrasted. The single phase shell type power transformer is

compared with the bench 3p-3s system, whose banks consist of single phase shell type transformers.

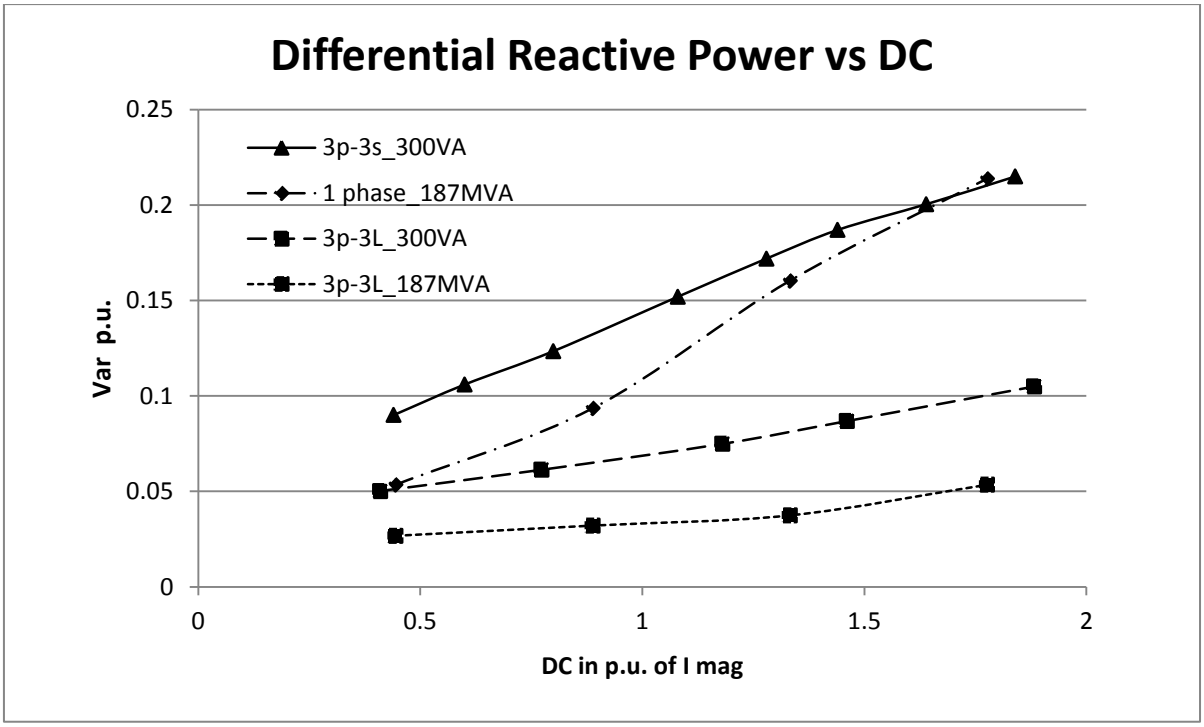

Figure 65: A comparison of the differential reactive power due to dc excitation involving measured results from the bench scale system and field tests conducted by Kappenman (1989). The 1 phase 187 MVA transformer is not a three phase bank but a single transformer unit.

Figure 65 illustrates the similarities in the response of transformers of similar core structures. Looking at the *3p-3s* (300VA) and the single phase (187MVA) transformers; both consisting of shell type single phase transformers, the shape of the reactive power versus dc in per unit seems to be related, especially when it comes to the steepness of the response. The *3p-3L* systems also appear to have a correlated response, with the 300VA response appearing to be an offset of that of the 187MVA.

However the results may be of great value for two reasons: (a) they demonstrate similarities in the shapes of the core structure differential *Q-dc* responses, and (b) the curves can easily be mapped onto the anticipated non-active power response (based on observations in section 6.4). This therefore opens up possibilities for power utilities like South Africa's Eskom to predict a very good estimate of not only the reactive power, but more importantly the non-active power demand that will arise from a predicted magnitude of GIC during a geomagnetic disturbance.

6.4.4 Harmonic analysis and Voltage collapse

First, the current harmonics will be presented in their spectra or bar graph form to enable the analysis of the individual harmonic components. The total demand distortion that arises at varying levels of dc will then be discussed and light will be shed on the differences that come with each core structure. Only the current harmonics in the red phase will be under consideration in this section. The rest of the results showing the harmonics yellow and blue phases, along with their corresponding THD's are given in Appendix C.

6.4.4.1 Current harmonics no load bench transformers

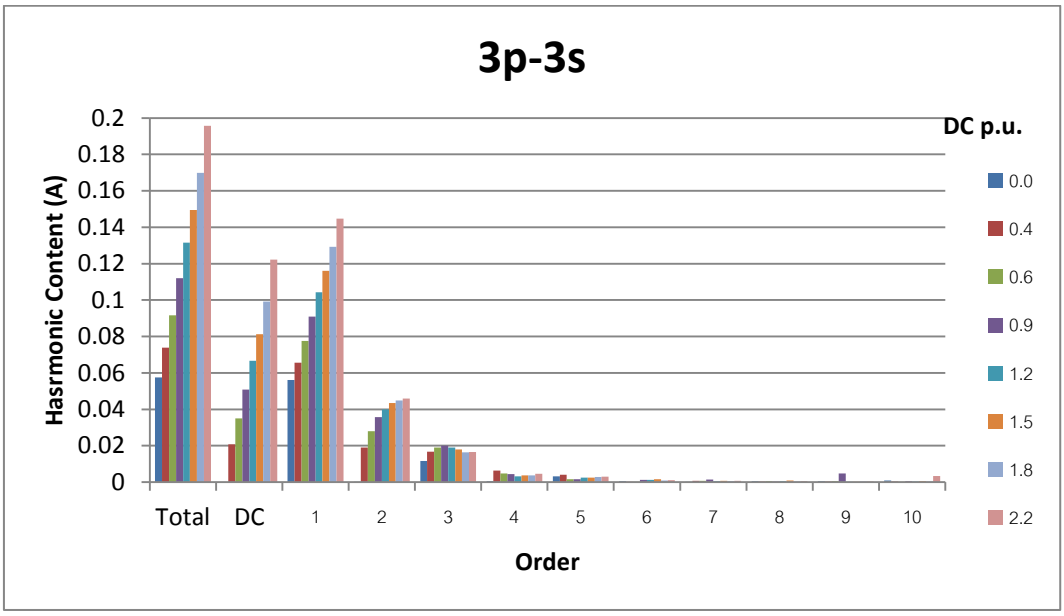

Figure 66: Harmonics generated with increasing levels of dc in the three phase bank of single phase shell type transformers –red phase.

Figure 66 shows the harmonic spectrum of the *3p-3s* transformer. As seen from earlier tests, there appears to be an increase in both even and odd harmonics as the levels of dc increases. The size of the fundamental increases linearly with dc as the magnetising current component is directly affected by the imposition of a dc component

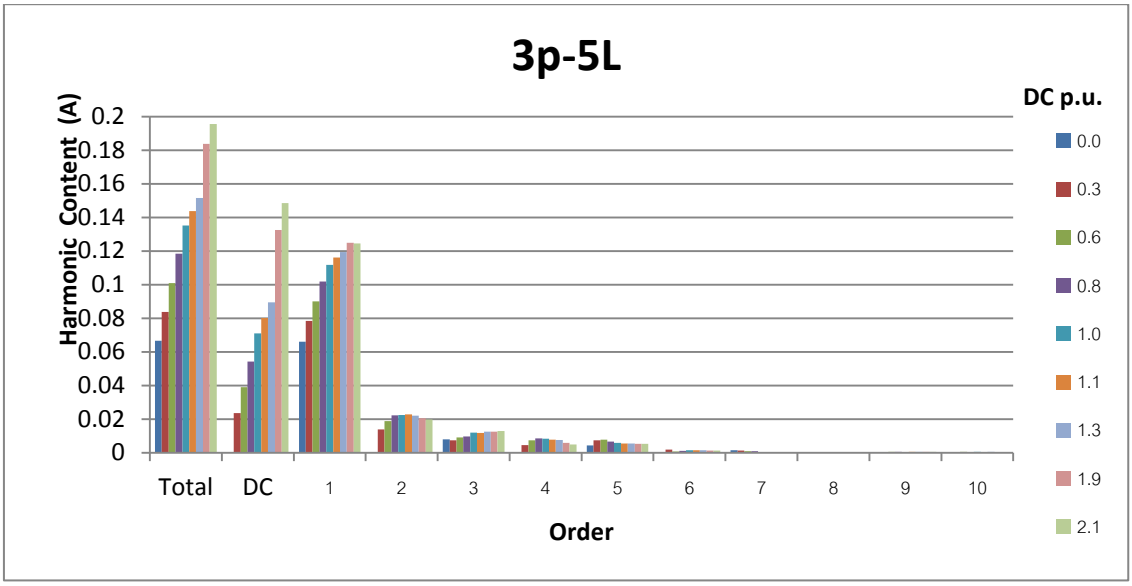

Figure 67: Harmonics generated with increasing levels of dc in the three phase five limb transformer – red phase

In Figure 67 the *3p-5L* transformer seems to generate harmonics similar to those of the *3p-3s* transformer. The saturating harmonics however appear to be of smaller magnitudes. Appendix C3 shows the harmonic profiles of each phase of the *3p-5L* transformer and it is clear the phase *r* and *b* (the two outer limbs) have similar harmonic order profiles. The 3rd harmonic of phase *y* (centre limb) rises more significantly with increasing dc. These results are similar to a *3p-5L* transformer model's response under dc bias reported by Li, *et al.* (2010).

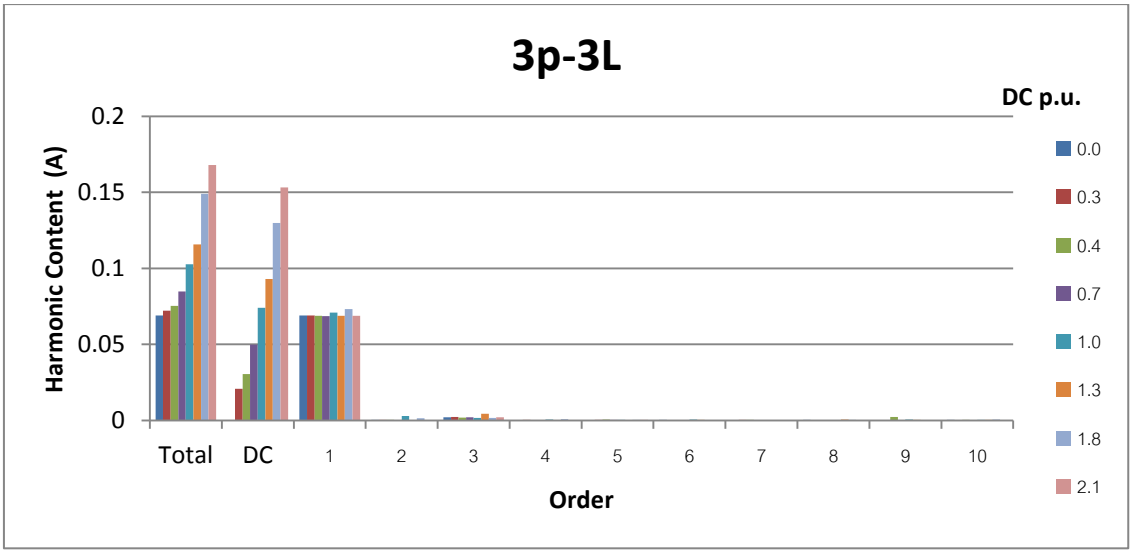

Figure 68: Harmonic spectrum of the three phase three limb transformer with increasing levels of dc – red phase.

The *3p-3L* transformer does not generate any noticeable harmonics at all levels of dc, illustrated in Figure 68. The fundamental remains intact at all levels of dc signifying a zero effect on the magnetising current of the transformer.

In order to analyse further the differences between how each core type behaves, the TDD is plotted against direct current on the same curve (see Figure 69). The curves indicated clearly that the *3p-3s* exhibits the highest amount of distortion which is closely followed by

the *3p-5L*. Initially, their TDD seems to rise sharply with increasing dc up to 1 p.u., after which the distortion levels of for the *3p-3s* and diminishes for the *3p-5L*. The 3p-3L does not seem to have a significant amount of distortion despite the increasing levels dc imposed on it.

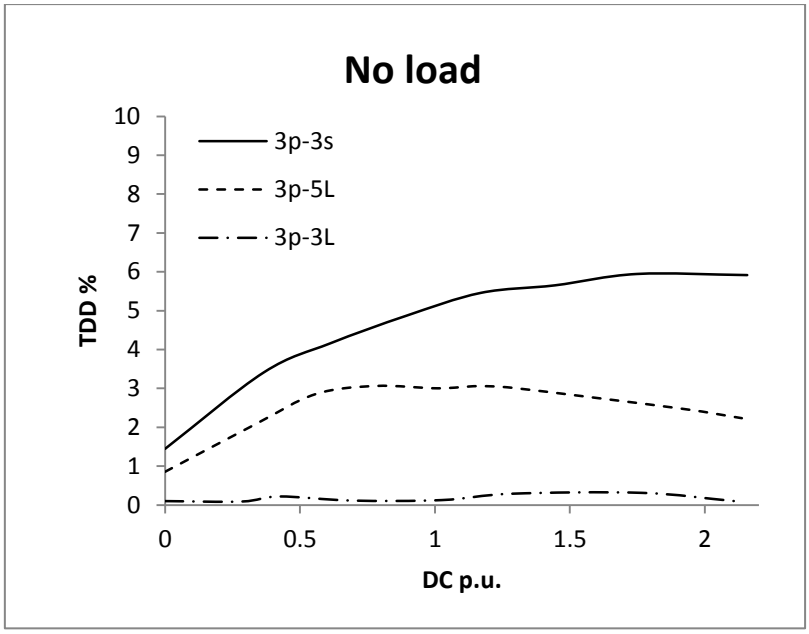

Figure 69: Total Demand Distortion (TDD) of each core type with increasing direct current

6.4.4.2 Volt drop (no load) – bench transformers

When an increasing amount of dc is imposed on a transformer non-active power losses are experienced as has been observed in earlier sections. This brings rise to increased inefficiencies in the transfer of energy which may result in a voltage depression. Though the voltage waveform per se was not experiencing any significant distortion at dc levels up to 2 p.u., it was carefully monitored to see how it behaved at each dc injection level. The voltage response of each transformer core structure is seen shown in Figure 70

The 3p-3s transformer exhibits the most extreme amount of voltage drop with its voltage dropping down to by 50% at the highest dc value. The 3p-5L transformer system also experiences a significant voltage drop with a maximum drop of 20%. The 3p-3L transformer did not show any signs of voltage drop throughout the full range of dc injection up to and including 2.0 p.u., which was unexpected according to theory.

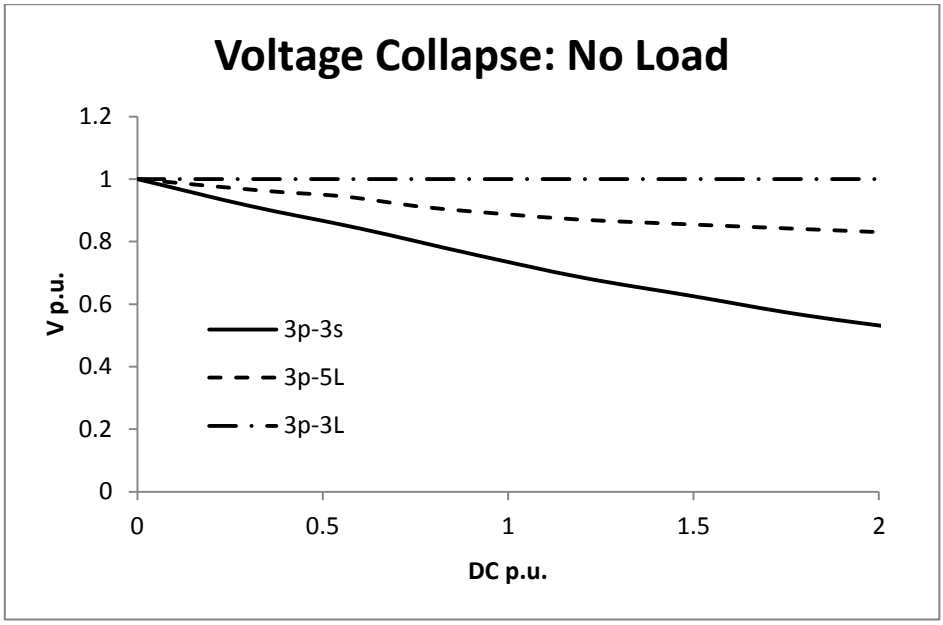

Figure 70: Measured results of the voltage drop across the transformer at no load with increasing dc

6.4.4.3 Harmonic analysis (loaded)-bench transformers

The next investigation involved the harmonic analysis of the line current when the transformers were loaded. An arbitrary resistive loading configuration of 70% of their rated capacity was incorporated into the system. Showing in Figure 71 is the THD response of each core type under loaded conditions (the corresponding harmonic spectra can be seen in Appendix D. The curves indicate that the distortion in the line current is significantly reduced due to the dominant load current whose component is much larger than the injected both the injected dc and the transformers magnetising currents (by a factor of >10 times).

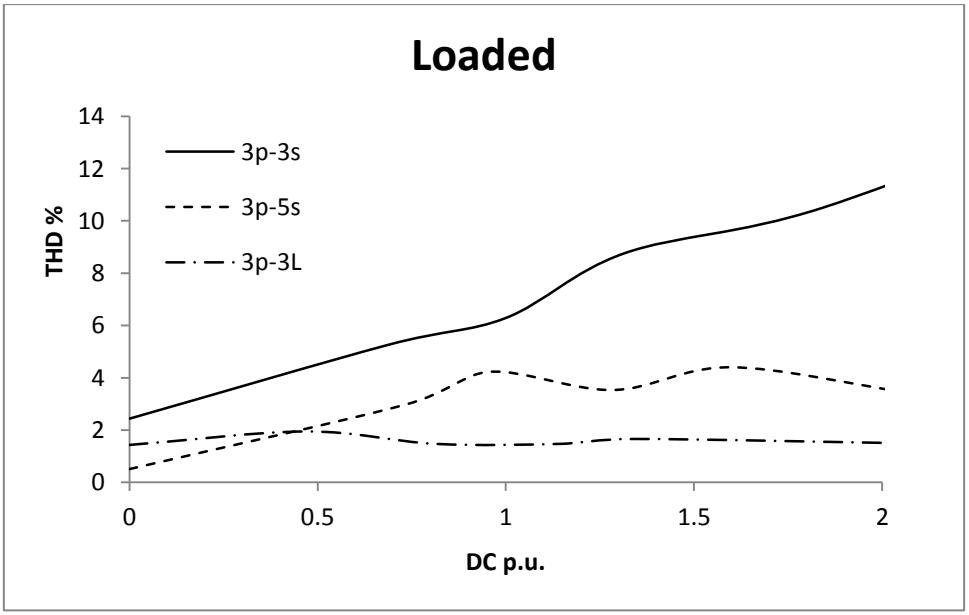

Figure 71: THD response of the different core types to increasing dc under loaded conditions

6.4.4.4 Volt drop (loaded) – bench transformers

It can be seen from Figure 72 that the presence of resistive load, ideally characterized by unity power factor conditions, the volt drop in the presence of dc is somewhat alleviated. The 3p-3s transformer system has the most significant voltage drop of about 19% at 2 p.u. dc while the other two core type do not show any significant drop in their voltage profiles.

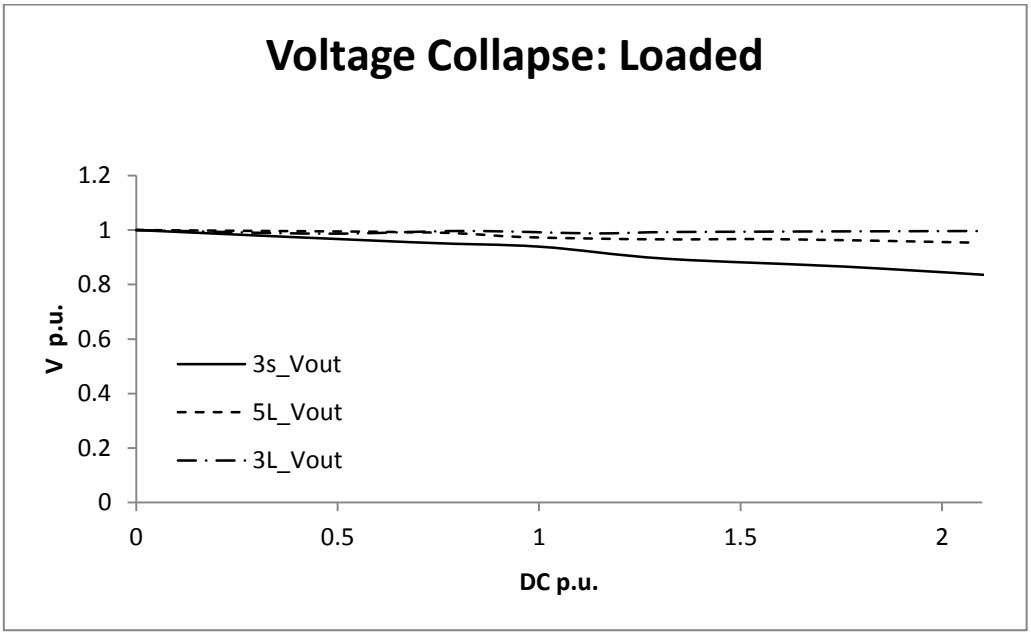

Figure 72: Measured results of the bench transformer output voltages with increasing dc

6.4.5 Discussion

The resultant Q-dc response differs with each core type. The differences between reactive power and non-active power have been demonstrated in the context of differing core structures and the non-active power is higher in all instances.

There is an association between the intensity of dc and the levels of current distortion and it also differs with core type. The shapes of the TDD curves at no load show that beyond dc input of 1p.u. both the *3p-3s* and the *3p-5L* transformers diverge from having a linear relationship with magnitude of dc, and that the *3p-5L* is pushed into the 'air-core region' at relatively lower dc levels than the *3p-3s*.

The differences that arise in the transformers' response when they are loaded are determined by the dominant resistive load current. Because the load draws a largely

sinusoidal current, there is less distortion in the system. This also has the effect of requiring a much larger dc to push the transformer core into the 'air-core region' and ultimately complete voltage collapse. Therefore in this light a resistive loading condition (tending to unity power factor at the output) has a 'helping effect' with current distortion and the rate at which the voltage is depressed.

The voltage collapse caused by the imposed dc on the *3p-3s/5L* transformers is due to the rate at which power factor, which can be seen as a measure of efficiency of energy transfer, drops with increasing dc and is dependent on the resistive loading condition. If the no load condition is taken to be the base case, the voltage collapse is less severe when there is a resistive load because the line current is largely sinusoidal (power factor tends to 1). At no load, when virtually the (non-sinusoidal) magnetizing current is flowing in the system, the power factor is very low and is dramatically affected by the imposed dc which therefore leads to severe voltage collapse.

6.5 Simulations

The simulation procedure in section 5.4 was investigated on the two transformer models available in PSCAD. The results are presented in subsequent sections.

6.5.1 Classical Approach

PSCAD's inherent classical modelling approach, which can only model single phase transformers, was investigated in the form of a three phase bank system (*3p-3s*). The results from the simulation protocol are displayed below.

6.5.1.1 Transformer selection and parameterization

Table 13: Parameter values of each single phase unit of the test transformer bank.

Parameter	Value
Base MVA	0.0000667 [MVA]
Base frequency	50.0 [Hz]
Leakage reactance (primary)	0.009 [p.u.]
No load losses	0.046 [p.u.]
Primary winding voltage (RMS)	0.080 [kV]
Primary side magnetizing current	6.60 [%]
Secondary winding voltage (RMS)	0.150 [kV]
Air core reactance	0.020 [p.u.]

Table 13 shows the parameter values that were used to model the *3p-3s* test transformer's configuration and saturation characteristics. The *S* base was 33.3% below the actual transformer's name plate rating as per McLyman's definition of linearity. The base frequency for all tests was 50 Hz. The leakage reactance and the no load losses were derived directly from the short circuit and open circuit tests respectively. According to the EMTDC manual, the air core reactance which is usually not known is approximated to be twice the leakage reactance as a rule of thumb**.** Therefore the same approximation was applied in the model.

6.5.1.2 Open circuit test

Table 14: Simulated open circuit test results compared against measured results

Parameter	R		Y		B	
	meas.	sim.	meas.	sim.	meas.	sim.
I (A)	0. 055	0.060	0.055	0.060	0.055	0.060
P (W)	3.10	3.11	3.10	3.11	3.10	3.11
Q(Var)	3.33	3.56	3.33	3.55	3.33	3.57

The PSCAD model was energized at a voltage representing 1.0 p.u. (V_{in}=V_{knee} = 80V) as per the O.C procedure described in the simulation protocol (section 5.4). The results are displayed in Table 14 and it can be seen that the simulation parameters represented the measured results quite adequately.

6.5.1.3 Loaded tests

Table 15 Simulated loaded test results compared against measured results

Parameter	R		Y		B	
	meas.	sim.	meas.	sim.	meas.	sim.
I (A)	0.724	0.728	0.727	0.728	0.723	0.728
P (W)	52.1	53.4	52.2	53.4	52.1	53.4
Q(Var)	3.33	3.56	3.33	3.55	3.33	3.57

Running the PSCAD model with about a 90% resistive load (on a 200VA base) yielded the results shown in Table 15. The slight discrepancy between the simulated and measured phase powers were due to the internal impedance (*IZ*) of the bench transformers causing a slightly bigger volt drop at the output when the transformer is heavily loaded i.e. voltage regulation (Sen, 1997).

6.5.1.4 Dc injection scheme

Table 16: Measured and simulated dc currents for the instance of a neutral dc injection of 151 mA.

Neutral dc (A)		R (A)		Y (A)		B (A)	
meas.	sim.	meas.	sim.	meas.	sim.	meas.	sim.
0.151	0.151	0.051	0.050	0.050	0.051	0.050	0.051

Table 16 shows the simulated dc values per phase compared against the measured results when a neutral dc of 151 mA is injected into the transformer neutrals. The dc component was determined by running an FFT for each line current in the model, and practically it was measured using the Yokogawa Power Meter (the dc neutral current in the laboratory was monitored with a current clamp). It can be seen that the expected 1/3 factor between line and neutral dc is consistent in both the laboratory and the simulation model.

6.5.1.5 Results

The complete PSCAD model was capable of simulating various aspects of the electrical and magnetic response of transformer shown below:

(a) BH loops

Using an XY plot of the magnetic flux linkage versus the magnetising current, a representation of the simulated hysteresis loop was generated. A dc value that was known to push the transformer into saturation was used and the simulation results were compared against the measured results.

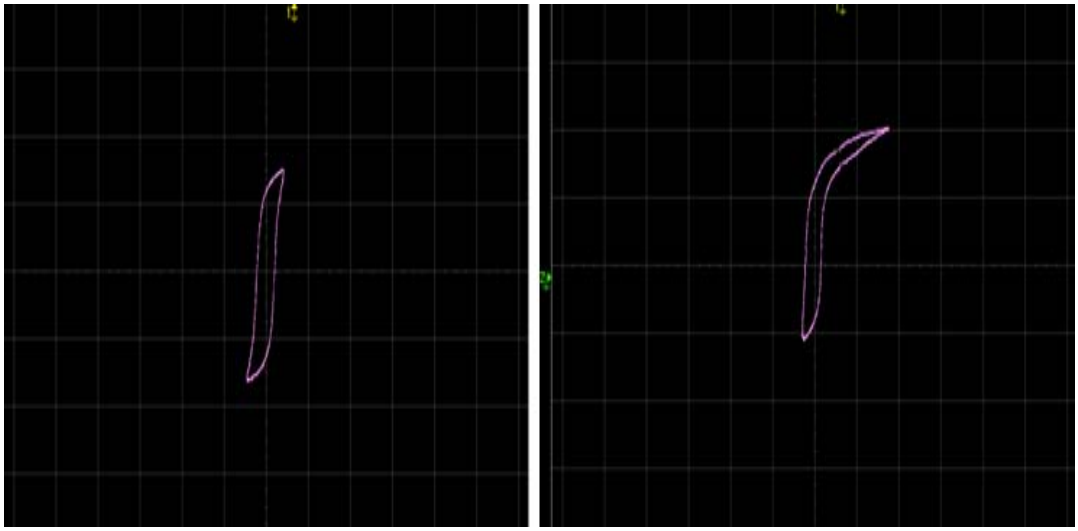

Figure 73: BH loop of the TuT in the laboratory at the knee voltage without DC (left) and with 70mA DC, 1.3 p.u. of Imag (right). Injection of DC leads to a vertical shift and a distortion of top of the loop.

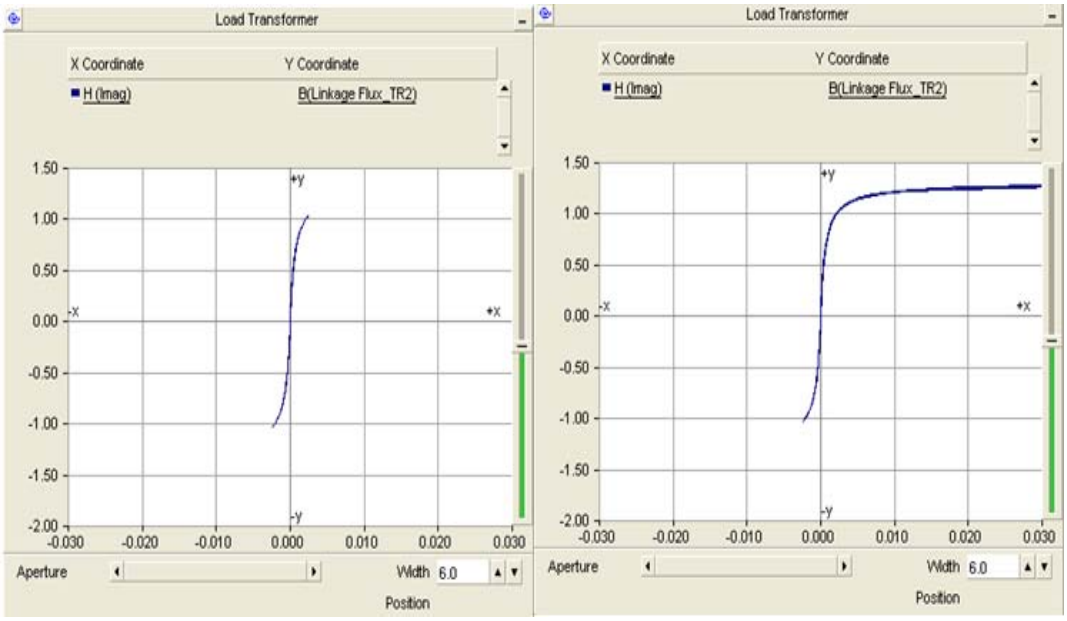

Figure 74: Hysteresis loop of TuT modelled in PSCAD using the magnetic flux versus the magnetising current. No DC (left), and 70mA DC injected (Right).

Figure 73 shows the measured effect of dc injection on the TuT operating at its knee point voltage at no load. The dc injection causes a vertical shift of the loop as well as the flattening of its top. This effect can be further amplified by increasing the level of dc, as also reported in Heindl *et al.* (2011), and the transformer will experience 'deep saturation'. Simulations in PSCAD/EMTDC showed agreement in terms of the shape that results from the distortion of the BH loop to the effect of different levels of dc injection (see Figure 74). The hysteresis loops of the source transformer for all values of dc in per unit of I_{mag} showed very little or no change both in the laboratory and in the simulations, as expected.

(b) Reactive and Non-Active power response

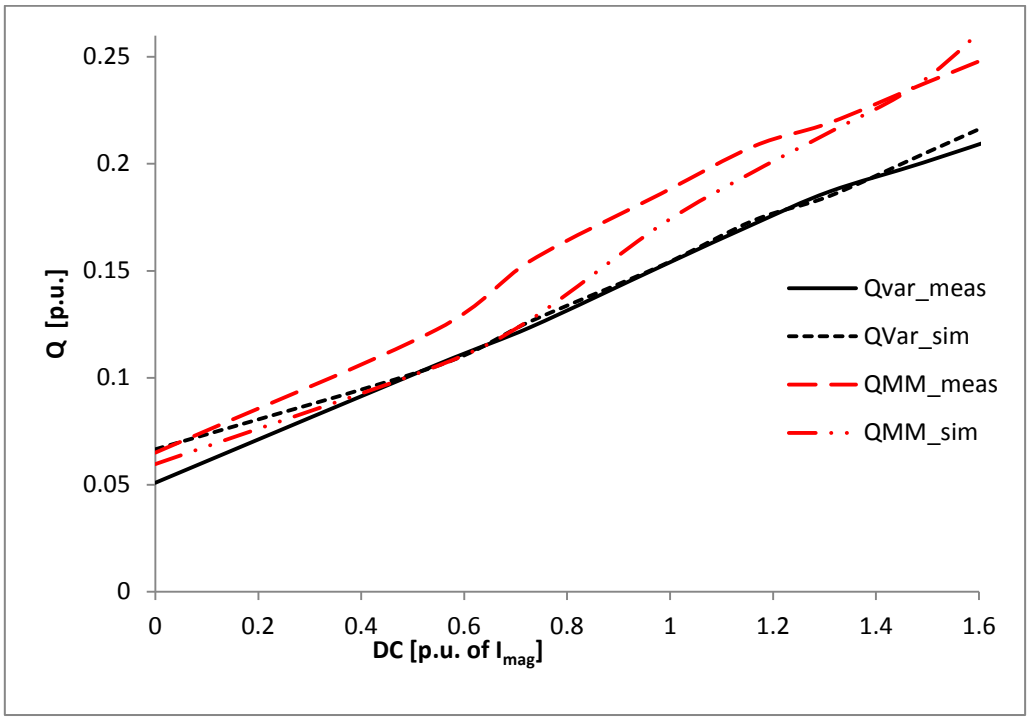

Figure 75: A representation of the measured and simulated and measured Q-dc response.

Figure 75 shows that the simulated Q-dc characteristic correlated quite well with the measured response. The reactive power Q_{Var} (black) seems to have a linear relationship with dc while the non-active power Q_{MM} (calculated using the general power theory - red) slightly diverges from linearity as the dc input approaches 1 p.u.

6.5.2 UMEC Approach

The PSCAD system modelled using the classical approach was then upgraded to the *UMEC* approach. The same protocol and transformer ratings were applied for each transformer core type in this part of the investigation.

6.5.2.1 Transformer selection and parameterization

The UMEC approach was used to investigate the following core structures:

- Three phase bank made up of single phase shell type units -3p-3s
- Three phase three limb -3p-3L
- Three phase five limb – 3p-5L

The configuration parameters were adjusted for each transformer core-type in the UMEC transformer models. The piecewise saturation curves were then taken directly from the transformers' magnetization curves (see sections 4.3 and 6.4.1), while the core aspect ratios were entered as measured from the actual transformers. For the multi-limb

transformers with mutual inductances, the average of the saturation curves in each limb was used to represent their *v- i* characteristics.

Table 17 shows the piecewise *v-i* inputs and corresponding *v-i* curve that were used for the *3p-3s* test transformer. The corresponding magnetization curve that the software generated can be seen in Figure 76. The saturation curve parameters and their corresponding *v-i* curves of the *3p-3L* and *3p-5L* transformers can be seen in Appendix E.

Table 17: Saturation curve parameters for the 3p-3s test transformer

Point [I,V]	I_{mag} [% of rated I]	V [p.u.]
1	0.00	0.00
2	2.11	0.078
3	3.56	0.254
4	4.45	0.525
5	5.24	0.758
6	6.62	1.01
7	10.1	1.30
8	12.1	1.43
9	15.9	1.59
10	23.8	1.82

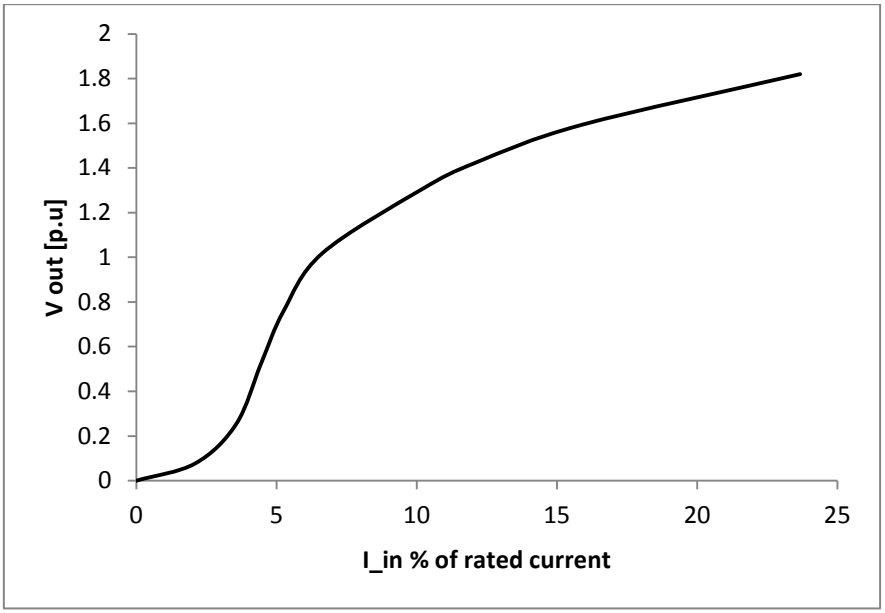

Figure 76: Corresponding Saturation curve used for the 3p-3s test transformer

6.5.2.2 Open circuit tests (UMEC)

The O.C test results when each transformer was energized to its relative 1p.u. (knee voltage) are presented below. It can be seen that the UMEC transformer model generated some bad correlation with respect to the magnetizing currents and phase reactive powers especially for the *3p-3s* and *3p-5L* models. The *3p-3L* UMEC model however yielded a better open circuit correlation with the measured results.

Table 18: Three phase banks system (3p-3s). Simulations severely dissimilar to measured results are shown in red.

Parameter	R		Y		B	
	meas.	sim.	meas.	sim.	meas.	sim.
I (A)	0. 055	0.237	0.055	0.237	0.055	0.237
P (W)	3.10	3.36	3.10	3.36	3.10	3.36
Q(Var)	3.33	17.7	3.33	17.7	3.33	17.7

Table 19: Three phase three limb system (3p-3L)

Parameter	R		Y		B	
	meas.	sim.	meas.	sim.	meas.	sim.
I (A)	0.088	0.102	0.066	0.066	0.083	0.110
P (W)	1.012	0.34	0.565	0.644	0.24	1.56
Q(Var)	3.52	4.13	2.73	2.61	3.52	4.173

Table 20: Three phase five limb system (3p-5L). Simulations severely dissimilar to measured results are shown in red.

Parameter	R		Y		B	
	meas.	sim.	meas.	sim.	meas.	sim.
I (A)	0.078	0.151	0.073	0.204	0.082	0.159
P (W)	4.53	1.17	4.52	1.79	4.80	3.80
Q(Var)	4.20	12.0	4.12	15.9	4.31	11.9

6.5.2.3 Response to dc injection

The transformer systems were then loaded and had dc injected into their neutrals. The following observations were made from the simulations:

1. ***3p-3s***

The UMEC model greatly exaggerated the magnetising currents (see Table 18), which was unexpected. The resultant *Qs* in each phase were too large even without the effect of dc excitation. Figure 77 goes shows that when a dc that was a function of the measured I_{mag} was injected into the system, there was no change in *Q* because the dc offset seen by the line current was almost negligible. Therefore the UMEC model for this transformer core type did not yield satisfactory results when compared against the actual lab transformers see Figure 77.

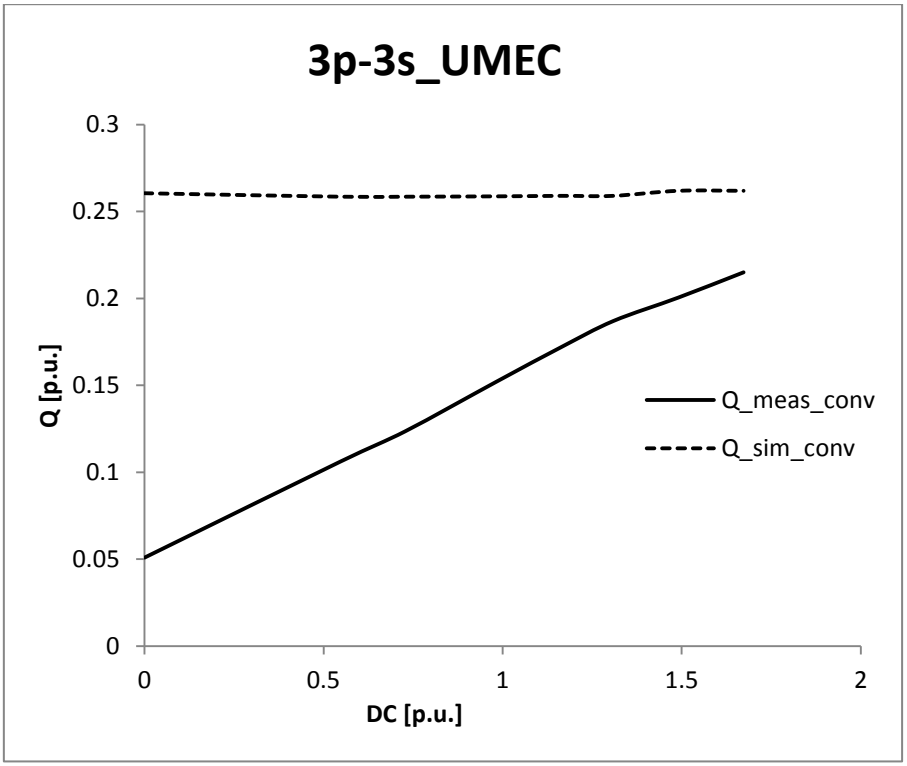

Figure 77: A comparison of the simulated and measured Q-dc response for the UMEC 3p-3s transformer system yielding unexpected results. The solid line represents the measured reactive power Q_meas_conv and the dotted line represents the simulated reactive power Q_sim_conv.

2. *3p-3L*

The modelled open circuit conditions seemed to correlate closely with the bench measurements (see Table 19); with the exception of minor deviations in the line currents due to the asymmetry of the core structure. However when various levels of dc were injected relative to the I_{mag}, no change was seen in the *Q* response of the transformer (see Figure 78). In the actual laboratory tests, the three phase three limb units did not have a steel tank enclosure. The effect that this possibly had on the results was a slight amelioration of the dc effects because of the absence of a dc flux path. In real power transformers with a steel tank enclosure, a dc flux return path is offered by the tank, effectively turning a *3p-3L* transformer to a *3p-5L* with very small outer limbs in the presence of GIC. The UMEC model did not simulate this effect satisfactorily in the case of a three phase three limb transformer.

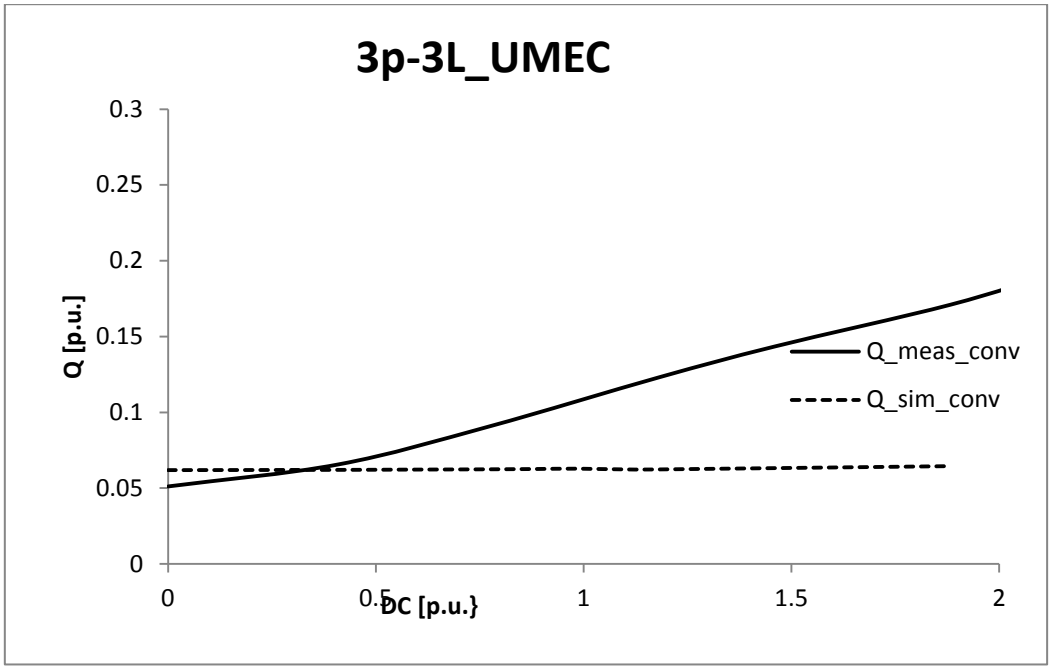

Figure 78: A comparison of the simulated and measured Q-dc response for the UMEC 3p-3L transformer system yielding unexpected results. The solid line represents the measured reactive power Q_meas_conv and the dotted line represents the simulated reactive power Q_sim_conv.

3. *3p-5L*

The response of the 3p-5L UMEC transformer model also yielded unexpected results with regard to the open circuit conditions (see Table 20), and the Q-dc response as shown in Figure 79.

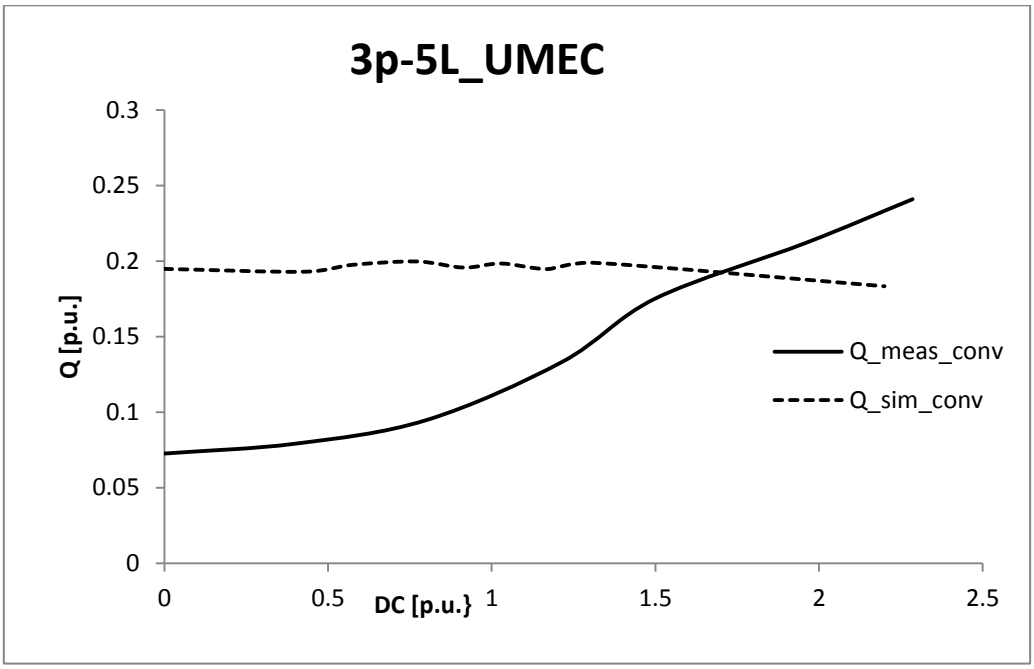

Figure 79: A comparison of the simulated and measured Q-dc response for the UMEC 3p-5L transformer system yielding unexpected results. The solid line represents the measured reactive power Q_meas_conv and the dotted line represents the simulated reactive power Q_sim_conv.

6.5.3 PSCAD MVA range investigation

Having evaluated the response of the PSCAD transformer models in the context of dc excitation, it was decided to further investigate the capabilities of the classical model, which had yielded the most agreeable results for the bench scale *3p-3s* transformers, in the MVA range. In order to be rigorous with the investigation it was consequently split into two parts: a) an up-scaled version of the bench scale system (to 200MVA), and b) a comparison of simulated and measured results from a field-tested 187MVA transformer. The above investigations and their outcomes are described below.

6.5.3.1 200MVA system

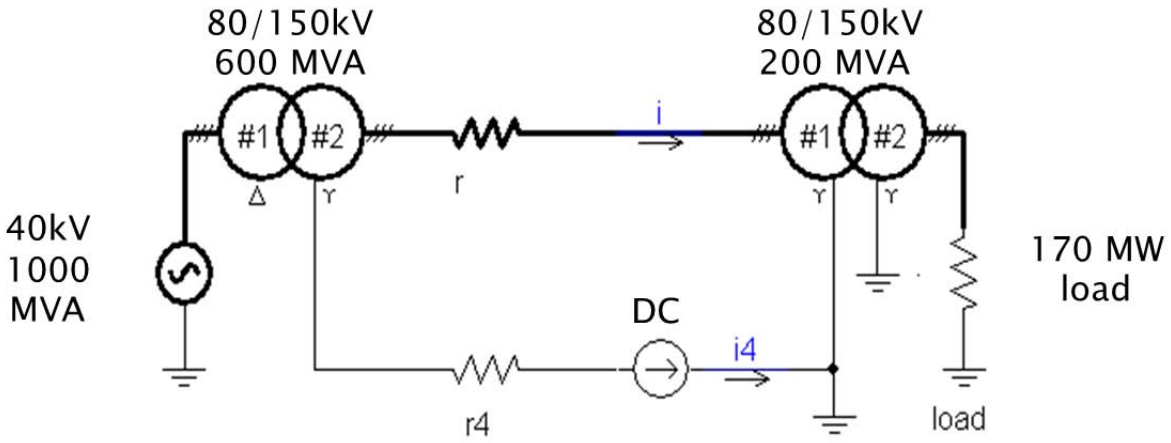

Figure 80: Simplified single phase respresentation of the the 200MVA test transformer model

Figure 80 is a single phase representation of how the bench-scale simulation model was scaled up to test a 200MVA load transformer. The test transformer was energized to its knee point and loaded with a relatively heavy resistive load. The dc was injected according to the protocol described in Chapter 4 whereby it is a function of the test transformer's magnetising current at the knee point voltage according to McLyman. The test transformer's parameters were per unitized according to the bases described in Table 21.

Table 21: Test transformer per unit bases.

Parameter	Base
S	200 MVA
V	80/150kV
dc	55 A

A very good correlation between the bench-scale measured and simulated results was demonstrated in section 6.5.1.; thus validating the classical PSCAD classical model in relation to the *3p-3s* transformer system. Further investigation with this model reveals that on a *per unit* scale the response of a transformer due to dc excitation is *independent* of the transformer *size* (see Figure 81 (a) and (b)).

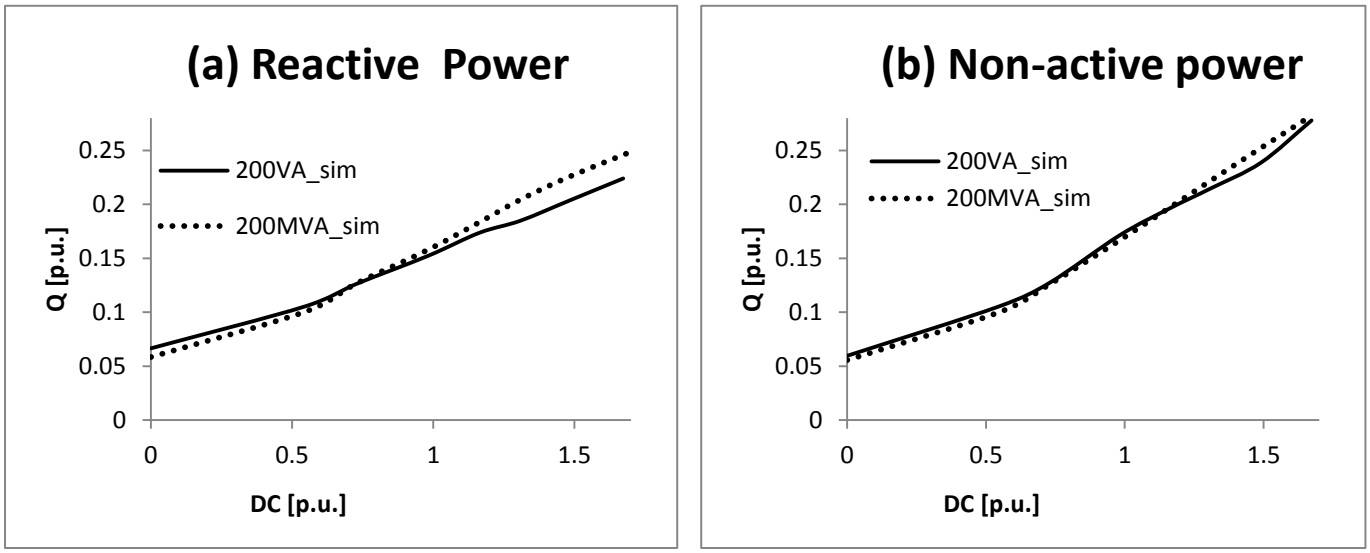

Figure 81: A comparison of the simulated *Q*-dc response between a 200VA and a 200MVA transformer on a per unit system. Reactive power is shown on the left (a), and non-active power as calculated with the general power theory is on the right (b).

6.5.3.2 187 MVA measured data

Kappenman reported the measured reactive power response of a large power transformer whereby varying levels of dc of up to 100 A were injected into the transformer neutral (Takasu *et al*., 1994 – discussion). The power transformer parameters that were provided by the author are given in Table 22. Figure 81 shows the PSCAD model that was used to simulate the effects of dc excitation on the load transformer. From earlier experiments it was seen that the effect of dc is the same in all phases of a three phase transformer bank. One phase (187 MVA) of the three phase bank was compared against the measured data.

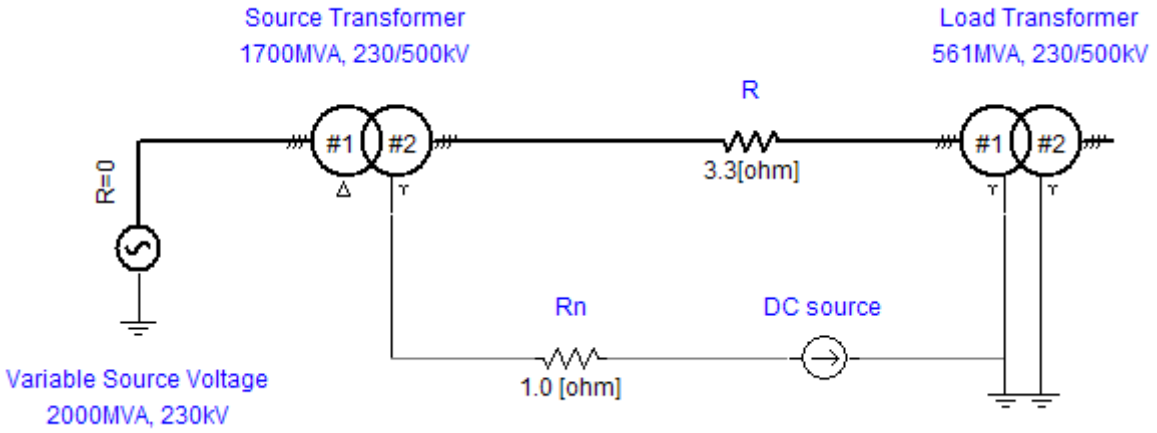

Figure 82: Single phase representation of the PSCAD model that used to simulate the Kappenman's measurements. The source transformer is approximately three times larger than the load transformer (test transformer), to make it immune to dc injection levels relative to the test transformer. The test transformer is a three phase bank of single phase power transformers (187MVA/phase).

It can be seen in Table 22 that these parameters were somewhat limited for the purposes of modelling in the PSCAD simulation environment. Some assumptions were made in the development of the 187MVA model.

First, a single phase shell type power transformer system (classical model) was selected and then it was subjected to an open circuit test, in which the magnetising current was adjusted to suit the initial conditions of *Q* given in the report (5 MVar/phase at no dc). The simulation software generated a corresponding current of 44 A/phase at open circuit. Since the O.C and S.C parameters were not given, the default parameters for a PSCAD power transformer were employed in the model i.e. leakage reactance - 0.1 p.u, air core reactance - 0.2 p.u. No load losses were arbitrarily set to 0.046 p.u. (taken from the bench-scale unit), as they had no bearing on the transformer model's response to dc excitation. The transformer was tested at no load as Kappenman's report did not specify the loading configuration (early tests showed that the *Q-DC* response is independent of a resistive loading condition *vide supra* section 4.5: *Varying Load Tests)*. Figure 82 shows the PSCAD model that was used to simulate the effects of dc excitation on the load transformer. From earlier experiments it was seen that the effect of dc is the same in all phases of a three phase transformer bank. Therefore one phase (187 MVA) of the three phase bank was compared against the measured data.

Table 22: Specifications for field tested power transformer. The dashes show the data that was not made available in the report and therefore had to be assumed using carefully considered parameters.

Parameter	Specification
Transformer Type	Single phase – shell type
Voltage	230/500kV
Capacity	187MVA
Knee point	-
Magnetising Current	-
O.C / S.C elements	-
Loading configuration	-

The method that was used to test the transformer was an upgraded version of the model used in previous simulations i.e. a *3p-3s* transformer system consisting of a deliberately larger source transformer (600MVA/phase) immune to dc, and a smaller load transformer (187MVA/phase). In Kappenman's report one single phase transformer was field-tested, therefore only one unit in the model's three phase bank was used to compare with the actual transformer (the response of each transformer in a three phase bank to dc is virtually the same).

Figure 83 shows a comparison of the measured reactive power (React_meas) due to dc excitation and the simulation (React_sim). In addition to these curves, the simulated non-active power (calculated using the general power theory) is shown on the same graph (Non-act_sim). The simulation model seems to correlate closely with Kappenman's measured results. The slight deviation between 1.p.u. and 1.5 p.u. dc may be due to the approximation of the several unknown parameters. It can also be seen that the non-active power of the power transformer diverges greatly from the reactive power beyond a dc injection of approximately 1.p.u. (44 A in this case), being approximately 25% higher for 2 p.u. dc.

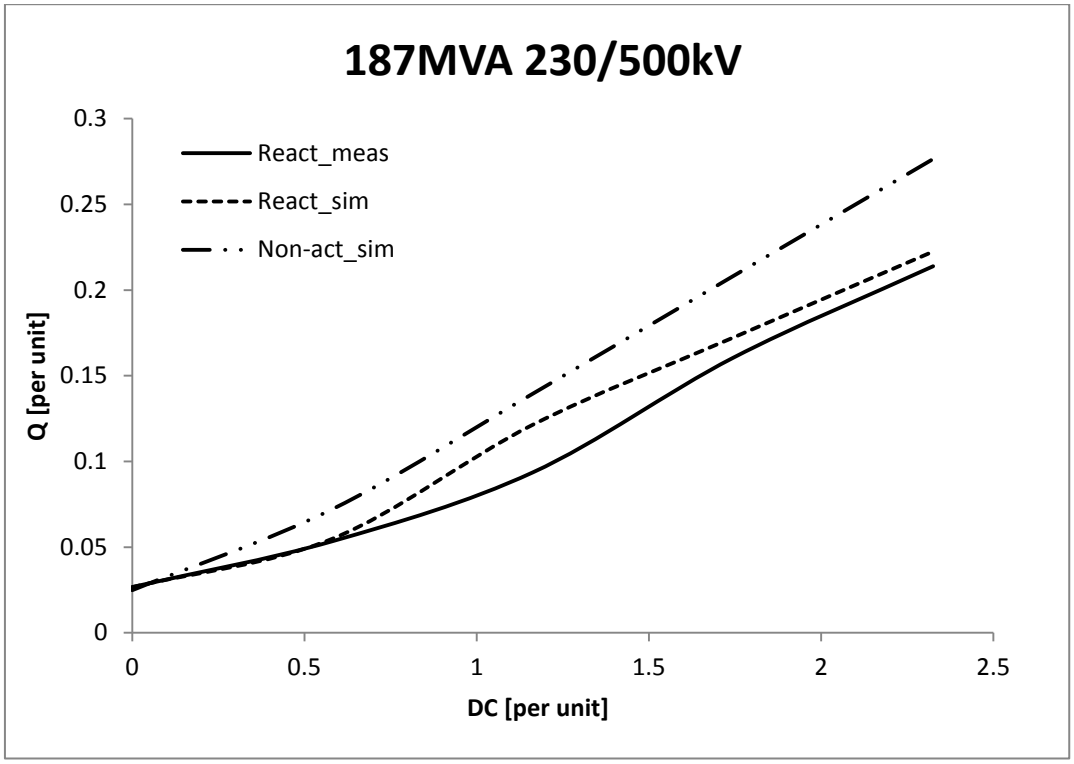

Figure 83: *Q-DC* measured and simulated response of a shell type single phase 187MVA power transformer. Kappenaman's measured reactive power, React_meas, is the solid line. The simulated reactive power, React_sim , is the dashed line. The simulated non-active power, Non-act_sim, r calculated using the general power theory is the dashed and dotted line.

6.5.4 Discussion

The electromagnetic transient simulation environment was rigorously investigated for the response of differing core structures of transformers, resulting in some illuminating findings.

The classical approach to modelling transformers in PSCAD was validated when compared against measured results from the actual bench transformers. After a series of investigations it was also found that this approach is be useful for modelling large power transformers in the MVA range; bringing about an important result: the response of a single phase transformer or three phase transformer bank to dc appears to be independent of the transformer size in the per unit domain that characterizes the magnitude of the dc as a function of the test transformer's I_{mag}.

The UMEC approach though more detailed did not represent three phase transformers adequately in the context of dc excitation. In his PhD thesis Berge (2011) also reported the same finding, recommending the PSCAD/EMTDC's developers (v4.0.0, 2003) to upgrade their UMEC three phase transformer models for compatibility with GIC studies.

6.6 Determination of *Q* using empirical formulae

The protocol developed in this study was successful for the testing of bench transformers of differing core structures and the characterization of their response from an electrical and magnetic perspective. Further tests were done in a system of 48kVA LV transformers (see chapter 7) in order to demonstrate the protocol's adaptability to larger transformers. While no tests have been performed on HV transformers, the validation of the applied simulation model (classical approach) using the bench scale measured results and data taken from measurements performed by Kappenman (1989) yielded some useful results. It was then concluded that using the proposed scaling method, the transformer *Q-GIC* response is independent of the size. This implies only the electrical and magnetic aspect of response. The noise and heating response varies with physical size and core designs; and these investigations were not within the scope of this study. The findings were then taken to generate empirical formulae that can be used to determine the amount of conventionally calculated reactive power that will be drawn by a transformer given the imposed GIC magnitude.

6.6.1 Q-GIC equations

A per unit scaled system is needed in order to apply the empirical formulae. A brief description of the parameters involved is given below:

- Magnetizing current I_{mag} – this is defined the current that is drawn by the transformer under no load at the knee point voltage (McLyman, 2004; Chisepo *et al.*, 2013) as seen from its *v-i* curve.
- GIC magnitude I_{GIC} - This is defined as the magnitude of the per phase GIC flowing in the transformer windings and it is in per unit of the I_{mag} as defined above.
- Reactive Power Q_{MVar} - This is defined as the reactive power drawn by the transformer as calculated using the conventional *IEEE* standards. It can be shown that the actual conditions in the transformer are better represented by the non-active power under condition distortion, unbalance and dc components such as those imposed by GIC (Gaunt & Malengret, 2012; Chisepo *et al.,* 2013); but currently reactive power is measured in the Eskom networks. This Q_{MVar} is in per unit of the transformer's MVA rating.
- Core structure – the transformer core configuration needs to be specified. Formulae for three core structures are provided.

Table 23: The options of equations that can be used to calculate the reactive power drawn by the transformer.

Core structure	Equation
Single phase / Three phase bank	$Q_{MVar} = 0.105 * I_{GIC} + 0.053$
Three phase three limb	$Q_{MVar} = 0.034 * I_{GIC} + 0.039$
Three phase five limb	$Q_{MVar} = 0.057 * I_{GIC} + 0.047$

6.6.2 Assumptions

The above formulae were generated from the bench-scale laboratory tests and simulation models. Only the single phase/three phase bank model was further validated using data taken from an actual power transformer of the same core structure measured by Kappenman. The PSCAD/EMTDC UMEC three phase three/five limb transformer models produced unexpected results. Also there was no available data for five limb power transformers. An assumption was therefore made that since the single phase model was validated, the other bench-scale models would be a good approximation of the Q-GIC response in MVA range. Scope for further work on this topic therefore should include the testing of power transformers of differing core structures in order to enhance these preliminary findings.

6.6.3 Extension to non-active power

The importance of incorporating non-active power measurements in the context of power transformers, power networks and GIC was investigated chapter 6 and it was found that the conventional calculation of reactive power in the presence of GIC may yield an optimistic perception of the energy transfer efficiency (the GPT calculation of non-active power consistently yields a higher Q under the same conditions). The operations and control for Eskom's power systems measure the reactive power flow using the conventional algorithm therefore the Q_{MVar}-*GIC* equations given in Table 23 will be compatible with their configurations. It is recommended however that power utilities incorporate non-active power measurements especially in distorted, unbalanced and dc component laden conditions so as not be over-optimistic about system conditions. Based on the assumptions described in section 6.6.2 and using the trends generated from the differential Q_{MM} responses, the following equations may be used to estimate the non-active power being absorbed by transformers during a GMD.

Table 24: The options of equations that can be used to calculate the reactive power drawn by the transformer.

Core structure	Equation
Single phase / Three phase bank	$Q_{MM} = 0.106 * I_{GIC} + 0.065$
Three phase three limb	$Q_{MM} = 0.066 * I_{GIC} + 0.044$
Three phase five limb	$Q_{MM} = 0.075 * I_{GIC} + 0.054$

7 APPLICATION AND EXTENSION OF PROTOCOL

Having successfully implemented the developed protocol on the new transformer systems, additional tests were performed on a three phase three limb transformer system of a much larger capacity (48kVA). A knowledge base on the response of three different core structures had been developed through the experimental procedures. The purpose of this investigation was therefore to test the protocol on transformer systems of a larger capacity than the bench-scale. These experiments were performed in the Medium Voltage Laboratory in the Department of Electrical Engineering. Here, the protocol had to be extended in some areas in order to compensate for the bigger transformers system. The measured results of the transformer response are presented in this chapter.

7.1 Test system

The test system consisted of the two identical three phase three limb 325/480V, 48kVA, $Y_n y_n$ transformers; both with a steel enclosure.

Figure 84 illustrates the 'back to back' set up in which the transformers were arranged in the laboratory. It was assumed that the transformer cores were of a much better quality than those of the bench scale units. A very sharp knee point close to the 1 p.u. voltage was anticipated which made it sound assume that the source transformer would not be affected by the dc in its under-excited state. A 10kVA isolated three phase generator was used to power the system and all measurements were taken using the Yokogawa power with the same calibration described in section 4.7: *Laboratory set up*.

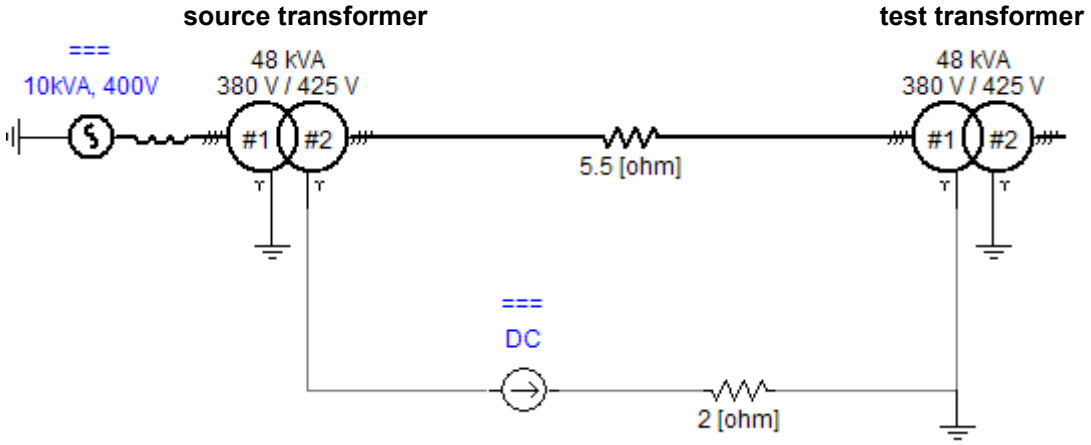

Figure 84: Single phase representation of transformer test system

7.2 Magnetization curves and characterisation

Using the procedures in the developed protocol, the magnetization curves of the transformer cores were generated and their linearity parameters were determined. It can be seen from

Figure 85 that magnetising currents of the transformers were largely asymmetrical with the current flowing in the centre limb being much smaller than those flowing in the outer limbs. In addition to this unexpected outcome, the transformer steel core characteristics seem to be linear at a voltage 40% below the name plate rating.

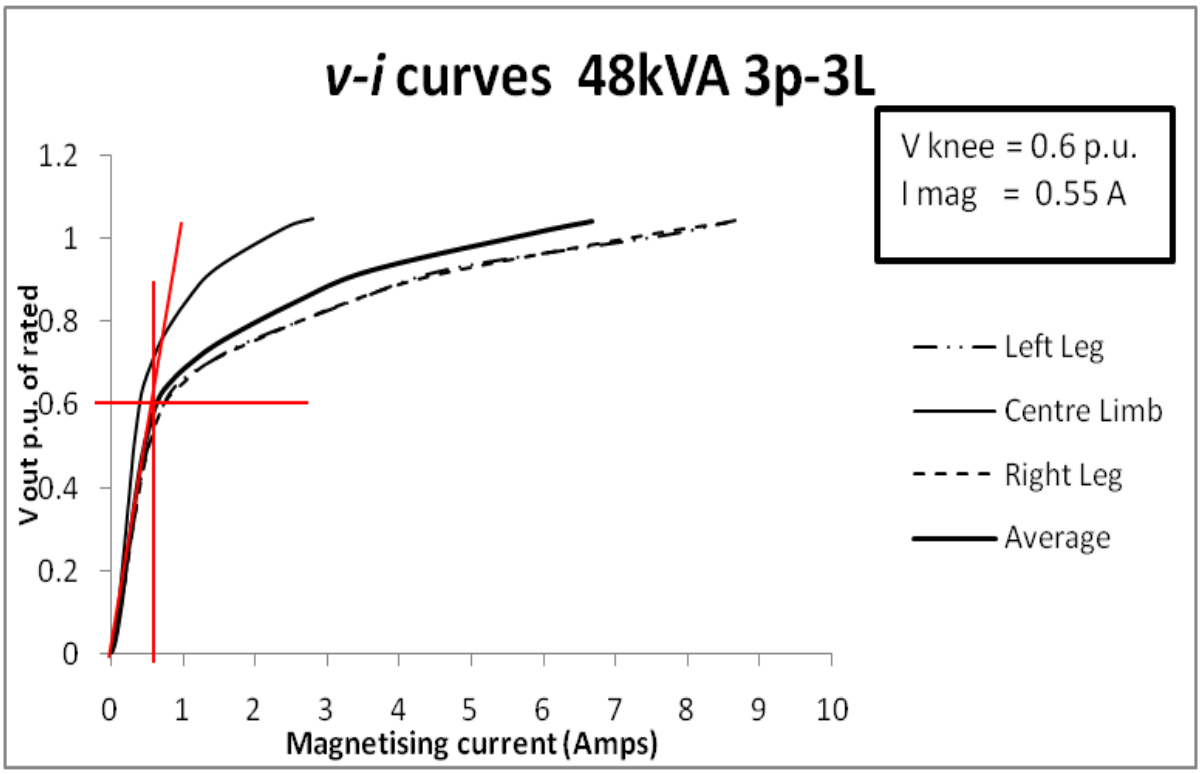

Figure 85: *v-i* characteristics of the test transformer.

In order to verify that the McLyman knee point was certainly 40% below the nameplate rating, a Fast Fourier Transform was run for the current waveforms along the *v-i* curve. When the current TDD was plotted on the same curve as the averaged *v-i* curve, this counter-intuitive region of linearity was confirmed (see Figure 86).

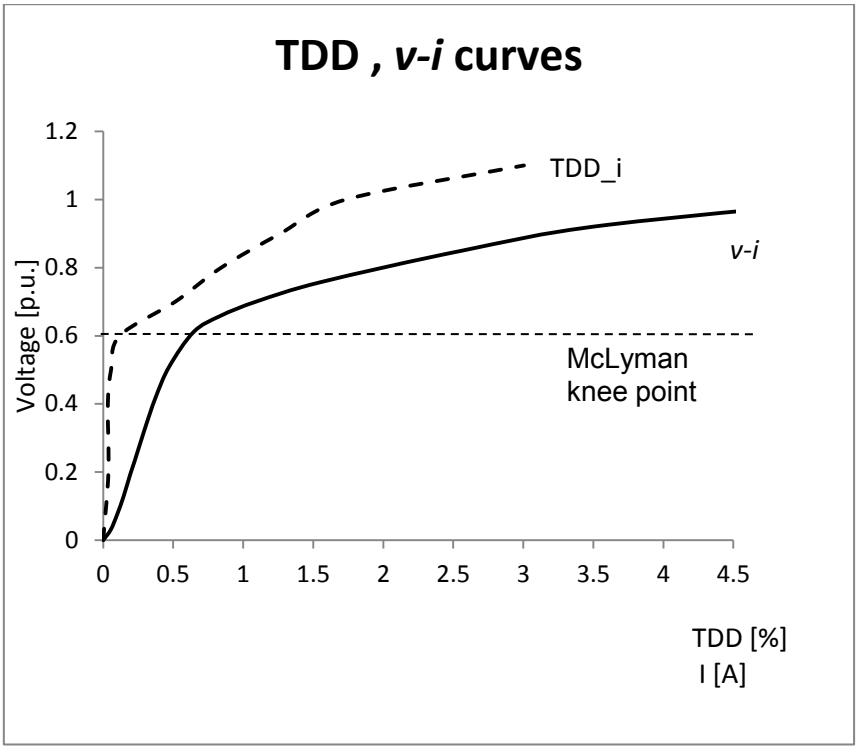

Figure 86:Total Demand Distortion of the red phase current and the averaged *v-i* characteristic.

7.3 *Q* response

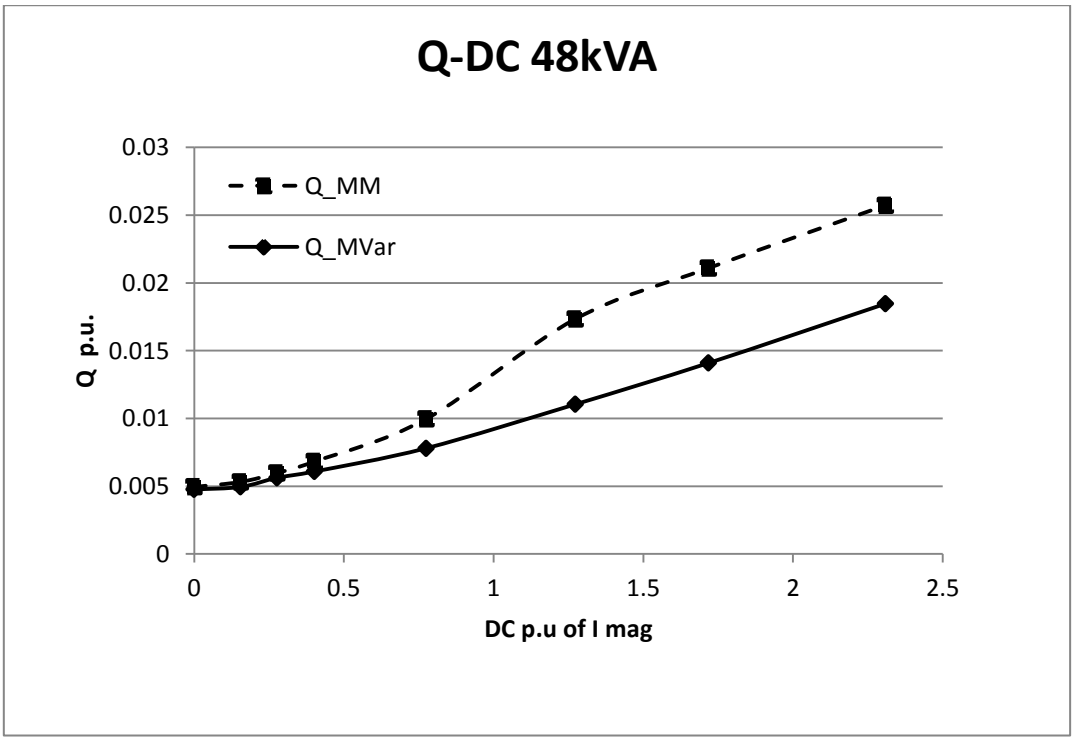

Figure 87: *Q-dc* response of 48kVA three phase limb test transformer.

Using the parameters defined the previous section, the test system was subjected to dc injections of varying levels and the corresponding *Q* responses were calculated. Figure 87 displays the measured reactive and non-active power responses against dc. The response is consistent with previous measured results from the bench-scale transformers in terms of the differences between the conventionally calculated reactive power and the non-active power calculated using the general power theory.

7.4 Discussion

The protocol was successfully applied to characterize and investigate test transformers of a larger VA rating relative to the bench units. For a large capacity transformer with good transformer core steel, the large asymmetries in the phase currents were unexpected. Moreover, the substantially underrated knee point voltage further reduced the test system's relevance for further investigations.

A good outcome however from this experimental undertaking was observed when the distortion was plotted on the same graph as the magnetization curve. The McLyman knee point was used throughout the study to distinguish the region without distortion (linear region) from the region with distortion (saturation region). It clear from Figure 85 that in the linear region the distortion is virtually negligible, and then it increase sharply in operating regions beyond the knee point.

8 CONCLUSIONS

The research carried out in this dissertation aimed at investigating the need for a rigorous testing protocol for transformers with dc currents in order to adequately characterize their response. The study developed a procedure for characterizing transformers based on their magnetization characteristics, and then uses these parameters to select adequate levels of dc injection to investigate various aspects of transformer electrical and magnetic response. This chapter firstly presents a discussion and interpretation of the results in chapters 6 and 7. Following that, conclusions are drawn for the research questions based on the hypothesis presented in chapter 1. Lastly, final thoughts on the validity of the hypothesis are stated along with a summary of the key process steps required to carry out the protocol.

8.1 Power Calculations in the presence of dc components

The bench-scale measurements and simulations showed that under distortion, unbalance and dc components, such as the conditions brought about by GICs, there is a substantial increase in the *Q* component of the apparent power that is delivered. The two methods of calculating power that were contrasted indicated that the conventionally calculated reactive power absorbed by transformers can be significantly lower that the non-active power calculated using the newer method. This significant reduction in the power factor implies that the effective capacity to deliver power can actually be lower than is indicated by the conventional calculations. Incorporating the measurement of non-active power using the newer methods like the general power theory could therefore help system operators approach better configurations for power systems during GMDs.

8.2 Transformer response to extreme levels of dc

It was shown in chapter 6 that transformer behaviour during the imposition of extreme levels of dc (based on the *3p-3s* system) results in a complex system response that leads to high levels of VAR absorption and voltage collapse. This response is similar to reports by Kappenman & Albertson (1990) of the extreme Quebec storm, stating observations of unusual real and reactive power swings and voltage dips. For low to moderate levels of dc (GIC), a linear relationship with the current THD/TDD is observed. However, when beyond a certain level of dc, the distortion begins to decline as the transformer will be operating in a region beyond the knee of the B-H characteristic, which is known to be linear. Using the I_{mag} per unitized system for characterizing the levels of dc injection made it possible to understand better the points at which the transformer response would deviate from its expected behaviour i.e. operation in the ‘air core region’.

8.3 Effect of reducing the operating voltage

In the development of the testing procedure (chapter 5), it was demonstrated that the amount of *Q* absorbed by a transformer is a function of the applied voltage and the level of dc injected in per unit of I_{mag}. Building on this expected result, the following question was formulated, “By what margin can the voltage be reduced for mitigation during GMDs, without breaching the limits for voltage depressions?”

It was found after a series of tests that dc levels comparable with the load transformer’s I_{mag} still pushed it into saturation despite dramatically reduced levels of applied voltage. Therefore in order to avoid going beyond the limits for voltage dips in power systems, it is concluded that reducing the voltage during a GMD is not feasible for mitigation.

8.4 Differential Core type response

The *3p-3s* transformer system was initially used as the platform to develop the protocol for the transformer test systems. The methods developed along with the experience obtained with dc injection then made it possible to test other core types of transformers to investigate their response. Though the transformers were not completely comparable, their ratings were similar and the per unit scaling which paid close attention to their core knee point characteristics made it possible to test them under relatively similar conditions and compare their response on the same scale yielding consistent results. . Completely comparable results require a deeper analysis of transformer design beyond the scope of this dissertation, but the testing protocol that has been developed offers a useful and consistent approach to testing different transformers.

8.4.1 *Magnetization curves*

The laboratory protocol initializes the investigation of each core type with the generation of a magnetization curve. While some manufacturers provide such details, the industrially made bench scale units had no such information; therefore it had to be rigorously generated. The knee point of the magnetization curves was then selected according its definition by McLyman (2004). This uniquely defined knee point was used to per unitize the magnitudes of the different levels of dc that were injected into the transformers, and it brought about a clearer picture as to how the transformers respond to certain of levels of dc at different loading configurations.

8.4.2 *Differential Q-dc investigation*

The results presented in chapter 6 pertaining to the differential *Q* response of transformers under dc excitation showed that there is an association between the relative amounts of *Q* absorbed by each transformer type and the level of dc in them. The *3p-3s* transformer

system was observed to draw relatively more *Q* than the *3p-5L* system, while the *3p-3L* system drew the least amount of *Q*. From a power system perspective therefore, *3p-3s* transformers will have the most severe implications in the stability of the transmission networks during a GMD when compared against the other two core structures of the same capacity and voltage ratings. These observations then led to the formulation of equations that can be used to calculate how much *Q* a transformer will absorb given a certain level of GIC.

8.4.3 *Harmonic Analysis and Voltage drop*

It can be seen from chapter 6 that the harmonics generated by the transformers are a function of the levels of dc injection and the transformer core structure; with the *3p-3s* generating relatively higher levels of distortion. Classifying the amount of dc flowing in the windings as a function of the relative magnetizing currents revealed that there may be a certain 'distortion knee point' associated with a 1.0 p.u. dc injection, when the transformers are not loaded. This is the point where the relationship between the levels of distortion and of amount of dc injected ceases to be linear as the distortion will start to reduce with higher magnitudes of dc.

The behaviour of the transformers when they are connected to a resistive loading configuration differs from that of the no load condition. With a power factor tending to one at the output, the input currents have much lower levels of distortion in the presence of dc. Therefore the current distortion-dc characteristic remains linear for low to moderate levels of dc. It was observed in the *'Effects of Extreme GIC levels'* (section 6.2) investigation that there is a second 'distortion knee point' in the distortion-dc relationship when the transformer is connected to a resistive load. In this experiment, the 'extreme GIC levels' at which this second knee point was reached were in the order of 50 p.u. dc ($50*I_{mag}$). These findings therefore give insight into the amount distortion that the transformers may generate at clearly defined magnitudes of dc in their no load and loaded states.

8.4.4 *Consistency of Laboratory protocol*

In the theory development stage of the study (chapters 3 and 4), the fundamentals of the procedures that were to be applied were laid down, and the *3p-3s* transformer system was used for a preliminary practical implementation. This protocol was then extended to test other transformer systems varying in core structure (bench scale) and size (48kVA three phase three limb transformers), bringing about out consistent results in the characterization of each transformer system.

8.5 Simulations

After a convincing literature survey it was decided that a suitable simulation environment for transformer studies in the context of GICs was PSCAD/EMTDC which a available at the university. The main reason for modelling in this simulation program was because the inherent transformer models incorporate core saturation due to dc excitation, which was a crucial aspect of the study. The two transformer models in the PSCAD/EMTDC library (v4.2.1 Educational) were rigorously investigated in the simulation protocol presented in chapter 5. Having sufficiently generated and modelled the required parameters, the classical transformer model, which can only model single phase transformer systems, was validated against the bench *3p-3s* laboratory measurements.

With this validated model, an arbitrary transformer system was simulated in the HV/MVA range according to the requirements in the protocol and it was found that in PSCAD, the transformer Q-DC response is independent of the transformer size. This finding can be extended to suggest that the electrical and magnetic response of a transformer is independent of the transformer size. It was then pertinent to rigorously test the simulation against large power transformers and it was found that after approximating for unknown parameters, there was as good correlation between the simulation and measurements done by Kappenman (Takasu, *et al.,* 1994 - discussion). Though no actual power transformers were tested in this study, satisfactory simulation results (classical model) were achieved from the bench scale and literature measurements.

It was shown in chapter 6 that the UMEC transformer model did not give satisfactory results despite the input of sufficient parameter information generated from the bench units. Further investigations involving more updated versions of the UMEC transformer models is needed therefore to test the validity of these models.

8.6 Equations for different core structures

It is widely reported in literature (see chapter 2) that the response of transformers differs with core structure; therefore this study investigated and characterized the response of three different laboratory scale core configurations. In order to compare the different core structure responses against each other, a per unit system defined by transformer magnetization characteristics, was applied according to the developed laboratory protocol. The per unit system was then extended to generate some equations that may be used to predict the amount of *Q* absorbed by a transformer based on its magnetizing current, core configuration, and empirically generated trends from the experimental and validated simulation tests. These preliminary equations are useful to be further investigated against

large power transformers' response in order to yield a more refined predictive tool for stability and control operations in power utilities like Eskom during a GMD.

8.7 Answers to Research Questions

A summary of the answers to the research questions formulated in Chapter 1 are presented below:

(a) What are the available methods of laboratory testing and monitoring that will facilitate measurements in compliance with the most up to date power calculation conventions?

Using standard testing method's available in open literature, the measurement and calculation of power fulfilling the requirements of the conventional and newer method (general theory of power) were successfully carried out using equipment with a facility whereby the adequately sampled numerical waveform data could be processed both on-line and off-line for post processing.

(b) In relation to (a), what are the differences between reactive and non-active power in the context of transformers and GICs?

This study showed that under dc excitation conditions, the calculated Q and apparent power using conventional approaches differs greatly from those using the general power theory. This may therefore result in over-optimistic measurements of the power transfer capacity of networks in the presence of distortion, unbalance and dc components of current (GICs).

(c) How does the sizing of a transformer in terms of VA rating and operating voltage relate to the magnitude GICs?

The effect of GIC on the magnetization characteristics of a transformer depends on the relative capacity and operating voltage of the transformer.

(d) What is the effect of reducing the transformer voltage in the presence of GIC?

Reducing operating voltage reduces *Q* in the presence of dc. However if the dc is big enough the transformer may still go into saturation and simultaneously generate harmonics. Therefore from system stability perspective it is not feasible to reduce the voltage as this may also be accompanied by a voltage collapse.

(e) Is there a standard for defining the relative size of the dc imposed on a particular transformer?

The magnetization curve can be used to characterize the linear region of a transformer core steel. The corresponding magnetizing current at the defined knee point should be used as reference for dc injection levels to monitor pre and post distortion conditions.

(f) For the same rated capacity (VA) and voltage, what is the differential transformer core structure's response to dc?

It was observed from the laboratory tests that the response of transformers to dc differs with core structure as widely reported in literature. The single phase shell type (three limb) is the most vulnerable to the effects of GIC as it readily offers a dc flux return path through the two unwound outer limbs. The three phase five limb transformer also offers dc flux return path but it is not as significant as the single phase, as five limb transformers have outer limbs that are smaller than the inner limbs. The three phase three limb transformer is the least vulnerable to GIC attack, but is not immune to it as draw of reactive power and generation of harmonics have been reported. Its relatively less severe response to GIC is because three limb transformers do not readily offer a dc flux return path as every limb is wound. Any stray flux caused by GICs must therefore flow through the transformer steel tank, whose dimensions are significantly smaller than the actual transformer core limbs.

(g) How accurate is the carefully chosen simulation software in modelling actual transformers' responses to dc?

The electromagnetic transients PSCAD/EMTDC's classical model was validated using not only laboratory measured results (three phase bank test transformer), but also by data taken from Kappenman's measurements of a 500/230kV single phase transformer.

An unexpected response was however observed for the UMEC transformer models and therefore requires further investigation with updated versions of these transformer models.

8.8 Validity of Hypothesis and Final thoughts

In chapter 1 an introduction to this study was presented along with its motivation. This then led to the formulation of the following hypothesis:

"The development of a rigorous testing protocol for transformers subjected to GIC-like currents is needed for a better understanding of the response."

Section 8.7 showed that the hypothesis was valid for answering the research questions that were posed to test it. Consequently, the hypothesis and work done in the study led to the restating of the hypothesis to the following:

"The development of a rigorous testing protocol for transformers subjected to GIC-like currents including, but not limited to, the identification of the magnetizing current at a uniquely defined 'knee point' on the *B-H* characteristic, the testing of harmonics, and interpreting the power data as conventional reactive power and non-active power is necessary for a better understanding of the response."

In summary, the following key aspects are fundamental to the application of the protocol:

- Ensuring adequate supply and measurement conditions
- The generation of the magnetization curve and the identification of the magnetizing current I_{mag} at the McLyman knee point of this *v-i* characteristic.
- The definition of the levels of dc injection in per unit of the I_{mag}.
- The measurements of voltages and currents and their harmonics, calculation of power and the interpretation of the responses as a function of the dc in per unit of I_{mag}.

9 REFERENCES

Abdulsalam, S. G., Xu, W., Neves, W. L. & Liu, X., 1996. Estimation of transformer saturation characteristics from inrush current waveforms. *IEEE Transactions on Power Delivery,* 21(1), pp. 170-177.

Albertson, V. D. *et al*., 1993. Geomagnetic Disturbance effects on power sytems. *IEEE Transcaction on Power Delivery,* July, 8(3), pp. 1206-1216.

Amuanyena, L. A., 2002. Effect of geomagnetically induced currents on power transformers and reactors. *MSc. (Eng) Thesis.* University of Cape Town, South Africa.

Amuanyena, L. A. & Gaunt, C. T., 2002. Effects of Geomagnetically Induced Currents (GICs) on power transformers and reactors.

Berge, J. E., 2011. *Impact of GIC on Power Transformers.* PhD Thesis.

Ontario: Western Libraries.

Berge, J., Marti, L. & Varma, R. K., 2011. *Modeling and Mitigation of Geomagnetically Induced Currents in a Realistic Power System Network.* In IEEE EPEC proceedings. Winnipeg, pp. 485-490.

Berge, J., Varma, R. K. & Marti, L., 2011. *Laboratory Validation of the Relationship betwee GIC and Transformer Absorbed Reactive Power.* In IEEE EPEC proceedings. Winnipeg, pp. 491-495.

Blooming, T. M. & Carnovale, D. J., 2006. *Application of IEEE STD 519-1992 Harmonic Limits.* In Pulp and Paper Industry Technical Conference. Appleton, pp. 1-9.

Bolduc, L., 2002. GIC observations and studies in the Hydro-Quebec power system. *Journal of Atmospheric and Solar-Terrestrial Physics ,* Volume 64, pp. 1793-1802.

Bolduc, L., Gaudreau, A. & Dutil, A., 2000. Saturation time of transformers under dc excitation. *Electric Power Systems Research,* Volume 56, pp. 95-102.

Bolduc, L., Gaudreau, A. & Dutil, A., 2000. Saturation Time of Transformers under DC Excitation. *Electric Power Systems Research,* Volume 56, pp. 95-102.

Boteler, D. H., Pirjola, R. J. & Nevanlinna, H., 1998. Effects of geomagnetic disturbances on electrical systems on the Earth's surface. *Advances in Sapce Research,* 22(1), pp. 17-27.

Chandrasena, W., McLaren, P. G., Annakkage, U. D. & Jayasinghe, R. P., 2004. An Improved Low-Frequency Transformer Model for use in GIC studies. *IEEE Transaction on Power Delivery,* 19(2), pp. 643-651.

Chisepo, H. K., Gaunt, C. T. & Oyedokun, D. T., 2013. *Testing the response of laboratory bench transformers to geomagnetically induced currents.*In SAUPEC*.* Potchefstroom, pp. 37-42.

De Klerk, P. J. & Reynders, J. P., 1999. *Winding Slackness monitoring as a diagnostic for insulation ageing in oil-paper insulated power transformers.* In 11th International Symposium on High Voltage Engineering*.* London. vol 1, pp.185-188.

Dlamini, M., 2008. Measurement of harmonics generated in a transformer carrying Geomagnetically Induced Currents. *BSc. Eng. Thesis.* University of Cape Town, South Africa.

Emanuel, A. E., 2004. Summary of IEEE standard 1459: Definitions for the Measurement of Electric Power Quantities under Sinusoidal, Nonsinusoidal, balanced or unbalanced conditions. *IEEE Transactions on Industry Applicaitons,* May-June, 40(3), pp. 869-875.

Enright, W., Nayak, O. B., Irwin, G. D. & Arrillaga, J., 1997. *An Electromagnetic Transients Model of Multi-limb Transformers Using Normalized Core Concept.* Seattle, pp. 93-98.

Eskom Holdings Ltd, 1998. *Theory, design, maintanence and life management of power transformers.*Johannesburg: Y-Land Design, Print & Promotions.

Fehr, R., 2004. *Harmonics Made Simple.* [Online]
Available at: http://ecmweb.com/powerquality/electric_harmonics_made_simple/index.html
[Accessed 14 February 2012].

Gaunt, C. T., 2014. Reducing uncertainty – responses for electricity utilities. *J. Space Weather Space Clim.,* Volume 4, pp. A01:1-6.

Gaunt, C. T. & Coetzee, G., 2007. Transformer failures in regions incorrectly considered to have low GIC-risk. *IEEE Powertech.*

Gaunt, C. T. & Malengret, M., 2012. *Why we use the term non-active power, and how it can be measured under non-ideal power supply conditions.* In IEEE Power Africa. Johannesburg, pp.1-4.

Griffiths, D. J., 1999. *Introduction to electrodynamics.* 3 ed. New Jersey: Prentice Hall International, Inc.

Heindl, M. *et al.*, 2011. *Investigation of GIC related effects on power transformers using modern diagnostic methods.* Hanover.

Hock-Chuan, T. & Swift, G. W., 1984. A Novel Method of Detecting Asymmetrical Transformer Core Saturation Due to GIC. *IEEE Transactions on Power Apparatus and Systems,* January, PAS-103(1), pp. 183-189.

IEC, 1979. *Reactive power and distortion power.*

Jenneson, J. R., 2002. *Electrical principles for electric trades.* 5th ed. Australlia: McGraw-Hill.

Kappenman, J. G. & Albertson, V. D., 1990. Bracing for the geomagnetic storms. *IEEE Spectrum,* March.

Koen, J., 2002. *Geomagnetically induced currents and their presence in the Southern African electriciy transmission network.* PhD Thesis. University of Cape Town.

Koen, J. & Gaunt, C. T., 2002. *Disturbances in the Southern African Power Network due to Geomagnetically Induced Currents.* Paris.

Li, X., Wen, X., Markham, P. N. & Lu, Y., 2010. Analysis of Nonlinear Characteristics for a Three-Phase, Five-Limb Transformer Under DC Bias. *IEEE Transactions on Power Delivery,* 4(25), pp. 2504-2510.

Li, Z. & Yun, Y., 2012. *Harmonic Distortion Feature of AC Transformers.* Shanghai, Inst. of Electr., EPRI of Shandong, pp. 1-4.

Lundstedt, H., 2006. The sun, space weather and GIC effects in Sweden. *Advances in Space Research,* Volume 37, p. 1182–1191.

Malengret, M. & Gaunt, C. T., 2008. Decomposition of current in three- and four-wire systems. *IEEE Transcation on Instrumentation and Measurement,* Issue IM-57, pp. 963-973.

Malengret, M. & Gaunt, C. T., 2011. General theory of average power for multi-phase systems with distortion, unbalance and direct current components. *Electr. Power Syst. Res.,* Volume 84, pp.224-230.

Malengret, M. & Gaunt, C. T., 2011. General theory of instantaneous power for multi-phase systems with distortion, unbalance and direct current components. *Electr. Power Syst. Res.,* Volume 81, pp. 1897-1904.

Malengret, M. & Isumbingabo, E. F., 2010. *Evaluation of a the performance of a power transformer under varying dc injection and mitigation of adeverse effects.* SAUPEC. Johannesburg, pp. 248-253.

Manitoba, 2005. *EMTDC/PSCAD User Manual.* 4.2.0 ed.HVDC Research Center.

Marti, L., Berge, J. & Varma, R. K., 2013. Determination of Geomagnetically Induced Current Flow in a Transformer From Reactive Power Absorption. *IEEE Transactions on Power Delivery,* 28(3), pp. 1280-1288.

Masoum, M. A. S. & Moses, P. S., 2008. *Influence of Geomagnetically Induced Currents on Three-phase power transformers.* In AUPEC. Sydney, pp. 1-5.

Massachusetts Institute of Technology, 1944. *Magnetic Circuits and Transformers.* 2 ed. New York: John Wiley and Sons, Inc..

McLyman, C. W., 2004. *Transformer and inductor design handbook.* 3rd ed. Carlifornia: Marcel Dekker, Inc.

Milanés, M. I., Miñambres, V., Romero, E. & Barrero, F., 2009. *Quality Meter of Electric Power Systems based on IEEE Standard 1459-2000.* CPE. Badajoz, pp. 86-92.

Minhas, M. S., Reynders, J. P. & de Klerk, P. J., 1999. *Failures in power system transformers and appropriate monitoring techniques.* Eleventh Internat. Symposium on HV Eng. London, pp.94-97

Mohan, N., Undeland, T. M. & Robbins, W. P., 2003. *Power electronics: Converters, Applications and design.* 3rd ed. John Wiley and Sons, Inc.

Molinski, T. S., 2002. Why utilities respect geomagnetically induced currents. *Journal of Atmospheric and Solar-Terrestrial Physics,* Issue 64, pp. 1765-1778.

NERC, 2012. *GMDTF Interim Report: Effect of Geomagnetic Disturbances on the Bulk Power System,* North American Electric Realibity Corporation.

Ngwira, C. M., 2008. Geomagnetically induced current characteristics in Southern Africa. *MSc.Thesis.* University of Cape Town, South Africa.

Pinto, L. M. *et al.,* 2005. *Geomagnetically Induced Currents: The Ultimate Threat to System Security.* Russia. pp.1-7.

Price, P. R., 2002. Geomagnetically Induced Effects on Transformers. *IEEE Transcaction on Power Delivery,* October, 17(4), pp. 1002-1008.

Public Intelligence, 2012. *NASA Solar Flare Photos 2010-2012.* [Online]
Available at: http://publicintelligence.net/nasa-solar-flare-photos-2010-2012/
[Accessed 1 February 2012].

Pulkkinen, A., Thomson, A., Clarke, E. & McKay, A., 2009. April 2000 geomagnetic storm: ionospheric drivers of large geomagnetically induced currents. *Annales Geophysicae,* Issue 21, pp. 709-717.

Sen, P. C., 1997. *Electric Machines and Power electronics.* 2 ed. Canada: John Wiley and Sons.

Takasu, N., Miyawaki, F., Saito, S. & Fujiwara, Y., 1994. An experimental analysis of DC excitation of transformers by geomagnetically induced currents. *IEEE Transactions on Power Delivery,* April, 9(2), pp. 1173-1179.

Thomson, A. *et al*., 2010. Present day challenges in understanding the geomagnetic hazard to national power girds. *Advances in Space Research,* Volume 45, pp. 1182-1190.

U.S.A. FERC, 2013. *Reliability Standards for Geomagnetic Disturbances,* United States of America Federal Energy Rrgulatory Commission.

Zhang, B. *et al.*, 2011. Effect of load current on leakage flux of transformerwith geomagnetically induced current. *European Transactions on Electrical Power,* 1(21), pp. 165-173.

Zureks, S., 2009. *Permeability of ferromagnet.* [Online]
Available at: http://en.wikipedia.org/wiki/File:Permeability_of_ferromagnet_by_Zureks.svg
[Accessed 2012 February 2012].

10 APPENDIX

A. O.C. AND S.C. PARAMETERS

A1. 3p-3s Test Transformer

Req	Xeq	No Load Losses
0.06725 p.u.	0.00910 p.u	0.02291 p.u.

A2. 3p-3L Test Transformer

Req	Xeq	No Load Losses
0.000984 p.u.	0.03280 p.u.	0.009348 p.u

A3. 3p-5L Test Transformer

Req	Xeq	No Load Losses
0.01543 p.u.	0.00494 p.u	0.02083 p.u.

B. MV LAB SUPPLY SCHEMATICS

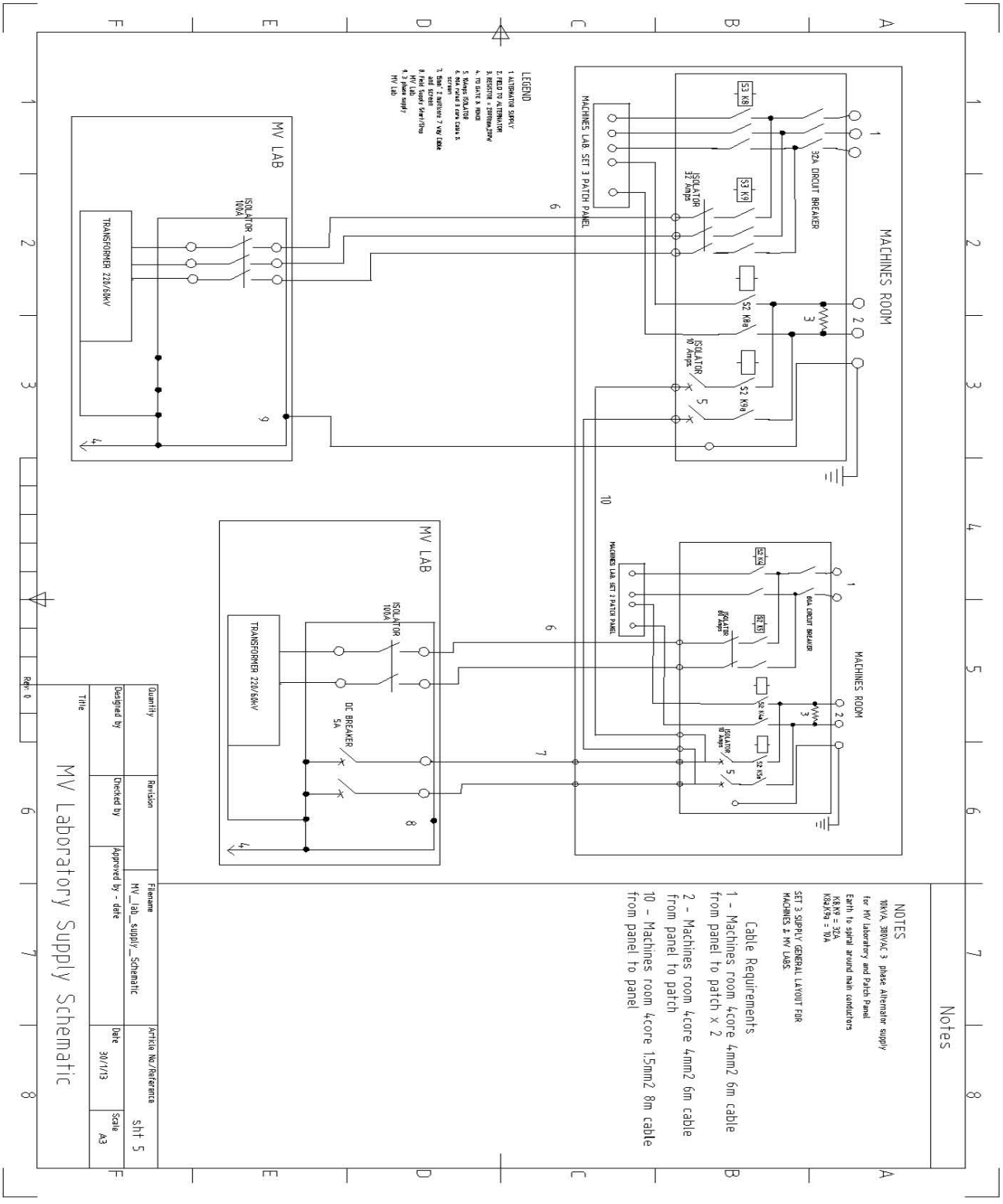

C. DIFFERENTIAL HARMONICS – NO LOAD

C1. PHASE HARMONICS AND THD: 3p-3s

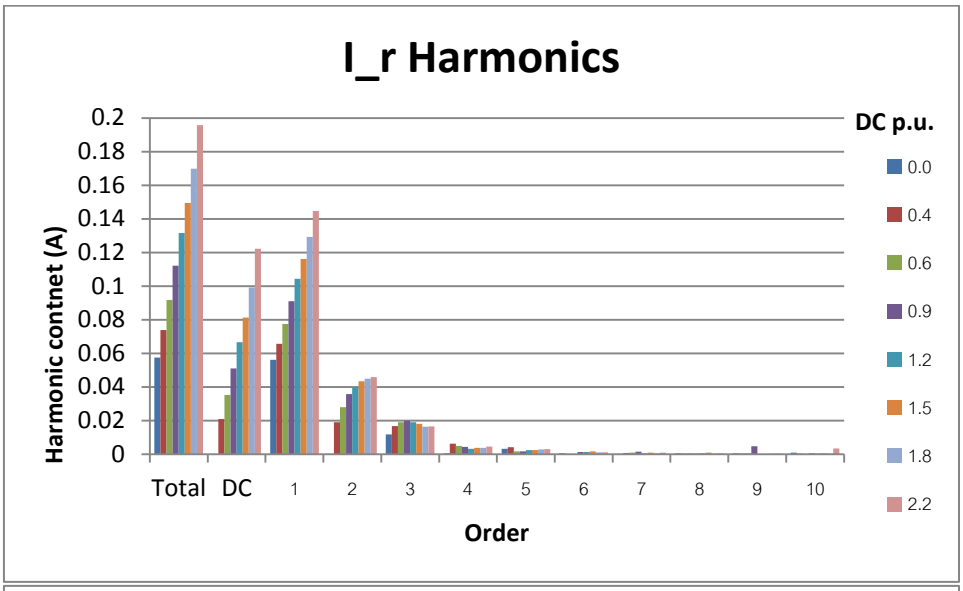

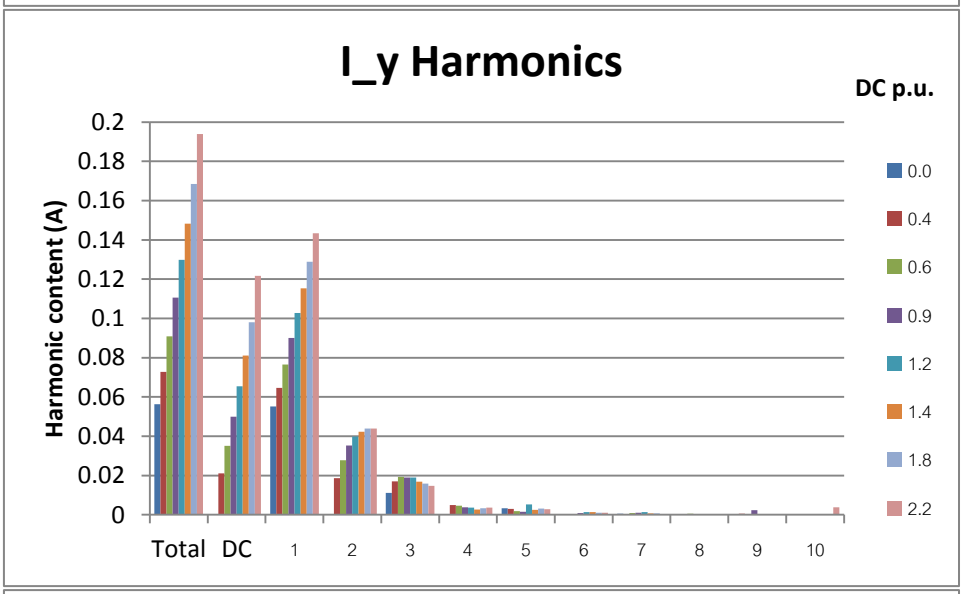

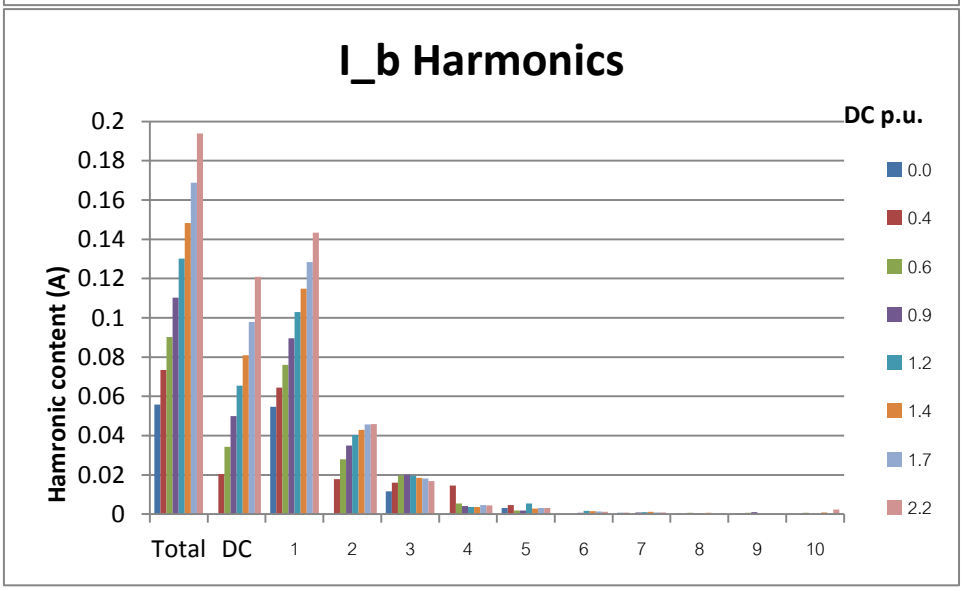

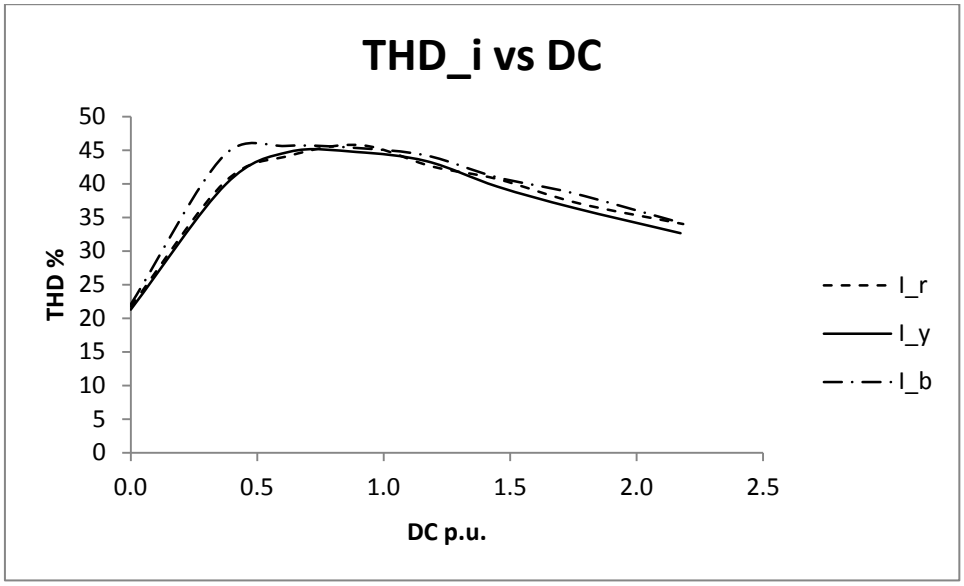
THD_i vs DC
THD %
50
45
40
35
30
25
20
15
10
5
0
0.0
0.5
1.0
1.5
2.0
2.5
DC p.u.
I_r
I_y
I_b

C2. PHASE HARMONICS AND THD: 3p-3L

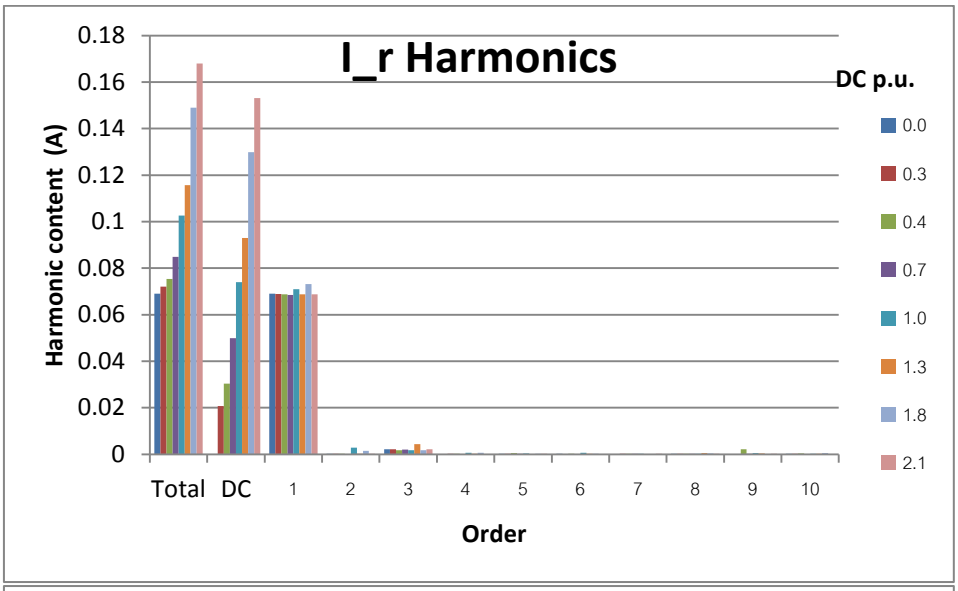

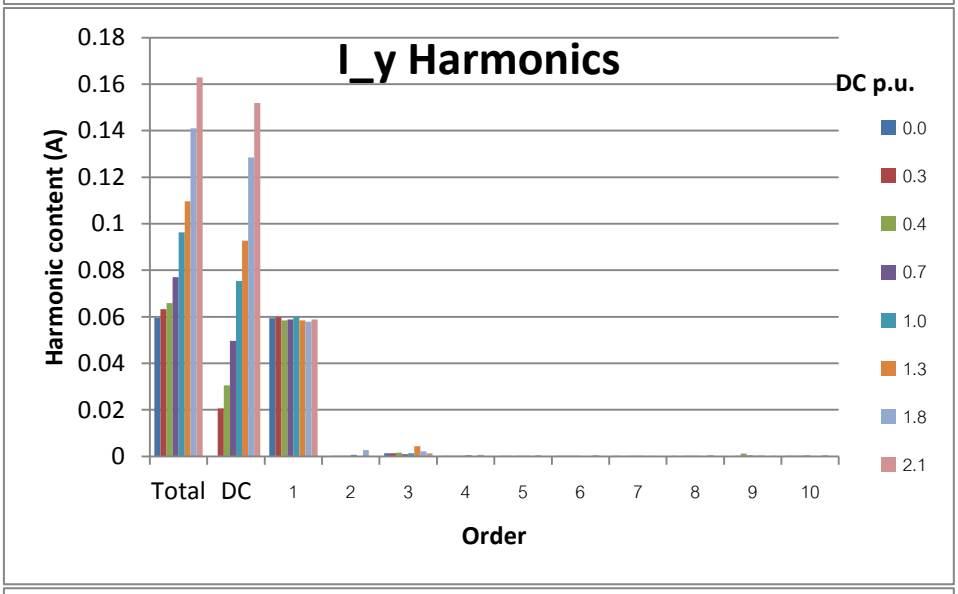

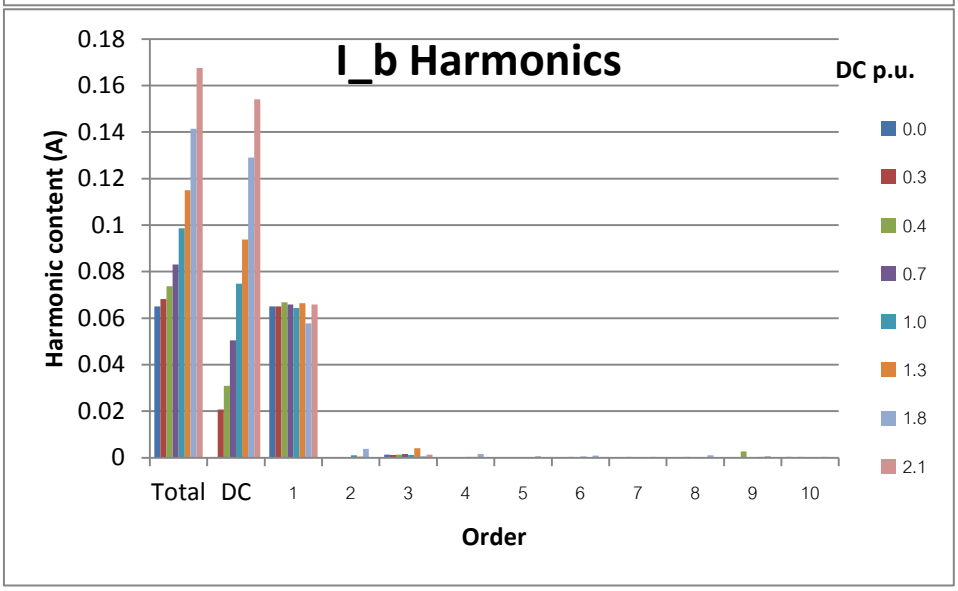

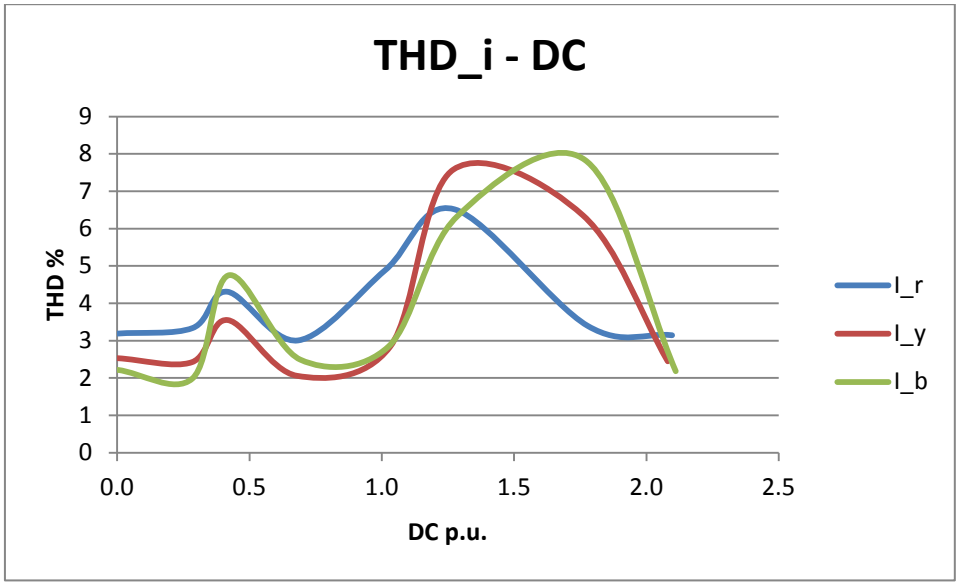
THD_i - DC
THD %
9
8
7
6
5
4
3
2
1
0
0.0
0.5
1.0
1.5
2.0
2.5
DC p.u.
I_r
I_y
I_b

C3. PHASE HARMONICS AND THD: 3p-5L

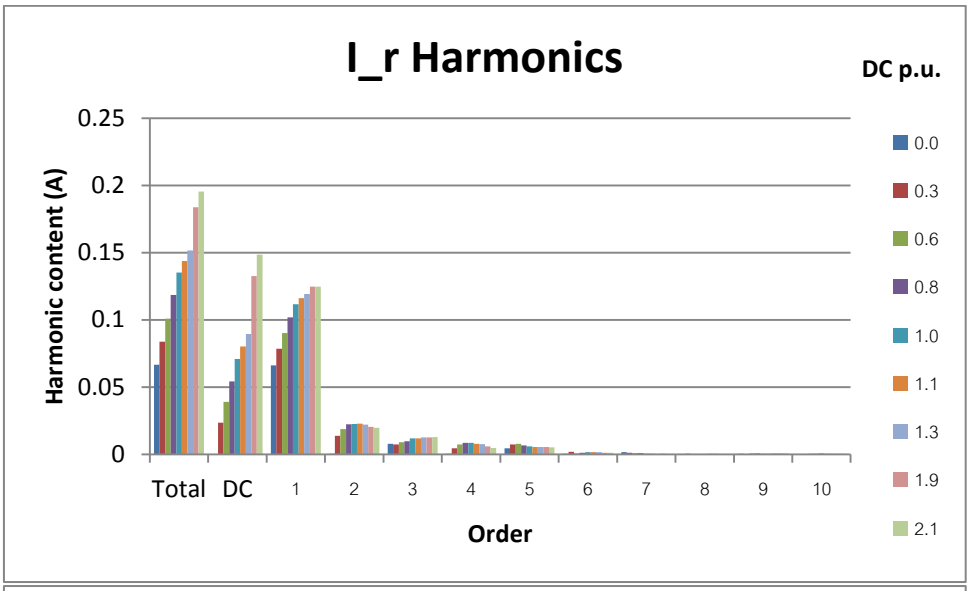

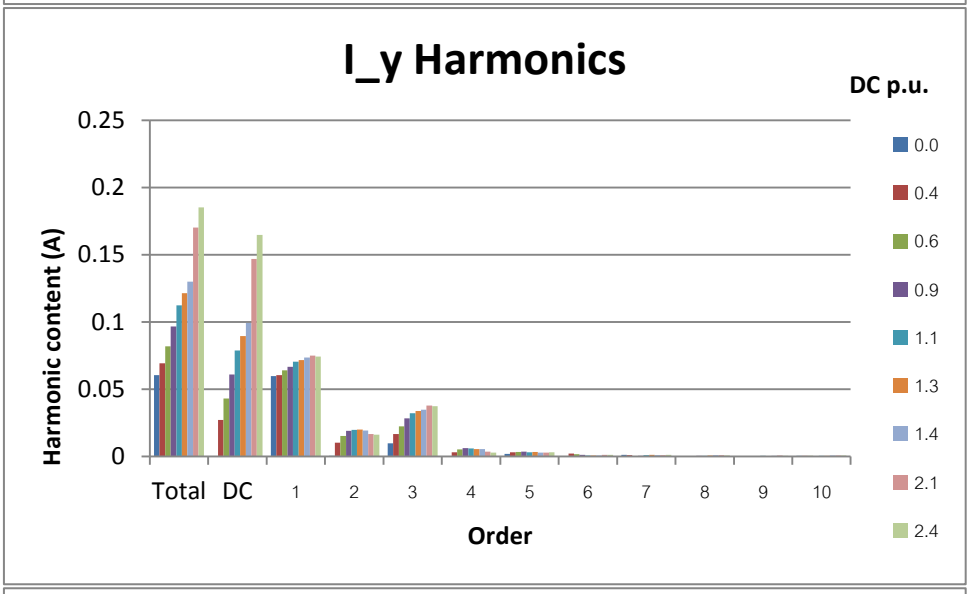

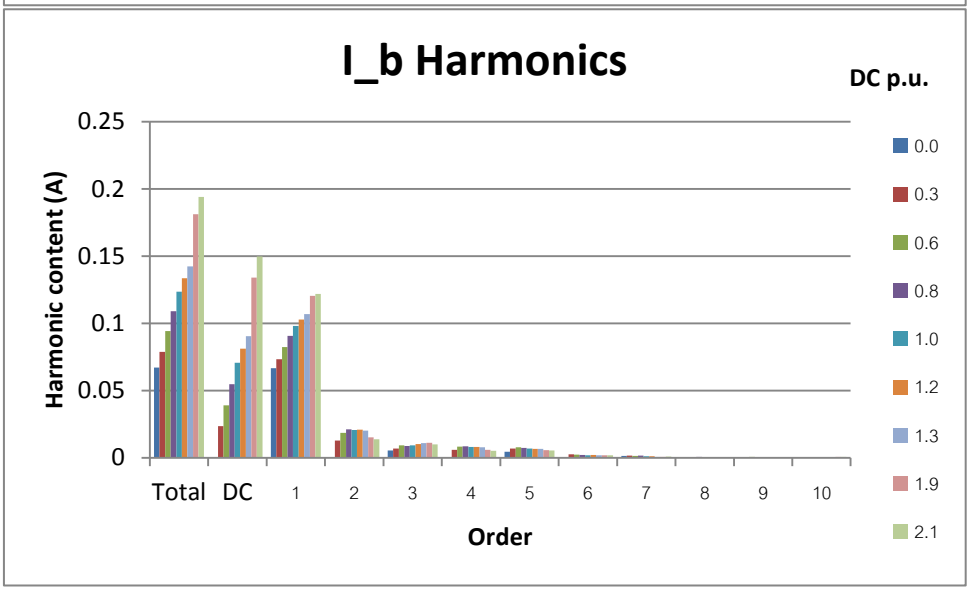

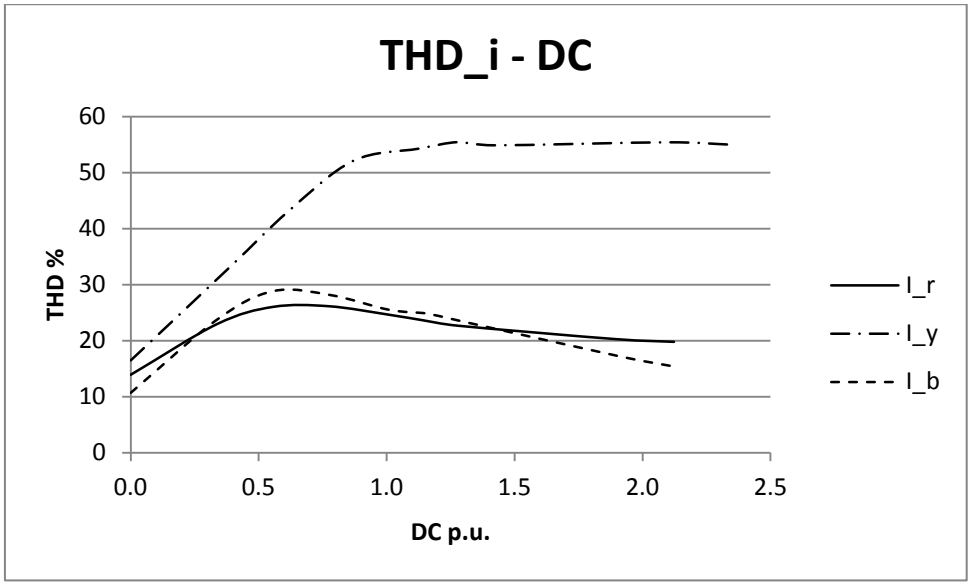
THD_i - DC
60
50
40
30
20
10
0
THD %
0.0
0.5
1.0
1.5
2.0
2.5
DC p.u.
I_r
I_y
I_b

D. DIFFERENTIAL HARMONICS – 70% LOADED

D1. PHASE HARMONICS AND THD: 3p-3s

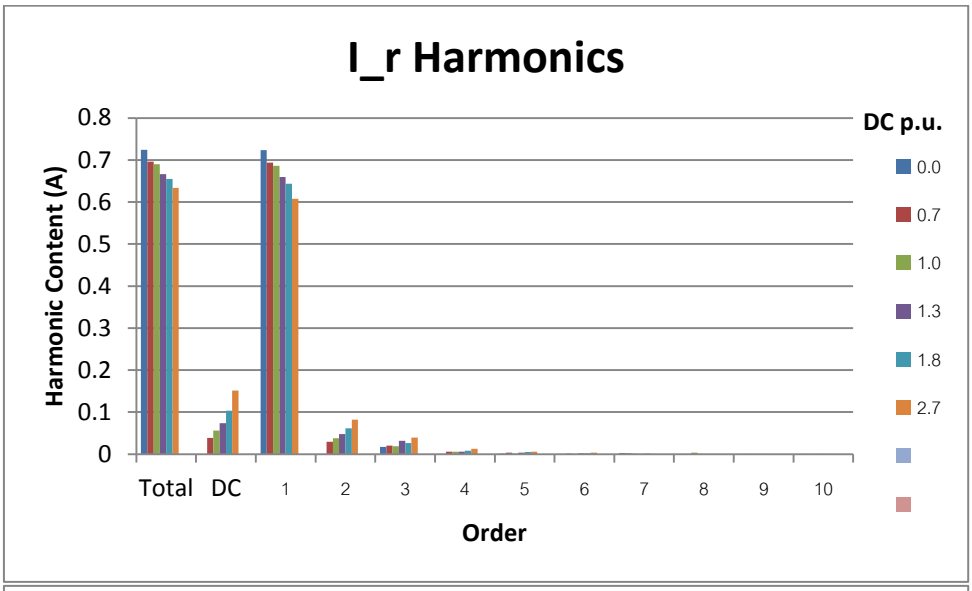

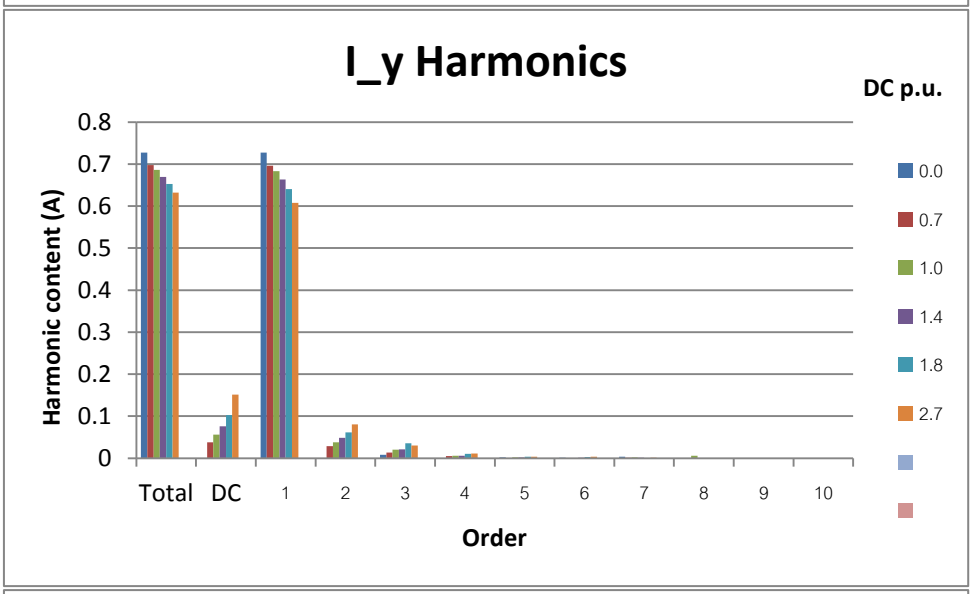

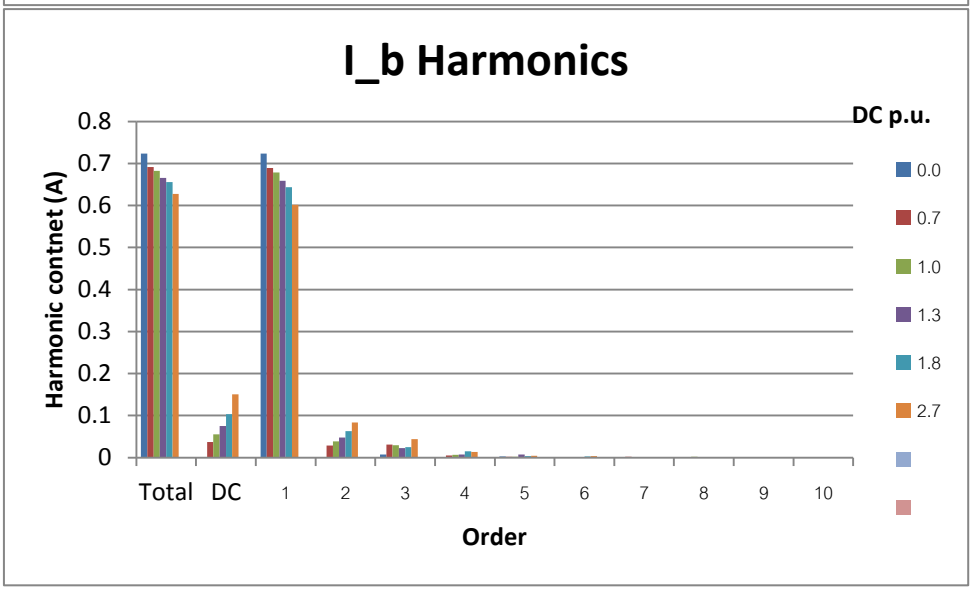

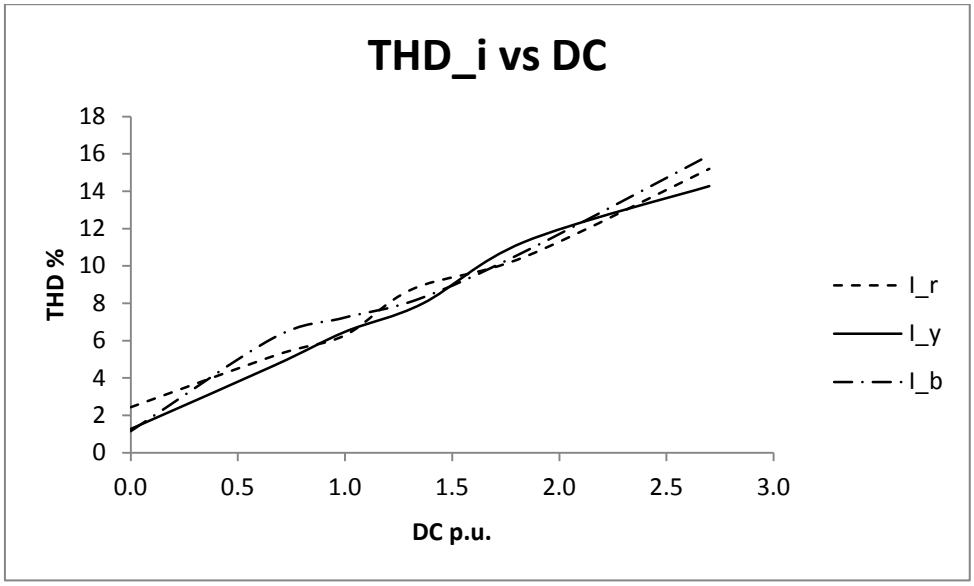
THD_i vs DC
THD %
18
16
14
12
10
8
6
4
2
0
0.0
0.5
1.0
1.5
2.0
2.5
3.0
DC p.u.
I_r
I_y
I_b

D2. PHASE HARMONICS AND THD: 3p-3L

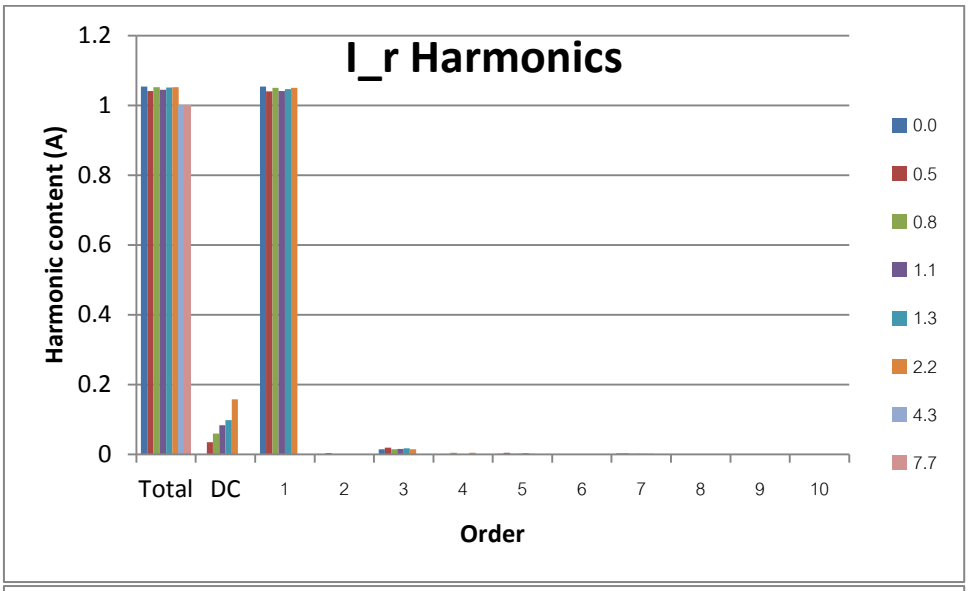

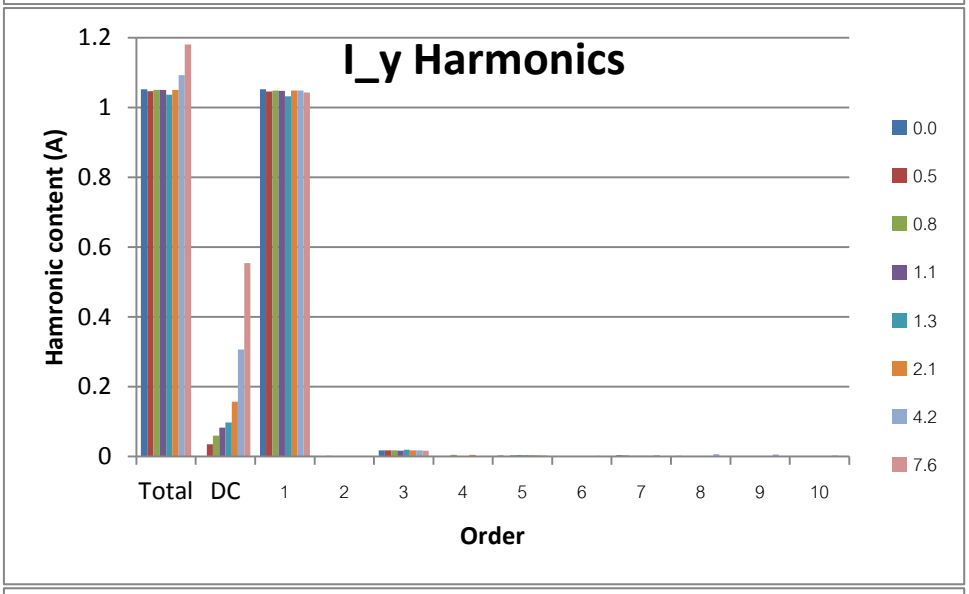

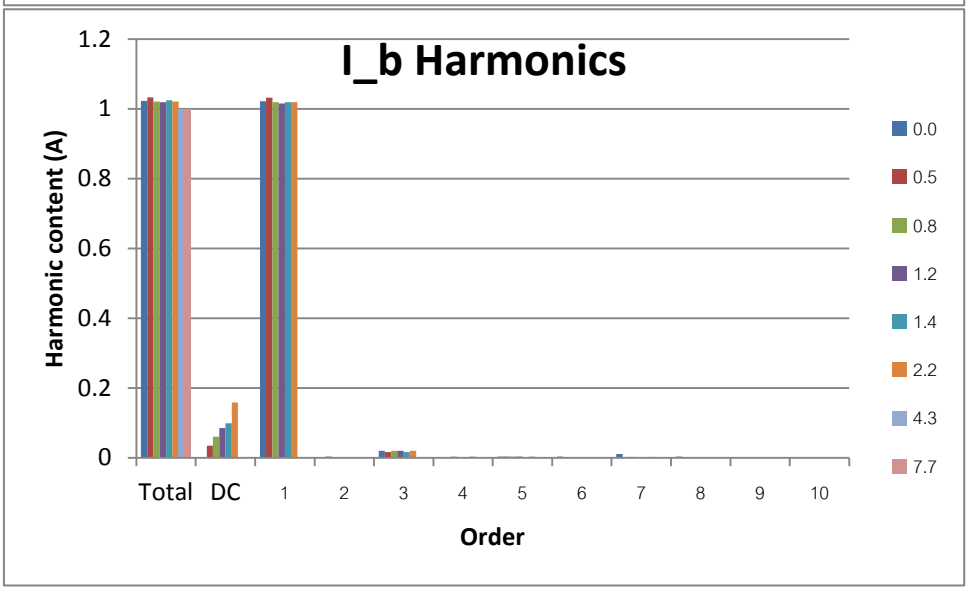

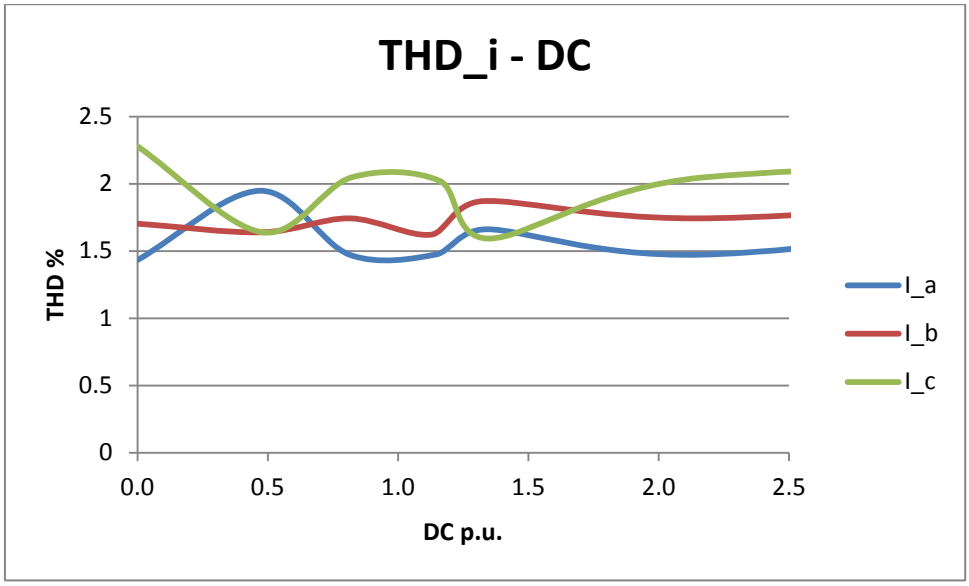
THD_i - DC
2.5
2
1.5
1
0.5
0
THD %
0.0
0.5
1.0
1.5
2.0
2.5
DC p.u.
I_a
I_b
I_c

D3. PHASE HARMONICS AND THD: 3p-5L

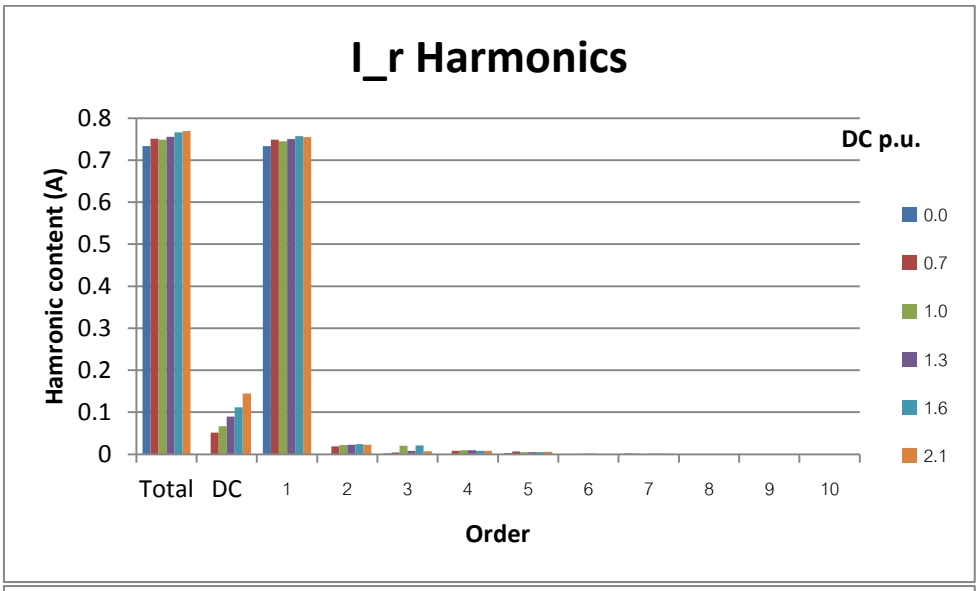

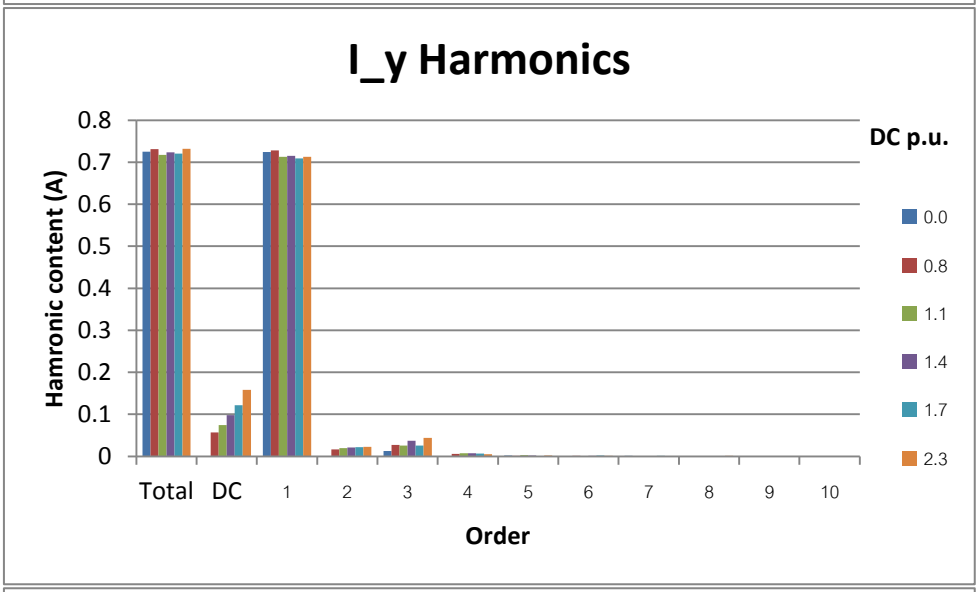

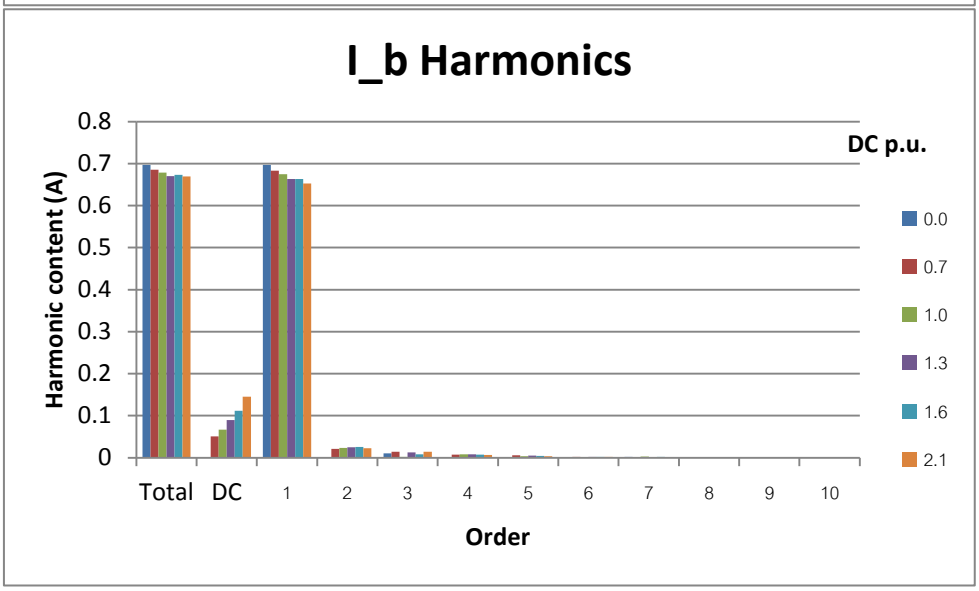

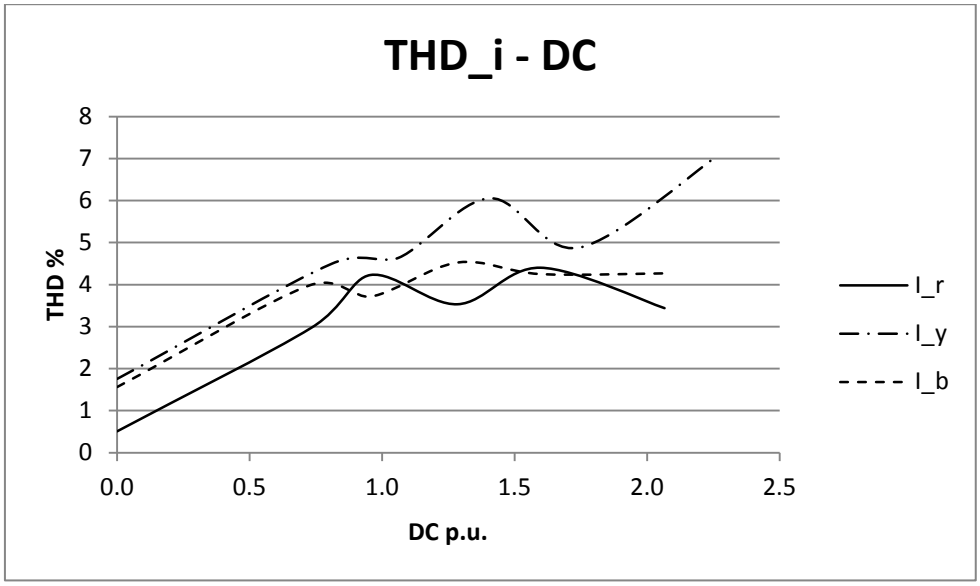
THD_i - DC
THD %
DC p.u.
0
1
2
3
4
5
6
7
8
0.0
0.5
1.0
1.5
2.0
2.5
I_r
I_y
I_b

E. PSCAD SATURATION CURVE INPUTS

E1. 3P-3L UMEC MODEL

Point [I,V]	I_{mag} [% of rated I]	V [p.u.]
1	0	0
2	1.583333	0.145504
3	2.895833	0.28203
4	4.229167	0.411153
5	6.006944	0.568311
6	7.354167	0.675985
7	9.229167	0.80945
8	11.96528	0.96998
9	15.27778	1.10997
10	19.1875	1.198593

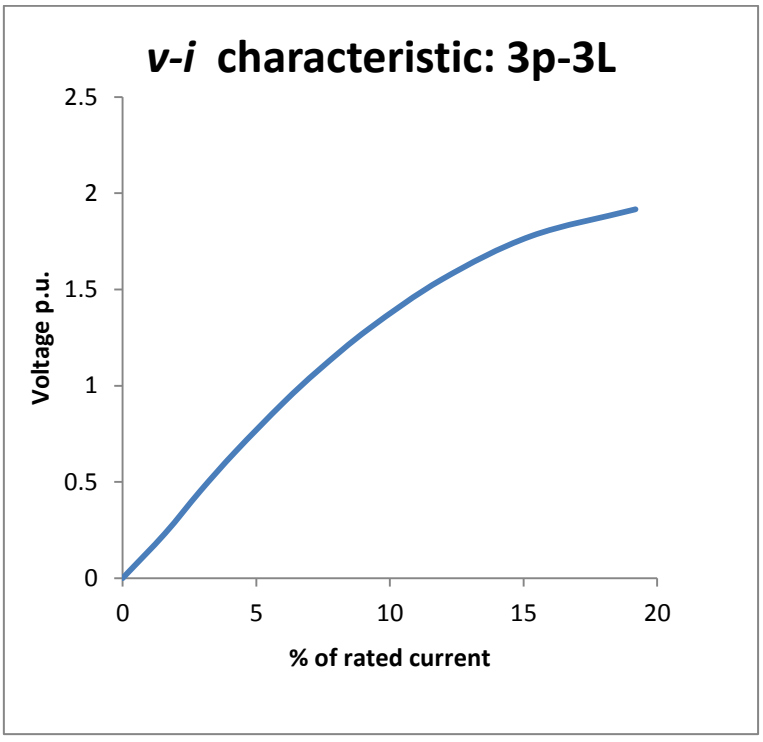

E2. 3P-5L UMEC MODEL

Point [I,V]	I_{mag} [% of rated I]	V [p.u.]
1	0	0
2	3.42	0.14096
3	5.064	0.34062
4	6.312	0.55467
5	7.524	0.78131
6	8.676	0.94911
7	11.592	1.15007
8	18.864	1.37811
9	26.784	1.53804
10	36.66	1.67938